UNIVERSITY OF LIÈGE

FACULTY OF MEDICINE

Resting Brain and Mind

How brain dynamics are associated with ongoing cognition

Sepehr MORTAHEB

Physiology of Cognition, GIGA-CRC In Vivo Imaging
University of Liège
Belgium

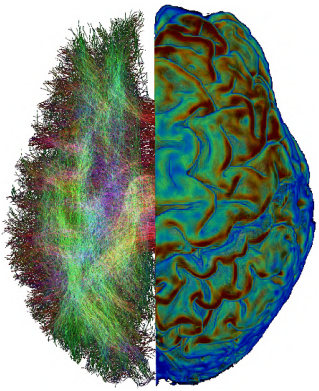

Supervisor
Dr Athena DEMERTZI

A thesis submitted in partial fulfilment of the requirements for the degree of Doctor of Philosophy in Biomedical Sciences and Pharmacology

Academic year 2022-2023

UNIVERSITY OF LIÈGE

FACULTY OF MEDICINE

Resting Brain and Mind

How brain dynamics are associated with ongoing cognition

Sepehr MORTAHEB

Physiology of Cognition, GIGA-CRC In Vivo Imaging
University of Liège
Belgium

Supervisor
Dr Athena DEMERTZI

A thesis submitted in partial fulfilment of the requirements for the degree of Doctor of Philosophy in Biomedical Sciences and Pharmacology

Academic year 2022-2023

To those for whom I wish I were more present.

Acknowledgements

I would like to acknowledge and give my warmest thanks to my great supervisor, Dr. Athena Demertzi, who has supported my ambitious career goals. During these years, she was not only my mentor but a dear friend and a kind sister whom I could rely on for both academic and personal life. I can't thank her enough for all her efforts, guidance, and kindness. Indeed, she changed the way I looked at the world.

I would like to give my special thanks to the members of the jury and thesis committee for their time to examine this research from different perspectives and for their valuable comments and feedback that improved different aspects of the thesis.

I am also grateful to all our national and international collaborators, especially Prof. Johannes G. Ramaekers (University of Maastricht), Prof. Floris Wuyts (University of Antwerp), Prof. Dimitri Van De Ville (École Polytechnique Fédérale de Lausanne), Prof. Steve Majerus (University of Liège), and Dr. Federico Raimondo (Jülich Research Center) whom I had the pleasure of working with on different projects of this thesis. Thanks for their effort in acquiring the unique datasets used in this thesis and their support to develop the methodological aspects of the projects. In addition, I would like to thank the funding agencies of F.R.S.-FNRS and Fondation Léon Fredericq whose financial support made this research possible. Also, special thanks to Prof. Steven Laureys and his team that gave me the opportunity to start my PhD in Belgium and to form the basis of my knowledge about the brain, consciousness, and cognition.

I would also like to give special thanks to my lovely lab members at the Physiology of Cognition lab (Matthieu, Camillo, Daphne, Paris, Larry, Stephania, Nikos, and Kévin) that I spent most of my time with, learning about science and enjoy life together. Also, I would like to thank my colleagues at GIGA-CRC In Vivo Imaging and GIGA-Consciousness for their support, friendship, and all the unforgettable good memories they made for me during these years. My very special thanks go to my Iranian colleagues, Soodeh, Roya, and Nasrin who not only were my colleagues, but also were my second family here. They were always supportive during the hardest moments of my life, and they were there whenever I needed them. I really cannot thank them enough.

Finally, my greatest thanks to my family. First, my parents, Parvin and Abbas. They always supported me spiritually throughout my life, putting my needs before theirs. Their belief in me has kept my spirits and motivation high during

these years while I did not have the chance to be close to them. I would also like to thank my sister Parinaz and my brother Soroush for being my best friends and all their emotional support. I really feel the absence of my family here and I wish I had them by my side.

Summary

When in a resting state, although it seems we are idle, our brain is not silent at all. It actually continues its activity by dynamically changing its functional organization. At the same time, our ongoing experience is also dynamic, characterized by rich exploration of a variant set of mental states. A fundamental question is how such dynamic neural organization during rest can support ongoing conscious experience. An answer to this question may help reveal the underlying intrinsic neural architecture which supports aspects of human cognition, in the absence of task performance.

In my Thesis, I tried to answer how ongoing brain activity and spontaneous cognition relate in four different ways: i) by decoding ongoing mental states during rest based on the brain's dynamic structural-functional (de)coupling profiles, ii) by exploring the neural correlates of mind blanking episodes during rest, iii) by checking the effects of external pharmacological perturbations with psychedelics on the brain-mind dynamics, and iv) by exploring the effects of new non-experienced environments after space travel on the brain's structural and functional organization. I show that while structural-functional (de)coupling profiles can predict ongoing mental states higher than chance-level, they also change regionally facing unseen environmental circumstances in an appropriate way to keep the brain's optimal functioning. Further, the exploration of the brain's functional dynamics showed that a recurrent profile of hyper-connectivity is associated with mind blanking (i.e., instances during which participants are unable to report mental contents) accompanied by high fMRI global signal amplitude compared to other mental states. The same connectivity profile was also found to be dominant in the brain's dynamical landscape under psychedelics. I show that this over-connected functional profile, accompanied by lower levels of global signal amplitude is associated with the experience of depersonalization and ego dissolution after psychedelic administration.

Taken together, the main findings of this thesis can be summarized as: i) regional structural-functional (de)coupling during rest is a signature of our ongoing mentation, ii) a spontaneously occurring functionally hyper-connected state affects our experience of self and environment during rest, and iii) the fMRI global signal can be used as a proxy of a physiological state, which plays an important role in our spontaneous subjective experience. I believe that these findings not only open new windows in brain-mind interaction investigations, but also suggest that a more general formulation based on brain-body interactions are needed to explore ongoing mentation.

Table of contents

Glossary

Term	Definition
Anxious ego dissolution (AED)	Feeling of ego disintegration and loss of self-control associated with anxiety because of psychedelics administration.
Audio-visual synesthesia	when auditory stimuli elicit visual sensations.
Auditory alterations (AA)	The experience of auditory hallucinations and acoustic alterations.
Auditory network	A network of cortical regions including bilateral superior temporal gyri/insular cortices, left pars opercularis, left superior temporal gyrus, and midcingulate cortex whose role is related to audition (tone and pitch discrimination), music, speech, phonological and oddball discrimination.
Auto-regressive model (AR)	A mathematical model to describe certain time-varying processes in which the output variable depends linearly on its own previous values and on a stochastic term.
Blissful state	A state of being extremely happy or full of joy, peace, and love.
Blood oxygen level dependent (BOLD):	When neurons of a certain brain area demand energy and oxygen, the cerebral vascular system responds to this demand by increasing the local blood flow which delivers oxygen to these neurons (neurovascular coupling). However, not all oxygen is consumed by the neurons. Changes in the oxygenated over deoxygenated hemoglobin ratio is the BOLD effect signal detected by fMRI.
Changed meaning of percepts	A state in which objects in an individual's environment appear more salient and personally significant than they ordinarily do.
Classification models	A group of supervised learning techniques that are used to identify the category of new observations based on training data. Using

	classification models, a program learns from the given labeled dataset or observations and then classifies new observation into several classes or groups.
Complex imagery	The state of having visual hallucinations of scenes and pictures after psychedelics administration.
Connectome	A matrix representing all possible pairwise anatomical connections between neural elements of the brain.
Default mode network (DMN)	A large-scale brain network primarily composed of the dorsal medial prefrontal cortex, precuneus and angular gyrus. It is best known for being active when a person is not focused on the outside world and the brain is at wakeful rest, such as during daydreaming and mind-wandering.
Disembodiment	Disruption of bodily self-awareness which induces a disturbing feeling of self-detachment or depersonalization.
Dynamic connectivity analysis	Analysis of functional connectivity alterations over the acquisition time course.
Dorsal attentional network (DAN)	Also known as task-positive network is a large-scale brain network composed of the intraparietal sulcus and frontal eye fields associated with voluntary orienting of visuospatial attention.
Ego dissolution	The experience of a compromised sense of self characterized by the reduction in the self-referential awareness.
Elementary imagery	Visual hallucinations of regular patterns, colors, or light flashes after psychedelics administration.
Executive control network (ECN)	Also known as fronto-parietal network is a large-scale brain network composed of dorsolateral prefrontal cortex and posterior parietal cortex, around the intraparietal sulcus. It is involved in sustained attention, complex problem solving and working memory.
Experience of unity	A critical dimension of mystical experiences after psychedelics administration in which

	representations of internal and external objects of consciousness blend together.
Exteroception	The perception of environmental stimuli originating outside of the body, e.g., visual, auditory, or tactile stimuli.
Functional connectome	The collective set of matrices representing brain functional connectivity.
Functional magnetic resonance imaging (fMRI)	A neuroimaging technique that measures the small changes in blood flow related to the brain activity. This technique relies on the fact that cerebral blood flow and neuronal activation are coupled. When an area of the brain is in use, blood flow to that region also increases.
General linear models (GLM)	Refers to conventional linear regression models for a continuous response variable given continuous and/or categorical predictors and is a compact way of simultaneously writing several multiple linear regression models.
Glutamate	The major excitatory neurotransmitter which is involved in the rapid production of excitatory postsynaptic potentials at axospinous synapses and in slowly developing neuroplasticity associated with learning, memory, and neuronal development.
Graph signal processing (GSP)	An extension of the classical signal processing algorithms which considers that signals are supported by irregular substrates defined by graphs. Signal points are represented as values, which reside on the graph nodes and are related to each other based on the edge weights of the graph.
Independent component analysis (ICA)	A computational method for separating a multivariate signal into additive subcomponents. This is done by assuming that at most one subcomponent is Gaussian and that the subcomponents are statistically independent from each other.
Information flow	In information theory, it is referred to as the transfer of information from a variable to another variable in

	a given process. In neuroscience, the variables can be considered and the brain's regional activity.
Insightfulness	Also known as unconstrained style of thinking, is a state after psychedelics administration in which one has very original thoughts and gains clarity into connections that puzzled him/her before.
Interoception	Collection of senses perceiving the internal state of the body such as feeling of heart beats or breathing, feeling of hunger, feeling of thirst, etc.
Limbic system	A set of brain structures including amygdaloid nuclear complex (amygdala), mammillary bodies, stria medullaris, central gray, and dorsal and ventral nuclei of Gudden involved in lower order emotional processing of inputs coming from sensory system.
Metastable state	A state in which brain signals (such as oscillatory waves) fall outside their natural equilibrium but persist for an extended period. It is a principle that describes the brain's ability to make sense out of seemingly random environmental cues.
Microgravity	Is the condition in which people or objects appear to be weightless. The effects of microgravity can be seen when astronauts and objects float in space.
Neuroplasticity	The ability of the nervous system to change its activity in response to intrinsic or extrinsic stimuli by reorganizing its structure, functions, or connections after facing the stimuli.
Oceanic boundlessness (OB)	Feeling of derealization and depersonalization associated with positive emotional states after psychedelic administration.
Orthonormal:	A set of vectors that have unity norm and are perpendicular to each other are known as orthonormal vectors.
Phase-based coherence	A measure to quantify the constant phase difference between two signals with the same frequency.
Phase-locking connectivity state	When performing dynamic functional connectivity analysis, if the connectivity matrices are calculated based on phase-based coherence, the estimated

	connectivity states are named as phase-locking states.
Positron emission tomography (PET)	A neuroimaging technique which reveals the metabolic or biochemical function of the brain using radioactive drug (tracer) to show both normal and abnormal metabolic activity.
Principal component analysis (PCA)	A dimensionality-reduction method that is often used to decrease the size of large data sets, by transforming them into smaller variables that still contain most of the initial dataset's information.
Psychedelics	A subclass of hallucinogenic drugs whose primary effect is to trigger non-ordinary mental states and/or an apparent expansion of consciousness.
Salience network	A collection of cortical regions including bilateral insular and anterior cingulate cortices (ACC). Activation of the insula and ACC are commonly observed in conflict monitoring, information integration and response selection. In resting state, the salience network is also thought to be involved in interoception and pain-related processes.
Sensorimotor network	A collection of cortical regions including supplementary motor area/ midcingulate cortex, and bilateral primary, premotor and somatosensory cortices involved in action-execution and perception-somesthesis paradigms.
Sliding window	A method of dynamic analysis in which a metric is calculated in different consecutive overlapping windows of data.
Spiritual experience	A subjective experience which is interpreted within a religious framework and goes beyond human understanding in how this experience could have happened in the first place.
Static connectivity analysis	Calculation of connectivity measure between pairs of regions based on the overall acquired data, considering that the connectivity measure is constant during the acquisition time.
Stimulus-dependent thought	Thoughts and mental images that are provoked by or reflect the features of one's surroundings.

Stimulus-independent thought	Thoughts that occur independently of input from the immediate external environment.
Structural decoupling index (SDI)	A measure of regional decoupling of functional activity from the underlying structure connectivity.
Structural harmonics	Defined as the eigenvectors of Laplacian of structural connectivity matrix, showing fully synchronous neural activity patterns with different frequency oscillations emerging on and constrained by the brain structure.
Transcranial direct-current stimulation (tDCS)	A form of brain stimulation and neuromodulation that uses constant, low, and direct electrical current delivered via electrodes on the head to modulate cortical excitability.
Transcranial magnetic stimulation (TMS)	A noninvasive form of brain stimulation in which a changing magnetic field is used to induce an electric current at a specific area of the brain through electromagnetic induction.
Visual network	A collection of cortical regions including primary and extrastriate visual cortices and inferior temporal gyri involved in low-level visual processing, viewing complex stimuli, and higher-level visual processing.
Visual Restructuralization (VR)	Perceptual and imaginational alterations including visual hallucinatory phenomena due to psychedelics administration.

1 Introduction

1.1 Network Representation of the Resting Brain

Suppose you are sitting somewhere, not engaging in any task, and your thoughts are free to wander between different contents, times, and places. This condition is referred to as the "resting state." Neuroscientific studies support that during resting state, and in the absence of an external input, the brain's ongoing activity is essential to its global functioning (Fox & Raichle, 2007). This was initially argued based on **positron emission tomography (PET)** imaging of healthy subjects showing that a system of mesiofrontal, posterior cingulate/precuneus cortices, and lateral parietal areas, broadly known as the **default mode network (DMN)**, was systematically deactivated during task as compared to a resting condition (Mazoyer et al., 2001; Shulman et al., 1997). This led to the assumption that the brain at rest is not silent, opening a new area to study the purpose of ongoing brain function in more depth.

One way to investigate the brain's resting activity is to acquire **functional magnetic resonance imaging (fMRI)** data while the subject is lying still in the scanner, known as "task-free condition." In this setup, the brain's resting activity can be detected using the **blood oxygen level dependent (BOLD)** signal which is characterized by spontaneous low-frequency fluctuations (in the range of 0.01–0.1 Hz). In the absence of specific tasks and external inputs, a primary goal in resting-state fMRI studies is to analyze synchronized activity of the BOLD signal between pairs or sets of brain regions, commonly referred to as functional connectivity (FC; Biswal et al., 1997). Earlier studies using data-driven statistical methods, such as **independent component analysis**, showed that the brain at rest is organized into specific consistent large-scale FC profiles known as resting state networks (RSN; Beckmann et al., 2005; Damoiseaux et al., 2006; De Luca et al., 2006; Heine et al., 2012; Figure 1.1A). These RSNs consist of anatomically separated, but functionally linked brain regions that show high FC during rest (Van den Heuvel & Hulshoff Pol, 2010) and are implicated in various cognitive domains. The default mode network (DMN), **executive control network** (ECN; a.k.a., frontoparietal network), **salience** (a.k.a., ventral attentional network), **sensorimotor** (a.k.a., somatomotor), **auditory**, **visual**, **dorsal attentional network** (DAN; a.k.a., task-positive network), and **limbic system** are among the most studied networks. The fundamental characteristic that distinguishes these RSNs from each other is high FC between regions belonging to the same network and low FC between nodes belonging to different networks (Raichle, 2011).

These findings led to the network representation of the functional associations that exist between distant brain regions. In general, brain regions

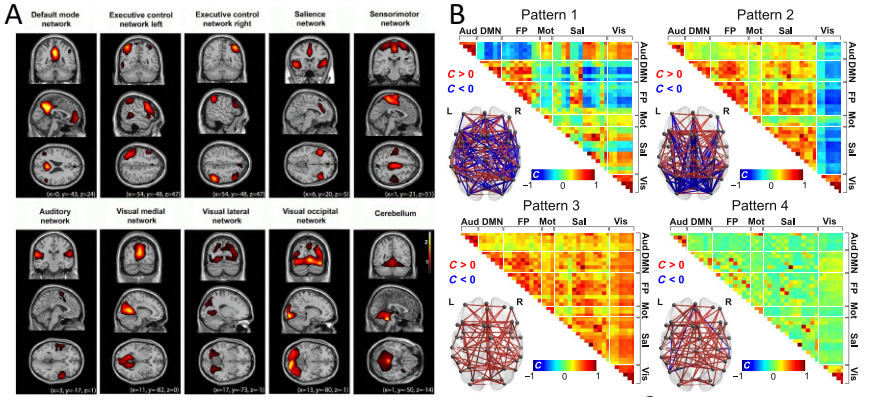

Figure 1.1 Brain in resting state can be characterized by distinct functional connectivity profiles. (A) Static analysis of synchronized activity of different brain regions leads to consistent and reliable functional connectivity networks identified by anatomically separated but functionally linked brain regions (Heine et al. 2012). **(B)** Time-varying analysis of BOLD time series shows that brain's functional connectivity during resting state is varying and can be explained by distinguishable recurrently emerging connectivity patterns (Demertzi et al. 2019).

can be defined as the nodes of a network that are connected using edges, describing the strength of structural/functional connectivity between them. Mathematically, this network can be demonstrated using a matrix representing all possible pairwise anatomical or functional connections between defined regions (Figure 1.1B). While the term **connectome** was initially suggested to describe the brain's anatomical network (Sporns et al., 2005), nowadays the term **functional connectome** is also used to describe a collective set of functional connections in the brain.

The RSN structure has been understood thanks to the "**static**" analysis of BOLD time series, i.e., taking the averaged time series to analyze synchronized activity. However, it is now known that brain function is rather a "**dynamic**" exploration of connectivity configurations over time (Gu et al., 2018; Watanabe et al., 2014). This means that brain activity configures in different ways as time goes by. Different methodologies such as **sliding window** FC estimation (Allen et al., 2014), **phase-based coherence** (Demertzi et al., 2019), and **auto-regressive modeling** (Liégeois et al., 2019) have been used to estimate the FC in shorter temporal resolutions. Accordingly, brain dynamics have been defined as spontaneous transitions between discrete **metastable states** of functional connectivity, a.k.a., "FC states" (Cabral et al., 2017; Cavanna et al., 2018; Hansen

et al., 2015). As an example (Figure 1.1B), it was shown that during rest, the brain organizes itself into four distinguishable recurrently emerging time-varying FC states described as i) a pattern of high complexity, including both positive and negative values of long-distance coordination, ii) a pattern of negative phase coherence between visual and other networks, iii) a pattern of cortex-wide positive phase coherence and iv) a pattern of low interareal coordination (Demertzi et al., 2019). These patterns have been shown to be quite reliable as they can be reproduced across different individuals, different paradigms, and different scanners (Mortaheb et al., 2022).

Dynamic transitions between FC patterns can be modeled by the Markov chain model, namely a stochastic model in which transition probabilities to other states are dependent on the current state (Gagniuc, 2017). Such dynamic transitions have so far been associated with level of consciousness (Demertzi et al., 2019; Y. Zhang et al., 2019; Zhou et al., 2019), cognitive performance (Cabral et al., 2017; Ikeda et al., 2022; Liégeois et al., 2019), and self-reported behavioral measures, e.g., life satisfaction (Casorso et al., 2019). However, what still needs to be answered is how these dynamic signal transitions are associated with the dynamism of ongoing experience. In other words, is there a cognitive relevance in task-free conditions?

1.2 Mental States During Rest

When the mind is unoccupied by environmental events, humans often spend most of their time focused on information that is self-generated but is not necessarily about the "here and now" (Karapanagiotidis et al., 2020; Mckeown et al., 2020). Such ongoing experience is dynamic and rich in content, taking the form of mental states. Mental states are transient cognitive or emotional occurrences that are described in terms of content (what the state is "about") and the relation we bear to this content (e.g., imagining, remembering, fearing; Christoff et al., 2016).

A fundamental characteristic of ongoing mentation is spontaneity, which means fluctuations of content independently from the immediate environment and without conscious control (Kucyi, 2018). From this perspective, when our attention is decoupled from external environment, our minds are occupied by thoughts (Smallwood et al., 2008), also known as **stimulus-independent thoughts** (Stawarczyk et al., 2011; Van Calster et al., 2017). Spontaneous thoughts are heterogeneous across people, places and situations (Smallwood et al., 2021), and vary in the dimensions of "content" and "form" (Karapanagiotidis

et al., 2017; Mckeown et al., 2020), which depends on the interplay between internal processes (e.g., self-generated thoughts) and environmental demands (Turnbull et al., 2019). In a simplistic model, the content of thought can be explained by three elements: time (past vs. future), reference (self vs. others), and emotional valence (negative, neutral, or positive). The form of thoughts can be about modality (from images to words), level of detail, and level of intrusiveness (Karapanagiotidis et al., 2017). These spontaneous thoughts with their different contents and forms are estimated to comprise ~30-50% of our daily life (Kane et al., 2007; Kucyi et al., 2018; Van Calster et al., 2017) and therefore are a significant source of variations during ongoing experience.

Apart from spontaneous thoughts, while being at rest we can also have perceptual contents of external stimuli (**exteroception**) or internal bodily states (**interoception**; Stawarczyk et al., 2011; Van Calster et al., 2017). External stimuli can involve the main five senses of visual, auditory, olfactory, gustatory, and somatosensory and internal bodily states can cover internal senses, such as feeling thirsty. In past studies, stimuli perceptions were sometimes confounded with thoughts related to the immediate environment, a.k.a., **stimulus-dependent thoughts**. This was due to the fact that those studies tended to distinguish between externally and internally oriented cognition (Vanhaudenhuyse et al., 2011) without considering possible mixed states, where internal mentation is simultaneously accompanied by some awareness of the external environment.

Finally, during ongoing experience, there can also be moments when we are unable to report or retrieve any mental content. This is often reported as “having no thought”(Van Calster et al., 2017), as if our mind “went away” (Ward & Wegner, 2013), or as if the mind “got blanked” (Kawagoe et al., 2019) widely referred to as Mind Blanking (Mortaheb et al., 2022).

Together, ongoing experience during task-free conditions can be modelled as a sequence of thoughts, which are comprised of different contents and forms, stimuli perception (exteroception vs interoception), and mind blanking states which occur spontaneously and recurrently over time. In this regard, mental state dynamics can be considered as spontaneous transitions between thoughts, perceptions, and mind blanking states.

Table 1.1 Resting state networks and their associated brain regions and cognitive roles.

Network	Brain Regions	Cognitive Role
Auditory	Superior temporal cortex Insular cortex Post central cortex	- Auditory processes
DAN	Intra parietal sulcus Frontal eye fields	- Goal-directed, voluntary control of visuospatial attention - Top-down selection of stimuli and responses
DMN	Medial prefrontal cortex Posterior cingulate cortex Angular gyrus	- Self-related cognitive processes - Mind wandering - Temporal perspective of self - Task-unrelated thoughts
ECN	Dorsolateral prefrontal cortex Posterior parietal cortex	- Sustained attention - Complex problem-solving - Working memory
Limbic	Amygdala Mammillary bodies Stria medullaris Central gray, dorsal and ventral nuclei of Gudden	- Lower order emotional processing of input from sensory systems
Salience	Anterior insula Anterior cingulate cortex	- Detecting and filtering salient stimuli - Recruiting relevant functional networks
Somatomotor	Post- and precentral gyrus Supplementary motor areas	- Performing and coordinating motor tasks
Visual	Striate cortex Extra-striate areas in the occipital lobe	- Visual processes

DAN: dorsal attentional network, DMN: default mode network, ECN: executive control network

1.3 Bridging the Resting Brain with the Spontaneous Mind

A fundamental question is how such specific neural organization during rest can support ongoing conscious experience. An answer to this question may help describe the underlying neural architecture which supports aspects of human cognition, useful for the cognitive evaluation of non-responsive individuals who are unable to communicate directly (Mckeown et al., 2020; Monti et al., 2010).

Considering the cognitive relevance of RSNs, there is evidence that resting state FC patterns have similarities with different task activation maps (Biswal et al., 1995; Smith et al., 2009; Tavor et al., 2016). In fact, FC architectures across a variety of tasks were reported to be highly similar (80% shared variance) to the resting-state FC architectures (Cole et al., 2014). Based on these similarities, a set

of cognitive roles were suggested for each one of the RSNs (summarized in Table 1.1). For example, the DMN was suggested to be associated with self-related cognitive processes, such as mind-wandering (Mason et al., 2007; Smallwood et al., 2021), task-unrelated thoughts (Stawarczyk et al., 2011; Van Calster et al., 2017), and temporal perspective of the self (D'Argembeau et al., 2010). Further, more detailed analysis showed that the RSNs not only have specific cognitive roles, but can also act as specific routes for **information flow** between different brain regions while subjects are performing cognitive tasks (Cole et al., 2016). Importantly, FPN, DAN, and ECN were suggested as main networks that globally control and coordinate task-related information flow (Ito et al., 2017).

Static connectivity analysis during rest showed that DMN and its interaction with other cortical regions, such as the hippocampus, support the occurrences of spontaneous thoughts (D'Argembeau et al., 2010; Karapanagiotidis et al., 2017; Mason et al., 2007; Smallwood et al., 2021; Stawarczyk et al., 2011; Van Calster et al., 2017). Additionally, parts of DAN and VAN are associated with stimuli perception (Van Calster et al., 2017). More detailed investigation of neural signatures regarding fluctuating conscious contents can be achieved thanks to the dynamic exploration of within- and between-network interactions during rest (Kucyi, 2018). For example, considering the role of DMN in the occurrences of spontaneous thoughts, it has been shown that more dynamic communication within DMN areas increases overall stimulus-independent thoughts (Kucyi & Davis, 2014). Using a retrospective evaluation of mental states after resting fMRI acquisition, it has also been shown that the neural activity which is commonly seen during demanding tasks and the time individuals spent in this state was associated with having thoughts about problem solving in the future. In addition, a second state that is commonly seen under less demanding conditions and the time individuals spent in this state was linked to reports of intrusive thoughts about the past (Karapanagiotidis et al., 2020). Also, individuals who reported greater frequencies of thoughts related to somatosensory awareness, auditory imagery, and visual imagery showed greater FC changes over time. These variations were more nuanced in the medial prefrontal cortex, insula, sensory regions, and basal ganglia, suggesting content-specificity of the relationship between different brain networks and spontaneous thoughts (Chou et al., 2017).

A limitation in these studies is the retrospective evaluation of ongoing mental states using questionnaires after data acquisition. Although this technique avoids interruptions in the flow of spontaneous mental states, it does not provide precise information about the occurrence time of each particular state, and is commonly subject to self-serving biases (Kucyi, 2018). To mitigate this limitation,

"experience sampling" or "thought probe" techniques were proposed, in which subjects are interrupted in random time points during rest to report their immediate mental state (Reed & Mihaly, 2014; Van Calster et al., 2017). This technique gives a better temporal resolution of mental state evaluation but leads to interruption in the flow on ongoing conscious experience. Due to this tradeoff, there is still a big gap in understanding the association of neural dynamics and ongoing mental states during rest.

1.4 Thesis Outline

In this thesis, the fundamental goal is to investigate the association between neural dynamics and ongoing conscious experience during resting state. In a general view, the thesis is planned based on four chapters to explore this question in two different settings: i) The investigation of brain-mind interactions in special conditions with the aim to see how this relationship is influenced by different parameters, i.e., intrinsic brain idiosyncrasy (mind blanking), perturbations (psychedelic drugs), and extreme environments (space flight); and ii) The design of a "brain-reading" model to decode ongoing mental states, with the aim to determine those neuroimaging features, critical to classify spontaneous mental content.

In Chapter 2, we investigate the association between resting state neural and mental dynamics in special conditions: a) in the form of spontaneous occurrences of mind blanking, b) under administration of psychedelics, and c) after space travel. Mind blanking is a unique, not widely charted mental state, that can occur also during normal wakefulness. As spontaneous occurrences of mind blanking suggest that the stream of consciousness might have intermittent gaps, exploring its neural correlates in terms of dynamic FC patterns can reveal valuable information concerning brain-mind interaction during rest. As perturbations are an efficient way to understand the underlying mechanism of a system, in the other two studies, we investigate the main question of the thesis while the whole brain-mind system is affected by an external factor. First, we study the effect of **psychedelics** (i.e., a class of psychoactive drugs that alter conscious experience) on the neural dynamics and how the identified neural changes lead to the changes in the conscious experience. Second, we study the effect of long-duration space flight. There are growing evidence that space travel leads to changes in brain structure and function. In this study we aim to explore the effects these changes have on the neural dynamics of cosmonauts who traveled to the International Space Station and the possible effects they can have on their mental flexibility.

Chapter 3 deals with mental state decoding. In this study, we use an experience-sampling technique to probe ongoing mental states during rest with the aim to characterize the dynamic behavior of ongoing conscious experience. Using machine learning tools, we designed a decoder which works based on the dynamic changes in the coupling and decoupling of functional activity to and from the underlying structural connectome. This decoder aimed to predict principal mental states that emerged during resting state solely based on the brain's neural dynamics.

Finally in Chapter 4, we summarize and discuss the main findings of this thesis in more detail. On the basis of outcomes and limitations, we suggest future directions that can be taken to complete this research.

2 Resting Brain in Special Conditions

This chapter is based on:

Mortaheb, S., Van Calster, L., Raimondo, F., Klados, M.A., Boulakis, P.A., Georgoula, K., Majerus, S., Van De Ville, D. and Demertzi, A., **2022**. Mind blanking is a distinct mental state linked to a recurrent brain profile of globally positive connectivity during ongoing mentation. *Proceedings of the National Academy of Sciences*, *119*(41), p.e2200511119.

2.1 Introduction

Exploring the underlying mechanism of action in a system in specific conditions helps to understand unique aspects of that system which are not visible in normal conditions. In this chapter, we examine the dynamic aspects of the brain-mind relationship in specific and unique conditions that can reveal more details about the way our brain supports ongoing experience during rest.

First, we observe that the brain's intrinsic organization constitutes by itself a substrate for variant cognition. An uncharted cognitive phenomenon is that of mind blanking. Therefore, we seek to answer what happens in the resting brain when we experience a blanked mind? Second, a typical way to better understand the mechanism of a system is to alter its characteristics through external interventions. A promising experimental framework for investigating such changes in the brain and mind is the psychedelic state. Psychedelic drugs lead to profound departures from normal waking consciousness and produce mystical experiences. How would these be reflected on brain dynamics? Third, studying the brain under long-term exposure to gravity alteration can provide a clear understanding about the effects of the environment on brain dynamic. Could structure-function relationship reveal subtle information about mental flexibility in space travelers?

2.2 Mind Blanking

Contemporary views of ongoing thought see spontaneous experience as an interplay between internal processes (e.g., self-generated thoughts) and environmental demands (e.g., task difficulty; Smallwood et al., 2021). For example, off-task thoughts and daydreaming can be observed more frequently when environmental demands are less pronounced (Turnbull et al., 2019). Ongoing experience can also show moments when we cannot report any mental content, often accompanied by a post-hoc realization that our mind "went away" (Ward & Wegner, 2013) or went "blank" (Kawagoe et al., 2019). This particular phenomenon is often referred to as mind blanking (MB). This mental state is a waking state during which we do not report any mental content. The phenomenology of MB challenges the view of a constantly thinking mind. So far, MB has been defined as "reports of reduced awareness and a temporary absence of thought (empty mind) or lack of memory for immediately past thoughts [that] can be considered as the phenomenological dimension of a distinct kind of attentional lapse" (Andrillon et al., 2019). This definition implies that MB can have various mechanistic causes, such as lack of content meta-awareness, failure

in memory retrieval, or lapses in attention. Regardless of the mechanistic counterpart, MB's phenomenology challenges the view of the mind as relating primarily to thoughts. Given this observation, what is the relation between MB and other mental states and what are the specific neural configurational processes that support this phenomenology?

To date, behavioral and neuroimaging studies have shown that MB can be reported with a low frequency compared to other mental states, it can occur either during resting state (Van Calster et al., 2017) or during a cognitive task (Andrillon et al., 2021), and it can be accompanied by particular neural activity. Behaviorally, it has been shown that, during focused tasks, MB was reported on average 14.5% of the times whenever subjects evaluated their mental state upon request (Ward & Wegner, 2013) and 18% of the time when participants reported MB by self-catching (Schooler et al., 2004). During resting state, this number was reported to be about 6% (Van Calster et al., 2017). Neuroimaging data showed that when participants were instructed to "think of nothing" as compared to "let your mind wander," there was lower fMRI functional connectivity between the default mode network and frontal, visual, and salience networks (Kawagoe et al., 2018). MB has also been associated with deactivation of Broca's area and parts of the hippocampus, as well as with activation of the anterior cingulate cortex, which was interpreted as evidence for reduced inner speech (Kawagoe et al., 2019). Decreased functional connectivity in the posterior regions of the DMN and increased connectivity in the DAN was also found in an experienced meditator who practiced content-minimized awareness, which can be considered a phenomenological proxy to sustained MB (Winter et al., 2020).

Collectively, these studies indicate that the investigation of MB is rising over the years. Yet, we observe that its neurobehavioral characterization remains inconclusive for several reasons. First, MB has been studied after deliberately inducing it or in highly trained individuals; therefore, its spontaneous occurrences are not generalizable. Second, in some cases MB has been studied in isolation from other mental states; therefore, its interstate dynamics are lacking. Third, current MB's neural correlates concern a limited number of brain regions, leaving the whole-brain functional connectome uncharted. Here, we aimed at addressing these issues by delineating the neurobehavioral profile of MB in a comprehensive way. For this purpose, we used fMRI-based experience sampling in typical individuals (Van Calster et al., 2017) to account for the behavioral quantification of spontaneous (noninduced) MB occurrences, to determine MB's inter-mental state dynamics, and to estimate MB's functional fine-grained connectome at the whole-brain level.

2.2.1 Characterization of Mind Blanking at Rest

Dataset

Data were previously collected from 36 healthy participants (27 women, 9 men, mean age: 23 y ± 2.9) within a 3-T MRI scanner while they were at rest with eyes open (Van Calster et al., 2017). Experience- sampling concerned randomly presented sounds (n = 50) that prompted the participants to evaluate and choose by button press the mental states in which they were engaged prior the probe. Possible mental states were absence (i.e., MB), perception of sensory stimuli (Sens), stimulus-dependent thoughts (SDep), and stimulus-independent thoughts (SInd) (Figure 2.1, Methods Box 1).

Behavioral Characteristics

Considering the occurrence rate over time, MB was reported significantly fewer times than the other mental states (median=2.5, IQR=3, min=0, max=9; Figure 2.2A). With respect to reaction times, there was a main effect of mental state ($\chi2[3]=66.63$, $p<0.001$; generalized linear mixed model analysis; Figure 2.2B), with MB being reported faster than SDep ($z=3.81$, $P=0.0008$) and SInd ($z=3.37$, $P=0.0042$) but with no significant differences from Sens ($z=0.73$, $P=0.89$; post-hoc Tukey test). The evaluation of the dynamic transitions between

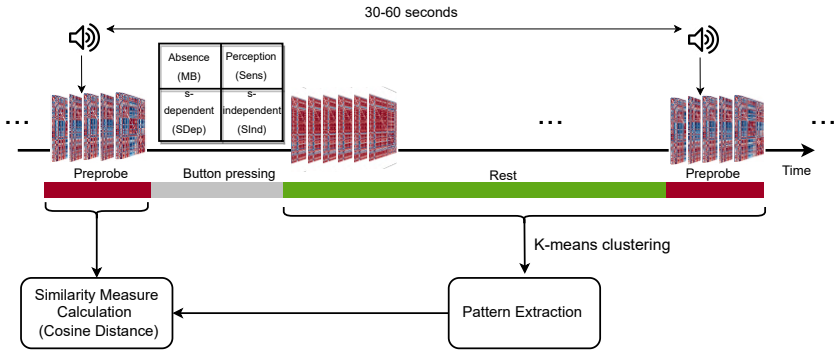

Figure 2.1 Data acquisition and analysis paradigm. While at rest, participants were randomly interrupted by an auditory probe to report their immediate mental state choosing between absence (MB), Sens, SDep, and SInd. To estimate which brain configuration corresponded to a reported mental state, connectivity matrices were estimated via phase-based coherence for each fMRI volume. The matrices were then organized in distinct patterns via k-means clustering, and the similarity between these patterns and the matrices relating to the reported mental states of the preprobe period was calculated. The pattern with the highest similarity to the preprobe matrices was assigned to that reported mental state.

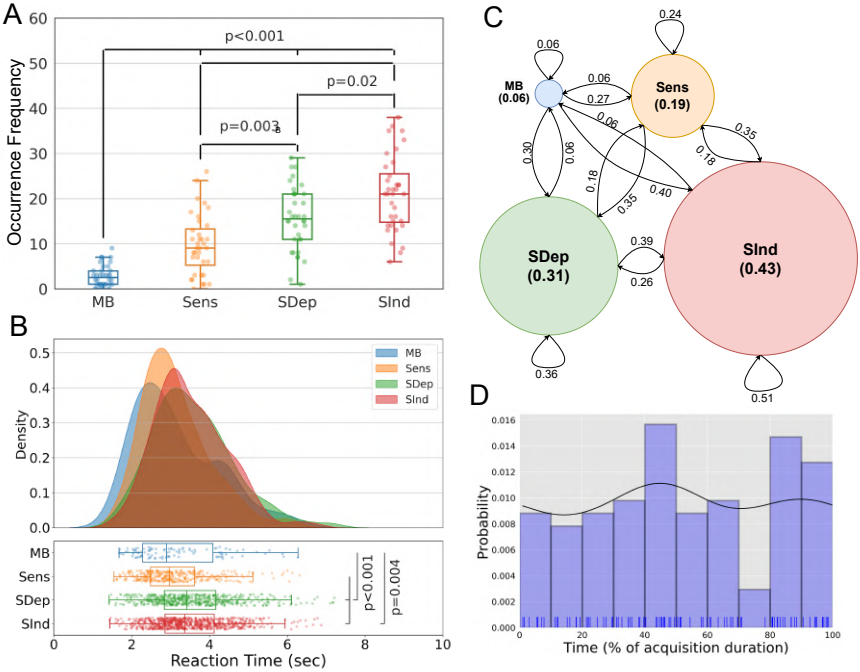

Figure 2.2 Mind Blanking (MB) is characterized by a distinct behavioral profile. (A) MB shows significantly low reportability by comparison to the other mental states, replicating past findings (FDR p<0.05). **(B)** MB is reported significantly faster than SDep and SInd mental states, possibly reflecting shorter cognitive evaluation due to the "absent content" as opposed to the thought-related reports. **(C)** The Markov model shows that the probability of reporting an MB state after exploring other mental states is low but equal (6%), suggesting that MB might serve as a transient mental relay during spontaneous mentation. **(D)** Uniform distribution of MB reports across the acquisition time shows that this phenomenon is not driven by tiredness or drowsiness. Sens: sensory perception of stimuli; SDep: stimulus-dependent thoughts; SInd: stimulus-independent thoughts.

different mental states showed exceptionally low but equal probabilities (0.06) for reporting MB when departing from a content-oriented state (Figure 2.2C). Also, the probability of rereporting MB was particularly low (0.04). Finally, the hypothesis of a uniform distribution of reports across the session could not be rejected for MB ($\chi2[9]=12.31$, $p=0.20$, $\phi=0.35$; Figure 2.2D), SDep ($\chi2[9]=5.25$, $p=0.81$, $\phi=0.10$), or SInd ($\chi2[9]=4.22$, $p=0.90$, $\phi=0.07$). Sens reports, though, were not uniformly distributed over time ($\chi2[9]=18.15$, $p=0.03$, $\phi=0.23$; Appendix D, Fig. D1).

Neural Characteristics

MB is associated with a distinct physiological state. To estimate MB's functional connectome, we first sought to delineate the contribution of the global signal (GS). This was because the GS has been previously shown to contain neural sources (Li, Kong, et al., 2019; Murphy & Fox, 2017; Schölvinck et al., 2010) and thus can be of functional significance. The spatially averaged time series were extracted from the regions of interest (ROIs), and their amplitude was estimated for five volumes (10.2 s) per probe, that is, two volumes preceding the probe and three after it (Figure 2.1) to account for the blood oxygen level–dependent (BOLD) hemodynamic response (see Methods Box 1), and their mean absolute value was calculated. By using this 10-s analysis window, we found a significant effect of mental state on the GS amplitude ($\chi 2[3]=12.474$, $p=0.006$; generalized linear mixed model), with higher amplitude relating to the volumes surrounding MB reports as compared to those linked to SDep ($z=3.3$, $p=0.005$) and SInd reports ($z=2.55$, $p=0.05$; post-hoc Tukey test; Figure 2.3). Similar results were obtained when the analysis window lagged between zero frames (i.e., five scans preprobe) up to three volumes (i.e., two preprobe and three postprobe scans; Appendix D, Fig. D2). As the GS contributes deferentially to the reportability of mental states, we decided to include it in the connectivity analyses. For comprehensive purposes, all analyses were performed without the GS as well. To

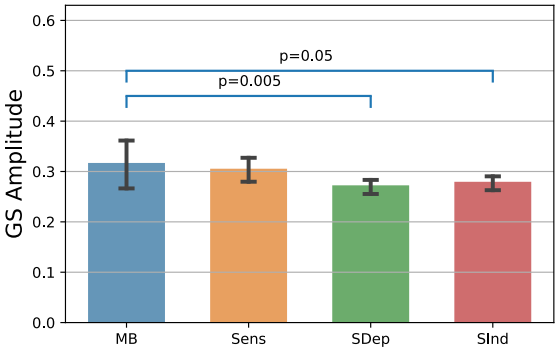

Figure 2.3 Volumes labeled as mind blanking (MB) are characterized by high global signal (GS) amplitude. The average value of the GS shows that the GS amplitude is significantly higher for volumes reported as MB compared to the GS amplitude observed in volumes reporting content-oriented states, pointing to a distinct physiological substrate supporting MB reportability. Bars show the mean absolute value, and error bars show 95% confidence intervals. Sens: sensory perception of stimuli; SDep: stimulus-dependent thoughts; SInd: stimulus- independent thoughts.

investigate the potential effect of the level of arousal on MB reportability, we also calculated the correlation between the GS amplitude and the reaction times of all MB reports. No significant correlation was found (Spearman's ρ=0.03, p=0.76; Appendix D, Fig. D2).

MB is accurately classified by means of phase-based coherence matrices. To check whether MB has a distinct neural profile, we first tested whether it can be classified among other mental states by using the functional connectome. Using the Hilbert transform, we estimated framewise phase-based coherence matrices for the above-mentioned period of five volumes (lag=3). Considering these connectivity matrices as feature vectors (five vectors per probe), a support vector machine (SVM) classifier with fivefold cross-validation and 10 repeats classified MB reports from all mental states with an average precision of 1, average recall of 0.81, and average balanced accuracy of 0.90. In addition, a one-versus-one strategy to classify MB from the other reports separately led to high classification performance (Table 2.1). To compare the results with the empirical chance level, a dummy classifier was further used to separate MB-labeled matrices from the matrices corresponding to the other mental states. This dummy classifier generated random predictions by respecting the training set class distribution (Table 2.1). This classification strategy also showed comparable performance for other analysis window lag values (Appendix D, Tables D1–D4). Collectively, by comparing all the performance metrics of the MB classification by using an SVM and the dummy classifier, we found that the SVM successfully separated the functional connectomes of MB reports from those belonging to the other mental states.

Table 2.1 Performance of SVM classifier when predicting MB reports based on phase coherence matrices (lag = 3)

	Balanced Accuracy	Recall	Precision
MB VS. SENS	0.97	0.95	0.99
MB VS. SDEP	0.96	0.92	1
MB VS. SIND	0.94	0.88	1
MB VS. OTHERS	0.90	0.81	1
MB VS. OTHERS (DUMMY)	0.50	0.05	0.06

Functional connectivity organizes into distinct recurrent patterns. Under the hypothesis that the MB's neural signature is contained in connectivity dynamics, we investigated how the framewise functional connectome organizes into distinct connectivity patterns. By concatenating all the estimated connectivity matrices across subjects and by applying k-means clustering, we determined four main functional brain patterns that appeared recurrently across the resting state periods, replicating previous results (Demertzi et al., 2019) despite different acquisition parameters and parcellation schemes. The patterns were characterized by distinct signal configurations: a pattern of complex interareal interactions, containing positive and negative phase coherence values between long-range and short-range regions (pattern 1), a pattern showing anticorrelations primarily between the visual network and the other networks (pattern 2), a pattern with overall positive interareal phase coherence (pattern 3), and a pattern of overall low interareal coherence (pattern 4; Figure 2.4A). In terms of occurrences, pattern 4 appeared at a significantly higher rate than pattern 1 ($t[35]=7.131$, $p<0.001$, Cohen's $d=1.18$), pattern 2 ($t[35]=7.495$, $p<0.001$, Cohen's $d=1.25$), and pattern 3 ($t[35]=5.857$, $p<0.001$, Cohen's $d=0.98$, p values false discovery rate (FDR) corrected at $\alpha=0.05$; Figure 2.4A). Importantly, these patterns also emerged when we used different cluster sizes (ranging from 3 to 7) and different analysis window lags (ranging from zero up to three frames; Appendix D, Figs. D3–D6).

Neurobehavioral Characteristics

To determine which brain pattern was the closest to the MB reports, we used the cosine distance as the similarity measure between five connectivity matrices of each analysis window and the four resting brain patterns (Figure 2.1). Using a generalized linear mixed model fit to the distance measures of each brain pattern separately, we found a significant effect of mental state for distance values to pattern 3 ($\chi2[3]=19.088$, $p=0.0002$). Pattern 3 further showed higher similarity to MB compared to the reports of Sens (estimate=0.114, low CI=0.027, high CI=0.202, $p=0.004$), SDep thoughts (estimate=0.137, low CI=0.053, high CI=0.221, $p=0.0002$), and SInd thoughts (estimate= 0.132, low CI=0.050, high CI=0.213, $p=0.0002$; post-hoc Tukey tests; Figure 2.4B). These results were also replicated with different analysis window lags (Appendix D, Figs. D16–D19). For comprehensive purposes, we performed a supplementary analysis of the neurobehavioral coupling by omitting the GS through subtraction or regression. Global signal subtraction (GSS) refers to withdrawing the GS from the ROI preprocessed time series, while global signal regression (GSR) concerns removing the GS from the preprocessed ROI time series via linear regression. After GSS and

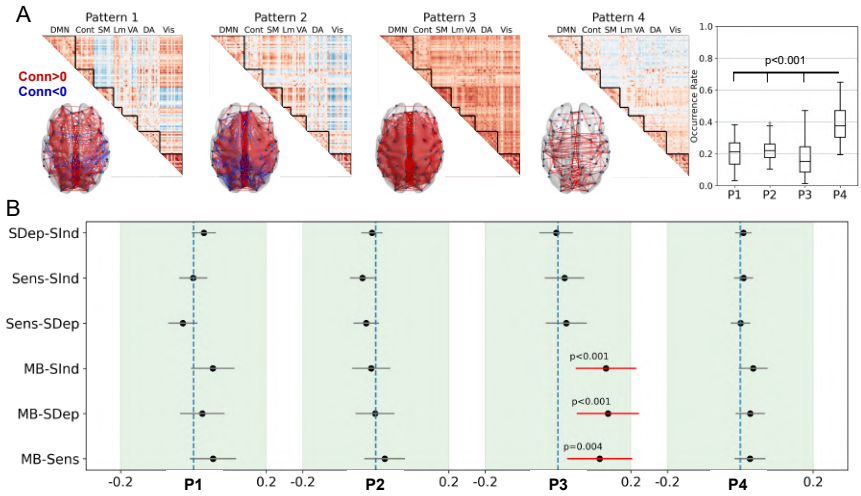

Figure 2.4 MB is associated with an overall positive interregional brain connectivity pattern. (A) Brain functional organization during rest can be summarized into four main connectivity patterns of complex cortical interactions (pattern 1 [P1]) visual network anticorrelations (pattern 2 [p2]), globally positive coherence (pattern 3 [p3]), and low inerareal connectivity (pattern 4 [p4]). There were similar occurrences rates across patterns, except for p4, which potentially reflects the underlying anatomy and therefore acts as a foundation upon which the others can occur. **(B)** The globally positive phase coherence P3 shows the highest similarity (positive contrast value of cosine similarity) to the connectivity matrices related to the MB reports compared to the other mental states. Black dots show the difference between similarity measures to the related connectivity pattern for each pair of mental states; error bars indicate 95% confidence intervals; vertical blue lines indicate the zero differences. Conn: connectivity (phase-based coherence); DMN: default mode network; Cont: executive control network; DA: dorsal attentional network; VA: ventral attentional network; Lm: limbic network; Vis: visual network; SM: somatomotor network.

GSR were applied, all brain patterns were reproduced except for pattern 3 (Appendix D, Fig. D15A), whose architecture shifted toward negative coherence values. The same observation was noticed on the clustering results with different cluster sizes (Appendix D, Figs. D7–D14). The overall effect of GSS and GSR on the connectivity patterns was the shift of connectivity value distributions toward negative values thus enhancing anticorrelations (J. S. Anderson et al., 2011; Leonardi et al., 2013; Murphy et al., 2009), also previously reported (Xu et al., 2018; Appendix D, Fig. D15B). In addition, inter-pattern correlation analysis showed that pattern 3 had the lowest similarity to itself after GSS and GSR (ρ=0.59; Appendix D, Fig. D15C). Considering a $p<0.05/4=0.0125$ threshold to correct for multiple tests, no significant effect of mental states on the similarity measures were found for any pattern, neither for GSS (pattern 1, p=0.931;

pattern 2, p=0.116; pattern 3, p=0.294; pattern 4, p=0.573), nor for GSR (pattern 1, p=0.109; pattern 2, p=0.022; pattern 3, p=0.276; pattern 4, p=0.093); Appendix D, Figs. D20 and D27). These results suggest that the GS carries partially independent neural information and contributes to the cerebral profile of MB reportability.

2.2.2 Discussion

We used experience sampling paired with fMRI to determine the neurobehavioral profile of MB in typical individuals to delineate its neurobehavioral profile in a comprehensive way. Collectively, our results show that MB is a unique mental state supported by a distinct neural state that contributes meaningfully to spontaneous mental activity. Behaviorally, we found that individuals report MB occurrences less frequently and faster than other mental states. This finding is in line with previous studies showing that MB gets reported significantly less often than thought-related states (Schooler et al., 2004; Ward & Wegner, 2013), although the opposite effect was also reported (Kawagoe et al., 2019). These discrepancies might be attributed to the study protocol, where in the latter study participants were encouraged to stay engaged in thinking about nothing (Kawagoe et al., 2019). This implies that MB might be a flexible and trainable mental state that, once introduced as an option, can be informative of one's ongoing mental experience. Our results also align with studies reporting similarly short MB reaction times while participants are involved in sustained attention to response tasks (Stawarczyk et al., 2020; Stawarczyk & D'Argembeau, 2016). Other investigations, however, show that MB is reported slower when compared to other mental states, which was interpreted as MB facilitating sluggishness in responses (Andrillon et al., 2021) or as the result of decreases in alertness and arousal during task performance (Unsworth & Robison, 2016). Here, we consider that the short reaction times for MB and the longer reaction times for thought-related mental states (Sdep, Sind) might be attributed to an additional cognitive evaluation of the latter. In other words, when thoughts are occupied by specific content, this is translated into longer cognitive evaluation as to the particularities of this content.

This stance implies that MB can be a mental state that is "content-free," and as such it is reported faster. This interpretation is supported by previous investigations using self-paced focused reading with self-catches of MB and mind wandering (Ward & Wegner, 2013). Although this is a tempting consideration, we recognize that the content-free nature of MB reports could not be directly addressed here. In attempting to uncover the mechanisms of MB, past work

shows that attention can act as a mediating process that drives content reportability (Pitts et al., 2018), so that participants do entertain content-full thoughts but fail to attend to them, therefore leading to attentional lapses (Stawarczyk et al., 2020; Unsworth & Robison, 2016; Van den Driessche et al., 2017). At the same time, it can be that MB is a matter of participants' metacognitive capacities, in that MB is more about a "cognitive evaluation free" or "meta-awareness free" mental state rather than lack of mental content. Equally, MB might be deprived of any experience altogether, reflecting a "transition mode" between modifications of experience (content) as we move from one state to the other. This last scenario fits with our results of the low probabilities to report MB when previously in another mental state. In that case, departures from MB are more likely to lead toward thought-related reports and less likely to return to MB. However, these findings should be considered within the temporal constraints of the experience sampling paradigm, namely, one cannot assume that this dynamic sequencing reflects actual mental state transitions because the temporal structure between the reports is not continuous. Consequently, other mental states might have appeared between reports. Despite this limitation, the finding that the equally small probabilities to report MB when previously in another state and vice versa indicates that MB might not be driven by any specific mental content, therefore serving as a transient mental relay (Fornito et al., 2012). This means that thoughts with reportable content can lead toward more mental contents due to semantic associations, hence creating the perception of a stream of consciousness (Christoff et al., 2016). Since MB is not semantically associated with any particular mental content, it may therefore occur scarcely during ongoing experience. Therefore, phenomenologically "empty" mental states might have less of an anchoring effect than content-full states. Finally, our finding of a uniform distribution of MB reports over time, also reported elsewhere (Ward & Wegner, 2013; Watts et al., 1988), further suggests that MB happens spontaneously across time and is not an artifact of fatigue or sleepiness, which would lead to more occurrences at the end of the recordings. Additionally, in the absence of direct physiological measures of arousal, such as electroencephalography or pupillometry markers, the BOLD GS amplitude can be considered as a proxy of arousal and also sleepiness (Fukunaga et al., 2006; Nilsonne et al., 2017). Although other studies relate sleepiness to an inflated number of MB reports and reduced reaction times (Stawarczyk et al., 2020; Stawarczyk & D'Argembeau, 2016), the lack of significant correlation between GS amplitude and reaction times shows that sleepiness is not a confounding factor of MB reportability in our dataset. Taken together, the behavioral results indicate that MB is a distinct

mental state with a unique position among thought-related reports. In order to shed light on the refined mechanisms underlying MB reportability we suggest that future work address MB in terms of content, attention, and metacognitive capacities.

In terms of MB's neural underpinnings, we first found that the amplitude of the GS was preferentially higher for scanning volumes associated to the MB reports. In addition, the supplementary analysis of the neurobehavioral coupling without the GS confirmed that the GS contributes meaningfully to the MB state as it dramatically changes the overall interregional positive coherence of pattern 3 after its removal. At the moment, we can only speculate about what the high GS amplitude might mean for MB reportability. In terms of physiological relevance, spontaneous GS amplitude was previously found to correlate negatively with electroencephalographic (EEG) vigilance (alpha, beta oscillations), while increases in EEG vigilance due to caffeine ingestion were associated with reduced GS amplitude (Wong et al., 2013). In macaques, electrocorticography showed that widespread transient and synchronous cortical activity was linked to low arousal in a series of sequential spectral transitions (i.e., from decreases in midfrequency activity, accompanied by increases in the gamma band, to be followed by increases in delta band; Liu et al., 2015). When these transient electrophysiological events in animals were linked to fMRI motifs in humans, there was a close association between the GS and these transitions, which corroborated the origins of arousal (Liu et al., 2018). These results, jointly with the elevated GS amplitude during MB described herein, show the possibility of neuronal silencing during wakefulness.

The scenario of neuronal silencing is further supported by the analysis of neurobehavioral coupling. With this analysis we first showed four distinct brain functional connectivity patterns, which recur dynamically during the resting periods of the experience-sampling task. These brain patterns bear great resemblance to what we previously reported as recurrent brain configurations during pure resting state fMRI acquisitions across healthy individuals and brain-injured patients (Demertzi et al., 2019). The fact that these patterns appear across independent datasets, and also in nonhuman primates (Barttfeld et al., 2015), under different paradigms, different brain parcellations, and different cluster sizes, points to their universality and robustness. Specifically, to MB, the pattern with the all-to-all positive interareal connectivity (pattern 3) had the highest similarity to the connectivity matrices preceding MB reports. Such high prevalence of comparable signal configurations was previously shown during non–rapid eye movement slow-wave sleep, wherein overall minimal neuronal

firing was translated as globally positive connectivity (Aedo-Jury et al., 2020; El-Baba et al., 2019). Studies in rats (Vyazovskiy et al., 2011) show that such periods of neuronal silencing can happen also during wakefulness in the form of neuronal firing rate reduction, leading to slow wave activity, which is indicative of local sleeps. When applied to humans, it has been argued that these instances of local sleeps can be the phenomenological counterpart of MB (Andrillon et al., 2021). In that respect, wakefulness does not only support constantly on periods of neuronal function. Rather, our brains can also show instances of neural down states even during wakefulness, possibly for homeostatic reasons (Bridi et al., 2020), which can be translated as global positive connectivity and phenomenologically interpreted as MB.

From a theoretical perspective, it seems that MB further challenges the boundaries of various models of conscious experience. For example, the global neuronal workspace theory (Dehaene et al., 2006) posits that a stimulus becomes reportable when some of its locally processed information becomes available to a wide range of brain regions, forming a balanced distributed network (Sergent & Dehaene, 2004). A key process of this global broadcasting is ignition (Dehaene et al., 2003). Ignition is characterized by the sudden, coherent, and exclusive activation of a subset of workspace neurons that code a particular content, while the remainder of the workspace neurons stay inhibited. If the global neuronal workspace ignition is always related to selective neural activation and inhibition (content), the theory cannot account for how MB can still be reported if it is linked to a functional connectome with only positive connections. This is similar for the integrated information theory (IIT) (Tononi, 2008). According to IIT, in order to generate an experience, a physical system must be able to discriminate between a large repertoire of states (i.e., information). This must be done as a single system that cannot be decomposed into a collection of causally independent parts (i.e., integration). So far, IIT can explain the inability to report mental content in brain states with extreme functional integration (i.e., functional hyperconnectivity), as during generalized epilepsy (Blumenfeld, 2012). In such a brain state, an abnormally large number of regions work in synchrony, and, as a result, the brain becomes no longer capable of processing information in a way that leads to conscious experience. The here-identified all-to-all positive connectivity pattern shows the highest level of integration and efficiency and the lowest level of segregation and modularity compared to the other brain patterns (Demertzi et al., 2019). Therefore, this may imply that such a neural configuration is unable to produce a balance between values of integrated information and its segregation, leading to limited experience, such as MB. If the role of integration

is emphasized over the role of segregation, as in the recent version of IIT, then MB challenges that approach, making a clear case for the importance of information segregation within neural configurations of conscious content. Importantly, though, the integration in IIT happens only when there is a content of experience, being reported or not, which is counterintuitive for MB. Both theories essentially start from the premise that experience is made up of various bits from which a unified experience arises. As MB does not provide such building blocks, it seems to be a kind of global state of unified experience, with conscious content being the modifications of such a basal conscious field, according to Searle's unified field model (Searle, 2000). If this interpretation is considered, then the current findings pose an important challenge to building block models of conscious experience.

Our analysis leaves several questions unaddressed. First, the current design does not permit us to determine the underlying mechanism that drives MB (i.e., whether it is an effect of attention, memory, or language). Such determination is expected to shed light on MB's modulatory mechanisms as well; and therefore, further indicate its functional significance in variant conditions. Second, apart from the intrinsic problems with the validity and reliability of self-reports during experience sampling (Nisbett & Wilson, 1977), we also used a probe-catching method. This means that participants were interrupted during spontaneous thinking by a probe, asking them to choose an appropriate option to describe their thought state. Such a probe-framing technique can restrict the estimation of potential phenomenological switches happening in between. Indeed, as the probes were appearing at predetermined time points, we cannot exclude the possibility of mental contents happening during the inter-probe intervals, and hence they were missed and could not be reported. Also, probe framing can be suboptimal in capturing spontaneous thinking because it might lead to an inflated number of MB reports. This is because participants may have chosen this category due to the fact that it was available, which, otherwise, they would not have reported if they were to identify it spontaneously (Weinstein et al., 2018). However, given that MB occurrences were not reported with a comparable high frequency to the content-oriented states, it might be that MB was evaluated in a representative way across the evaluation, leading to infrequent occurrences across participants. Third, the high repetition time (TR) during the fMRI acquisition (2.04 s) could also have echoed the temporal implications of the MB profiling. By means of simultaneous EEG and fMRI recordings, more light is expected to be shed on fine-grained temporal dynamics of MB. Such simultaneous multimodal recordings are expected to also illuminate the

assumption of slow-wave activity as the corresponding neural mechanism of MB. Finally, we cannot exclude the possibility that the mind is not absent in the first place, under the premise that if it were, participants would not have been able to report anything, including its absence. The term “mind blanking”, thus, may reflect different aspects (e.g., truly absence of the mind vs. absence of conscious access to mental events) that still need to be disentangled.

In conclusion, our study suggests that MB can be considered a default mental state occupying a unique position among thought-related reports. Its rigid neurofunctional profile could account for the inability to report mental content due to the brain’s inability to differentiate signals in an informative way. While we wait for the underlying mechanisms of MB to be illuminated, these data suggest that instantaneous nonreportable mental events can happen during wakefulness, setting MB as a prominent mental state during ongoing experience.

2.3 Resting Brain and Mind under Psychedelics

Psychedelics are a class of psychoactive drugs that have been used historically as a means to alter conscious experience (Mason et al., 2020; Metzner, 1998). Lysergic acid diethylamide (LSD), ayahuasca, psilocybin, N-dimethyltryptamine (DMT), and mescaline are some examples of these drugs. Among them, psilocybin, an ingredient in the so-called "magic mushrooms", is a well-known drug in psychedelic research because of its prolonged effects, rapid onset, and good absorption after administration (Griffiths et al., 2011, 2018; Hasler et al., 2004; Madsen et al., 2021; Tylš et al., 2014). While psilocybin has been used for centuries in healing ceremonies via mushroom ingestion, recently it has been considered as a potential therapeutic substance to treat different psychological disorders such as obsessive-compulsive disorder (Moreno, 2006), anxiety related to dying (Grob et al., 2011), depression (Andersen et al., 2021; Carhart-Harris et al., 2012, 2021; Ross et al., 2016), treatment-resistant depression (Carhart-Harris et al., 2016, 2017, 2018), major depressive disorder (Davis et al., 2021), terminal cancer-associated anxiety (Griffiths et al., 2016; Ross et al., 2016), demoralization (Anderson et al., 2020), smoking (Johnson et al., 2017), and alcohol and tobacco addiction (Bogenschutz et al., 2015; Garcia-Romeu et al., 2019; Johnson et al., 2014). Considering these therapeutic applications of psilocybin, as well as its consciousness altering capability in a profound way, it is important to study the way it affects the brain leading to such unique experiences (Tagliazucchi et al., 2014).

Psilocybin's underlying mechanism of action is to stimulate serotonin (5-HT2A) receptors located on cortical pyramidal neurons (Nichols, 2016; Vollenweider & Kometer, 2010) which eventually leads to release of **glutamate** (N. L. Mason et al., 2020; Vollenweider & Kometer, 2010). This mechanism leads to hallucinogenic effects and alters subjective conscious experience. In the acute phase, subjective experiences can be explained by **ego dissolution**, i.e., the reduction in self-referential awareness, ultimately disrupting self-world boundaries and increasing feelings of unity with others' and one's surroundings (Nour & Carhart-Harris, 2017; Studerus et al., 2010), unconstrained consciousness, i.e., hyper-association and profound alterations in the perception of time, space and selfhood (Carhart-Harris et al., 2014; Griffiths et al., 2006; Tagliazucchi et al., 2014), perceptual alterations, synesthesia, experiences of unity, profound changes in affect (Preller & Vollenweider, 2018), and transient elevations in mood (Majić et al., 2015). Other studies also reported long-term and lasting effects of psilocybin administration on personality and mood change, such as increases in the personality traits of openness and extraversion,

decreases in neuroticism and increases in mindful awareness (Erritzoe et al., 2018; MacLean et al., 2011; Madsen et al., 2020).

In terms of neural effects, functional neuroimaging studies have shown that the administration of psilocybin can result in decreased activity in the thalamus, posterior cingulate cortex (PCC), and medial prefrontal cortex (mPFC; Carhart-Harris et al., 2012), decreased connectivity within the DMN (Carhart-Harris et al., 2012; N. L. Mason et al., 2020) and ECN (McCulloch et al., 2022), increased global connectivity with reduced modularity (Preller et al., 2020; Roseman et al., 2014), altered connectivity of the claustrum (Barrett et al., 2020), decreased segregation of DAN and ECN (Madsen et al., 2021), and increased whole-brain network fractional dimension (Varley et al., 2020). These neural counterparts indicate that the subjective effects of psilocybin can be due to alterations in the activity and connectivity of important brain regions involved in information integration and routing. In order to better understand brain-mind interactions in this condition, one can further explore the brain's dynamic behavior during a psychedelic state.

Dynamic analyses of connectivity patterns after psilocybin administration have shown that the brain tends to visit more transient functional states with low stability and a smaller number of persistent ones (Petri et al., 2014). In addition, in this state the brain has the highest transition probability to a **phase-locking state** characterized by a global cortex-wide positive phase coherence (Lord et al., 2019). All these findings show that psilocybin affects the brain to make a more integrated and less modular system. However, a question that still needs to be answered is how these functional connectivity states and the alterations in their transitional dynamics are related to the unique experience individuals have during the psychedelic state.

In this section, we aim to explore the effects of a single dose of psilocybin on the brain's functional dynamics and to investigate how changes in the brain are associated with the subjective experience under psychedelics.

2.3.1 Effects of Psilocybin on the Brain and Mind

Dataset

We used previously acquired data (Mason et al., 2020) collected from 49 healthy participants with previous experience with a psychedelic drug but not within the past 3 months. Participants were randomized to receive a single dose of psilocybin (0.17 mg/kg, n=22 (12 men), age=23±2.9 y) or placebo (n=27 (15 men), age=23.1±3.8 y). Six minutes of resting state fMRI (ultra-high field, 7T)

were acquired from the participants with eyes open during peak subjective drug effect (102 minutes post treatment). In addition, the 5 Dimensions of Altered States of Consciousness (5D-ASC) scale (Dittrich, 1998) and the Ego Dissolution Inventory (EDI) (Nour et al., 2016) were evaluated 360 minutes after drug administration, as retrospective measures of drug effects.

Behavioral Counterparts

The 5D-ASC is a 94-item self-report scale that assesses the participants' alterations from normal waking consciousness (Studerus et al., 2010). In this questionnaire the participant is asked to make a vertical mark on the 10-cm line below each statement to rate to what extent the statements applied to their experience in retrospect from "No, not more than usually" to "Yes, more than usually." The 5D-ASC contains the 5 key dimensions, including ***auditory alterations*** (AA), ***anxious ego dissolution*** (AED), ***oceanic boundlessness*** (OB), *reduction of vigilance* (RV), ***visual restructuralization*** (VR), and which can be broken down into 11 subscales consisting of ***experience of unity***, ***spiritual experience***, ***blissful state***, ***insightfulness***, ***disembodiment***, *impaired control and cognition*, *anxiety*, ***complex imagery***, ***elementary imagery***, ***audio-visual synesthesia***, and ***changed meaning of percepts***.

The EDI is an eight-item self-report scale that assesses the participant's experience of ego dissolution (Nour et al., 2016). Sample items for the scale includes the following: "I experienced a dissolution of my self or ego" and "I felt at one with the universe." The participants answered the scale with endpoints of either 0 = "No, not more than usually" or 100 = "Yes I experience this completely/entirely." The EDI is scored by calculating the mean of all the 8 items (range 0–100). The higher the total score, the stronger the experience of ego dissolution. Administration of psilocybin was associated with significantly increased ratings on all (sub)dimensions of the 5D-ASC (AA: $U=529.5$, $p\leq0.001$, $d=0.78$; AED: $U=555.5$, $p<0.001$, $d=0.87$, OB: $U=583$, $p<0.001$, $d=0.96$; RV: $U=452$, $p=0.002$, $d=0.52$; VR: $U=589$, $p<0.001$, $d=0.98$; EDI: $U=487$, $p<0.001$, $d=0.64$; Figure 2.5).

Neural Counterparts

Whole-brain static connectivity increases after psilocybin administration. After applying the Schaefer atlas with 100 ROIs on the brain and calculating the average BOLD time series for each ROI, we used the Pearson correlation to measure the statistical dependency of BOLD time series between each pair of ROIs. This led to a 100×100 functional connectivity matrix for each participant

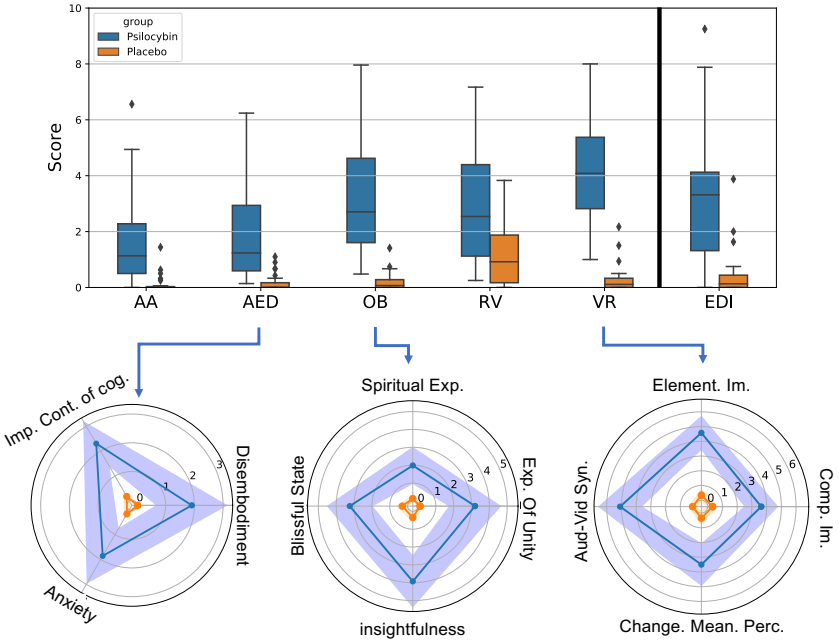

Figure 2.5 Substantial changes in subjective experience after psilocybin administration. Assessing five dimensions of altered states of consciousness (5D-ASC) and all its sub-scales, together with the ego dissolution inventory (EDI) score shows that administration of psilocybin significantly alters the subjective experience. AA: Auditory Alterations, AED: Anxious Ego Dissolution, OB: Oceanic Boundlessness, RV: Reduction of Vigilance, VR: Visual Restructuralization, Imp. Cont. of Cog.: Impaired Control and Cognition, Exp.: Experience, Aud-Vid Syn.: Audio-Visual Synesthesia, Element. Im.: Elementary Imagery, Comp. Im.: Complex Imagery.

which were averaged over the participants of each group (Figure 2.6A). After administration of psilocybin, the overall connectivity measure of the brain (i.e., average of the connectivity matrix for each participant) increased significantly (independent t-test: t=3.087, p=0.003; Figure 2.6B). An intra-network connectivity analysis showed that this increase was more dominant between the regions of the dorsal attentional network for the psilocybin group (independent t-test: t=2.620, p=0.042, FDR corrected; Figure 2.6C). An inter-network connectivity analysis also showed that the average connectivity between dorsal attentional network regions and all the other networks regions increased significantly in the psilocybin group (independent t-test; results are shown in Figure 2.6D and Table 2.2).

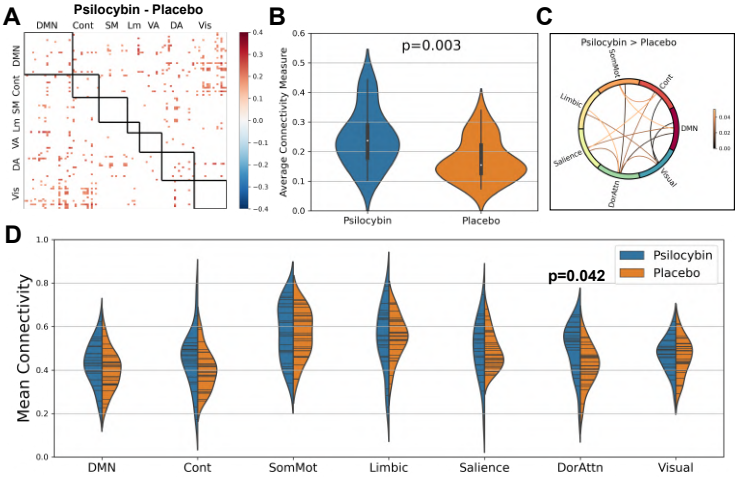

Figure 2.6 Overall increases in averaged connectivity after psilocybin administration. (A) Averaged connectivity matrix of the psilocybin group shows higher connectivity values between the brain regions compared to the placebo group. **(B)** This can also be seen statistically in the overall connectivity of the brain which significantly increases after psilocybin administration. **(C)** Between-network connectivity analysis shows that the connectivity measure between dorsal attentional network regions and all the other networks regions also increases significantly in the psilocybin group. **(D)** Further, within-network connectivity analysis shows that this increase in the connectivity values is more significant between the regions of the dorsal attentional network.

Brain activity tends to self-organize into a hyper-connectivity state after psilocybin administration. To investigate the effect of psilocybin administration on the dynamic changes of the whole-brain functional connectome at rest, we estimated the phase-coherence connectivity matrices at each time point of the extracted BOLD signals. After concatenating all the connectivity matrices of all the participants, we applied K-means clustering to summarize them into four recurrent connectivity patterns (Figure 2.7A). Using this method, we showed that the brain's resting functional connectome was organized into four distinct profiles of complex inter-network interactions, including both correlations and anti-correlations (Pattern 1), anti-correlation of DMN with other networks (Pattern 2), a global cortex-wide positive connectivity (Pattern 3), and a low inter-areal connectivity pattern (Pattern 4). An analysis of the occurrence rate of these patterns over the acquisition time showed that Pattern 3 was appearing significantly more often in the psilocybin group when compared to the placebo group (independent t-test: t=3.731, p=0.001, $\alpha_{\text{bonferroni}} = 0.05/4 = 0.0125$, Figure 2.7B). Furthermore, using Markov modeling and considering each one of the four

Table 2.2 Inter-network comparison of connectivity values between Psilocybin and Placebo groups (Psilocybin > Placebo).

connection	t	p	p(FDR)	connection	t	p	p(FDR)
Cont-DorAttn	2.57	0.007	**0.027**	DorAttn-Limbic	1.00	0.026	**0.045**
Cont-Limbic	0.93	0.180	0.189	DorAttn-Salience	2.48	0.008	**0.027**
Cont-Salience	1.97	0.028	**0.045**	DorAttn-SomMot	3.01	0.002	**0.011**
Cont-SomMot	2.19	0.017	**0.035**	DorAttn-Visual	2.32	0.012	**0.029**
Cont-Visual	3.81	<0.001	**0.002**	Limbic-Salience	1.52	0.067	0.083
Cont-DMN	1.79	0.040	0.059	Limbic-SomMot	0.99	0.163	0.180
DMN-DorAttn	3.17	0.001	**0.009**	Limbic-Visual	2.46	0.009	**0.027**
DMN-Limbic	0.16	0.436	0.436	Salience-SomMot	1.61	0.057	0.075
DMN-Salience	2.40	0.010	**0.027**	Salience-Visual	1.74	0.044	0.061
DMN-SomMot	2.03	0.024	**0.045**	SomMot-Visual	1.49	0.072	0.084
DMN-Visual	3.83	<0.001	**0.002**				

Cont: control executive network, DorAttn: dorsal attentional network, SomMot: somatomotor network, DMN: default mode network.

patterns as model states, we estimated the transition probability of each state to the others. The psilocybin group showed significantly higher transition probabilities towards Pattern 3 from Pattern 1 (Wilcoxon Rank-Sum test: z=2.744, p=0.006), Pattern 3 (z=2.291, p=0.022), and Pattern 4 (z=2.000, p=0.045; Figure 2.7C). In addition, the psilocybin group showed lower transition probabilities from Pattern 2 to itself compared to the placebo group (z=-2.452, p=0.014).

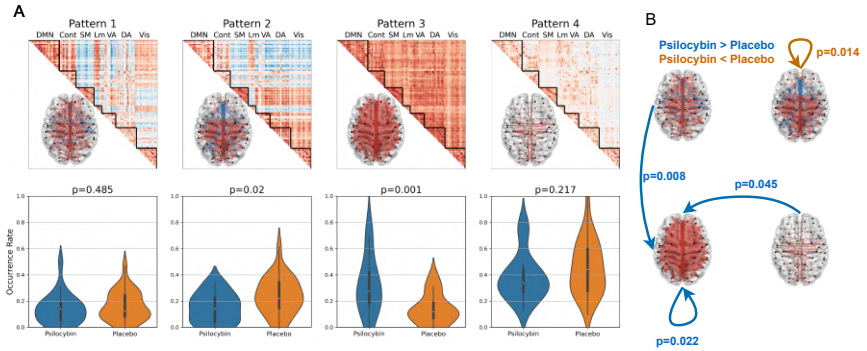

Figure 2.7 Brain tends to be functionally hyper-connected after psilocybin administration. (A) Functional connectome of the brain during resting state can be explained by four different recurrent connectivity patterns from a complex inter-network interaction (pattern 1) to a low inter-areal connectivity profile (pattern 4). **(B)** Occurrence rate analysis shows that after psilocybin administration, occurrence rate of the global cortex-wide positive connectivity (pattern 3) increases significantly. **(C)** Further, the transition probability from other configurations to the pattern 3 increases in the psilocybin group which shows the tendency of the brain to be reconfigured in this manner under psychedelics.

Regional BOLD signal amplitude decreases after psilocybin administration. Calculating the Euclidean norm of the BOLD time series related to each region of interest showed that the BOLD signal amplitude of the brain's posterior and anterior regions decreases significantly after psilocybin administration compared to the placebo group (Independent t-test (Psilocybin > Placebo), FDR-Corrected; Figure 2.8). While somatomotor and limbic networks and temporal regions of default mode network did not show significant change in their signal amplitude, the highest decrease was related to the posterior cingulate cortex and parietal regions of ECN and DMN.

Neurobehavioral Counterparts

To investigate the neurobehavioral counterpart of psilocybin administration, we performed a canonical correlation analysis (Mihalik et al., 2022) between behavioral measures and dynamic state transition probabilities estimated on the recurrent functional connectivity patterns. After estimation of the first canonical vector for both behavioral and neuronal spaces, we observed that the transition probabilities to pattern 3 have the highest correlation with the canonical vector related to the state transition probabilities (Figure 2.9A). On the other hand, considering the first canonical vector of the behavioral scores, OB, EDI, and VR showed the highest correlation with this vector (Figure 2.9B). These observations show that the depersonalization feelings after psychedelic usage comes from the

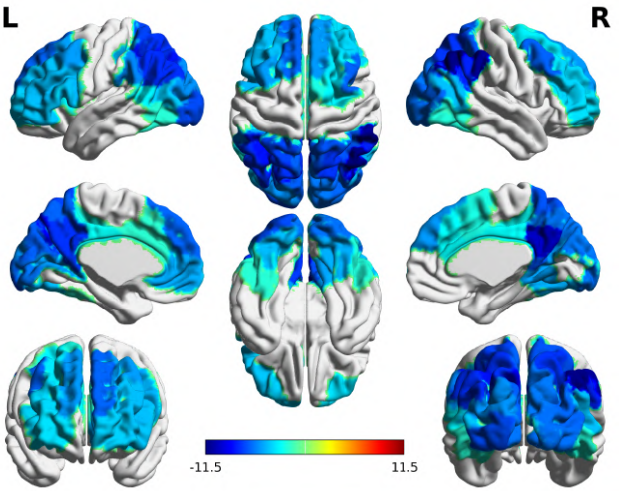

Figure 2.8 Posterior and anterior regional BOLD signal amplitude decreases after psilocybin administration. Difference between the mean value of Euclidean norm of BOLD time series in the psilocybin group and the placebo group at each ROI shows that the BOLD signal amplitude in the posterior and anterior regions decreases after psilocybin administration while this remains unchanged in the somatomotor and limbic networks as well as the temporal regions of DMN.

tendency of the brain to reconfigure itself into a global cortex-wide positive connectivity configuration. Considering the scatter plot showing the relationship between the first canonical vectors of both behavioral and neural spaces, the latent variable which derives the high correlation is group of the subjects (psilocybin vs placebo) which shows the results we observe here are directly due to psilocybin administration (Figure 2.9C). These results were further proved by a multiple-regression analysis. Fitting a linear model to each state transition probabilities, considering group and behavioral measures as factors of the model ($T_{i,j} = Group + AA + AED + OB + RV + VR + EDI$, with subjects as random factors), showed a significant effect of OB scores on the transition probability from pattern 1 to pattern 3 (t=3.160, p=0.003).

2.3.2 Discussion

Recent empirical and theoretical studies show that brain networks function near a critical state, defined as a state at the boundary between order and disorder (Aguilera & Di Paolo, 2021; Lee et al., 2019). At this state, the brain is maximally sensitive to internal and external perturbations (Signorelli et al., 2022). As a result, any externally exerted perturbation can cause significant changes in

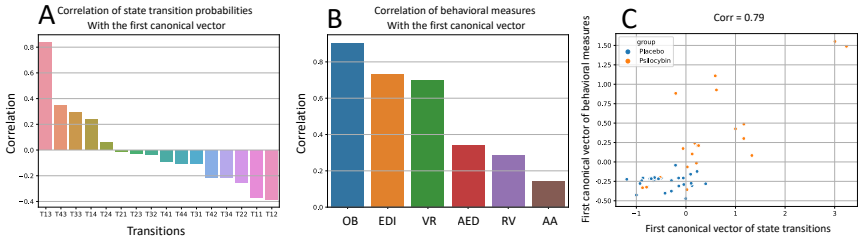

Figure 2.9 Depersonalization scores are associated with tendency of the brain to reconfigure itself with a global cortex-wide positive connectivity pattern. A) Canonical correlation analysis shows that the transition probabilities to the pattern 3 have the highest correlation with the first canonical vector of the state transition probabilities. **B)** In addition, the depersonalization scores such as OB and EDI have the highest correlation with the first canonical vector of the subjective scores. **C)** Showing two canonical vectors in relation with each other in a scatter plot, the separability of the points related to each group of subjects shows that psilocybin administration is the latent variable deriving the association between higher tendency of the brain to be configured as pattern 3 and depersonalization feeling after psychedelics usage.

the brain's functional organization and its dynamics, making external perturbation a useful tool to study the underlying mechanism of action of the brain. Brain activity can be perturbed magnetically (for example using **transcranial magnetic stimulation** (TMS; Siebner et al., 2009)), electrically (for example using **transcranial direct-current stimulation** (tDCS; Tu et al., 2021)), or pharmacologically, such as psychedelic drugs (Jobst et al., 2021). Among them, psychedelics can be an ideal candidate to study brain-mind interactions as they affect both brain dynamics and subjective experience rapidly and have prolonged effects (Madsen et al., 2021). In this study, we investigated the effect of a serotonergic psychedelic, psilocybin, on the brain dynamics and subjective conscious experience to understand how the resulted neural and mental alterations are inter-connected.

We found that psilocybin administration led to observation of the main characteristics of the psychedelic state: increase in feelings of ego dissolution, experience of unity with the surrounding environment, and significant alterations in RSNs (Carhart-Harris et al., 2013). We first observed an overall increase in the whole-brain functional connectivity in the psychedelic group, also reported elsewhere (Preller et al., 2020; Roseman et al., 2014). Previous work has also shown that the serotonergic psychedelics, including psilocybin, change the functional organization of the brain into a new architecture characterized by greater global integration (Petri et al., 2014; Tagliazucchi et al., 2016). More detailed analysis showed that this increase principally comes from the within-

network increased connectivity in DAN and between-network increased connectivity between DAN and other RSNs. The DAN is important in externally oriented attention (Fox et al., 2005) and there are also recent evidence that it gets desegregated after psilocybin administration (Madsen et al., 2021). This hyper-connectivity of DAN with the rest of the brain is aligned with the subjective psychedelic experience, explaining a perceived reduction in the borders between self and the external world (Carhart-Harris et al., 2013).

Dynamic analysis of FC patterns also showed that under psilocybin, the brain tends to spend more time in a globally coherent, highly integrated state. This was also observed in terms of higher transition probabilities from other FC states into this state. This pattern which is characterized by maximal integration and minimal segregation (Demertzi et al., 2019) is functionally non-specific and was also observed in previous psychedelic studies (Lord et al., 2019). Under psilocybin, this highly integrated FC state becomes the dominant attractor of the dynamic repertoire of the brain. This can be explained by the "flattened landscape" theory, stating that main functionally-specific FC states which act as attractors in normal conditions become less dominant under psychedelics (Carhart-Harris & Friston, 2019) and the brain consumes less energy to transit between those states (Singleton et al., 2022). This reduction in functionally-specific states leads to an increased transition probability into the globally coherent pattern which is interpreted as being functionally non-specific (Lord et al., 2019). Additionally, high functional integration in this state may lead to an atypical interregional communication profile (Lord et al., 2019) in which the brain retains the potentiality to entertain multiple contents simultaneously.

Considering the relationship between alterations in the brain dynamics and subjective conscious experience, we found that higher transition probabilities into the globally coherent FC state are predictors of oceanic boundlessness, ego dissolution, and visual restructuralization. OB can basically be explained by positively experienced depersonalization and derealization, deeply-felt positive mood, and experiences of unity (Studerus et al., 2010). In the same manner, ego dissolution has been interpreted as a disruption of ego boundaries, resulting in difficulty of distinction between self and surrounding objects, and precludes the synthesis of self-representations into a coherent whole (Nour et al., 2016). On the other hand, VR principally explains visual (pseudo)-hallucinations, illusions, auditory-visual synesthesia, and changes in the meaning of percepts (Studerus et al., 2010). Considering these definitions, we realize that the tendency of the brain to be in a highly integrated state brought by psychedelic drugs is associated mainly with the feelings of unity with the surrounding environment and

hallucinations. Feelings of unity may reveal the disruptions of the self-environment boundary due to the hyper connection of DAN with other RSNs, and hallucinations could be related to the simultaneous connection between different RSNs which alters the modular architecture of the brain as it tries to make sense of various information coming from different functional networks at the same time.

Another important observation in this study was a cortex-wide decrease of BOLD signal amplitude in the psychedelic state. This reduction was previously reported in two key structural hubs, namely PCC, and mPFC (Carhart-Harris et al., 2012) . We here showed that this amplitude reduction can be wider in the brain which is a proxy of decrease in global signal. GS amplitude has been shown to be an indirect measure of arousal (Fukunaga et al., 2006; Nilsonne et al., 2017). Indeed, previous studies have shown that the GS amplitude is negatively correlated with arousal and reduced GS amplitude is associated with increased vigilance measures of EEG (Wong et al., 2013). In addition, we recently showed that the high GS amplitude during wakeful rest is a proxy of low arousal and mind blanking (Mortaheb et al., 2022). So, together with previous results we can hypothesize that psychedelic state can be realized by high levels of arousal and information integration which leads to the unique subjective experience we have at the peak of drug effect.

This study was also exposed to limitations. First, the psilocybin administration dose was not high enough to induce total ego dissolution. Because of being in the MRI scanner at the peak level of drug effect, the administered dose was chosen in a way that the drug induces subjective experience alterations that can be handled in the scanner. The behavioral analysis results showed that the chosen dose was effective enough to induce both positively and negatively experience of ego dissolution and other subjective experience. However, future studies are needed to explore the effect of higher doses of psilocybin on the brain dynamics. Second, lack of direct physiological data acquisition during fMRI scan limits the preprocessing pipeline to remove the physiological fluctuations from the BOLD signals. In addition, acquiring data with an ultra-high magnetic field scanner (7T) leads to more prominent geometric distortions specially in the inferior regions (Jezzard, 2012). In the preprocessing pipeline, we tried to address this problem by susceptibility distortion correction techniques using 5 extra acquired EPI volumes with the inverted phase encoding direction. Comparable results of this study with other studies which acquired their data with lower field strengths, shows that the preprocessing pipeline was successful in handling such limitations. Finally, duration of the data acquisition was at the edge of having

reliable functional connectivity estimations (Birn et al., 2013). In fact, 6 minutes of acquisition is the minimum required time to have reliable connectivity estimates in the perspective of test-retest reliability. However, the repetition time of the acquisition sequence was short enough (TR=1.4 sec) to have acceptable time points (n=258) for robust correlation calculations.

In conclusion, in this study we found that an external pharmacological perturbation in the brain-mind dynamical system using psilocybin leads to profound alterations in both neural substrate and ongoing subjective experience. We showed that administration of psilocybin leads to an increase of brain tendency to be configured in a functionally non-specific hyper-connected organization which cognitively is realized as feelings of ego dissolution, depersonalization, and hallucinations.

2.4. Traveling to Space

Studying the brain in new non-experienced environments is a unique opportunity to understand the underlying mechanisms of its plastic abilities. In fact, when the brain confronts new circumstances, it dynamically adapts its structure and function to the new conditions, a process known as **neuroplasticity** (Lledo et al., 2006; Pascual-Leone et al., 2005). One such situation is long-duration space flights, during which the brain is profoundly affected by different factors such as **microgravity** (De la Torre, 2014), space radiation, social isolation and confinement, and circadian disruption (Roy-O'Reilly et al., 2021). These factors lead to structural and functional alterations by developing new and potentially compensatory ways to adapt the new environment. Eventually these modifications result in behavioral and performance changes (Bloomberg et al., 2015; Kornilova et al., 2017; Newberg & Alavi, 1998), which can reveal valuable information about the dynamism of the brain and its relation to cognition.

Considering structural alterations, studies so far have shown ventricular enlargement (Alperin et al., 2017; Barisano et al., 2022; Jillings et al., 2020; Kramer et al., 2020; Roberts et al., 2017; Van Ombergen et al., 2018, 2019), brain upward displacement with narrowing of the subarachnoid space at the vertex (Barisano et al., 2022; Jillings et al., 2020; Roberts et al., 2017, 2019; Van Ombergen et al., 2018), decreased grey matter (GM) volume in the frontal, temporal, and occipital cortex and decreased white matter (WM) volume and fractional anisotropy in some large WM tracts important for vestibular and proprioceptive processing (Jillings et al., 2020; Koppelmans et al., 2016; J. K. Lee et al., 2019; Van Ombergen et al., 2018), narrowing of central sulcus, supravermian cistern, and calcarine sulcus (Roberts et al., 2017), and increased volume of sensory motor areas and pre- and postcentral gyrus (Hupfeld et al., 2020; Koppelmans et al., 2016). These modifications can be principally attributed to the upward shift of the brain as a result of microgravity, which persist for several months or even a year after return to the Earth (Jillings et al., 2020; Kramer et al., 2020). The ensuing effects of such structural modifications, concern alterations in the left caudate which have been correlated with poor postural control, as well as alterations in the right primary motor area/midcingulate which were linked to the complex motor tasks completion times (Roberts et al., 2019). In addition, greater changes in the superior longitudinal fasciculus were found to be correlated with larger postflight balance disruptions (Lee et al., 2019).

Taking the brain's functional alterations into account, a case study on a Russian cosmonaut showed that exposure to long-term microgravity leads to significant differences in resting-state functional connectivity between motor cortex and cerebellum, as well as changes within the default mode network. In addition, during a motor imagery task, the cosmonaut showed changes in the supplementary motor area (Demertzi et al., 2016). Another study on a larger group of cosmonauts showed increases in the stimulation-specific connectivity of the right posterior supramarginal gyrus with the rest of the brain, strengthening of connections between the left and right insulae, decreased connectivity of the vestibular nuclei, right inferior parietal cortex and cerebellum with areas associated with motor, visual, vestibular, and proprioception functions, and decreased coupling of the cerebellum with the visual cortex and the right inferior parietal cortex (Pechenkova et al., 2019). A more recent study on the resting state functional connectivity changes after spaceflight showed persisting connectivity decreases in posterior cingulate cortex and thalamus and persisting increases in the right angular gyrus. In addition, connectivity in the bilateral insular cortex decreased after spaceflight, which reversed at follow-up (Jillings et al., 2023). Based on all these studies, brain regions that show functional changes due to microgravity are mainly associated with motor, vestibular and proprioceptive functions, or cognitive control, reflecting adaptations to unfamiliar and conflicting sensory input in microgravity (Jillings et al., 2023).

Together, the aforementioned studies indicate profound alterations in both brain structure and function caused by space travel. However, many important questions remain to be addressed in this research area, two of which will be the topic of investigation in the current chapter. First, how are brain functional dynamics affected due to the long-term living in microgravity conditions? An answer to this question will get us closer to a more comprehensive account about how the brain adapts to the extreme environments. Second, how does the relationship between the structural and function of the brain change in these conditions? By answering this question, one may reveal an underlying cognitive mechanism associated with these changes, especially when considering that associated behavioral tests during spaceflight are difficult to perform.

In this study, we aim to answer these questions by investigating brain dynamics in terms of transitions between FC patterns and the regional (de)coupling of functional activity from and to the structural connectome at rest.

2.4.1 Resting Brain after Space Travel

Dataset

Eighteen male cosmonauts (age = 44.92 ± 5.64 y.o.), engaged in long-duration space missions (185.35 ± 76.5 days) to the International Space Station, gave their consent to participate in the study. Resting state fMRI, diffusion weighted images (DWI), and structural data were acquired at three time points: before their mission (pre-flight), shortly after (post-flight), and approximately 8 months later (follow-up; Figure 2.10). Not all cosmonauts completed the whole protocol: 14 cosmonauts had the complete data for pre-flight, 14 for post-flight, and 7 for follow-up. Thirteen healthy participants (age = 42.55 ± 6.11 y.o.) matched for age, gender, education, and handedness were included as controls for time- and scanner-related effects. The control group was scanned at two timepoints, with an interval similar to that of the cosmonauts' preflight and postflight scans.

Effects of Space Travel on the Functional Dynamics

We first explored the effect of exposure to prolonged microgravity on the dynamics of the whole-brain functional connectome at rest. After preprocessing and denoising of the resting state functional data, we extracted the averaged BOLD time series from the Schaefer atlas with 100 ROIs concatenated with 19 subcortical regions. Then, we estimated phase-coherence connectivity matrices at each time point. After concatenating all connectivity matrices across

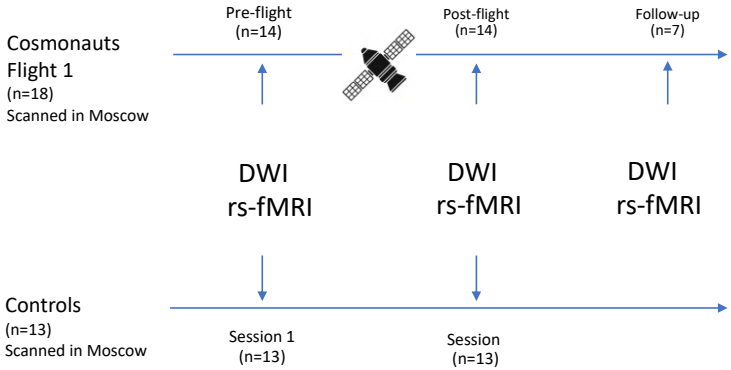

Figure 2.10 Data acquisition paradigm. Eighteen cosmonauts underwent resting state fMRI, DWI and structural imaging at three time points: i) pre-flight, ii) post-flight, and iii) follow-up. Thirteen matched control participants also underwent the same data acquisition session in two time points separated exactly as the duration between pre- and post-flights.

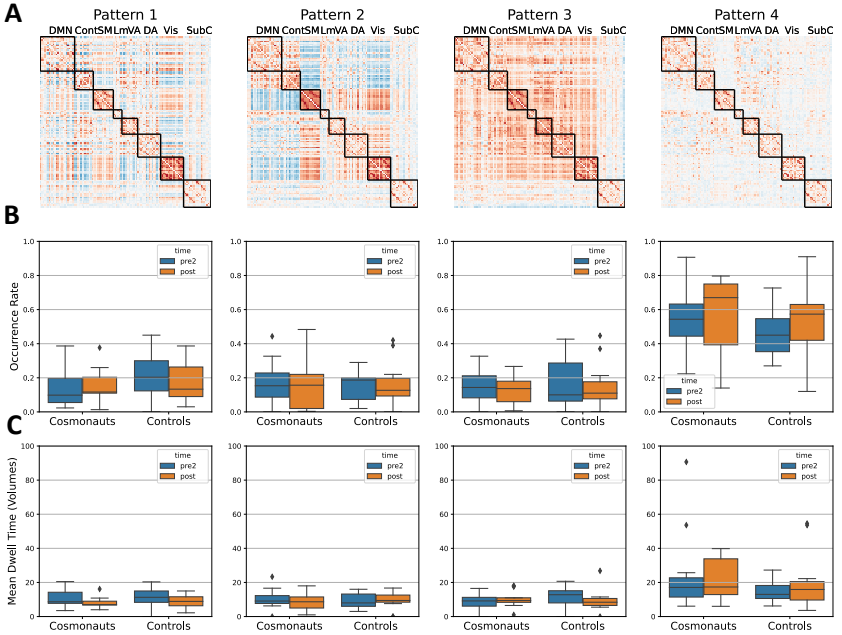

Figure 2.11 Exposure to prolonged microgravity does not affect functional dynamics. (A) Using phase-based coherence connectivity analysis on the cosmonauts' data, four patterns with distinct profiles were estimated. **(B)** The patterns' occurrence rate did not change after space flight (repeated-measure ANOVA, FDR correction for p-values). **(C)** In addition, the patterns' mean dwell time did not change after space flight (repeated-measure ANOVA, FDR correction for p-values).

participants, K-means clustering summarized them into four recurrent connectivity patterns (Figure 2.11A). We first found that the brain's resting functional connectome is organized into four distinct profiles of complex inter-network interactions, including both correlations and anti-correlations (Pattern 1), anti-correlations of DMN and ECN with other networks (Pattern 2), a global cortex-wide positive connectivity (Pattern 3), and a low inter-areal connectivity pattern (Pattern 4). No significant interaction was found between Time and Group in the occurrence rate of each pattern considering pre- and post-flights for both groups of subjects (linear mixed model analysis, Pattern 1 [χ^2=0.865, p_{FDR}=0.942], Pattern 2 [χ^2=0.100, p_{FDR}=0.942], Pattern 3 [χ^2=0.005, p_{FDR}=0.942], and Pattern 4 [χ^2=0.206, p_{FDR}=0.942]; Figure 2.11B). We also calculated the mean dwell time, namely the average time that brain stays in each specific pattern. No significant interaction was observed between Time and Group with respect to

mean dwell time of each connectivity pattern considering pre- and post-flights for both groups of subjects (linear mixed model analysis, Pattern 1 [χ^2=0.004, p_{FDR}=0.947], Pattern 2 [χ^2=0.254, p_{FDR}=0.819], Pattern 3 [χ^2=1.854, p_{FDR}=0.694], and Pattern 4 [χ^2=0.875, p_{FDR}=0.699]; Figure 2.11C). The analysis of transition probabilities among patterns did not show any significant differences between pre- and post-flights for either cosmonauts or controls (Wilcoxon rank-sum test, p_{FDR}>0.05 for all transition probabilities).

Effects of Space Travel on the Structural Connectivity

To investigate possible alterations in the cosmonauts' structural connectome, we estimated the structural connectivity matrix of each participant at each time point using tractograms estimated from the DWI images and the Schaefer atlas with 100 ROIs (see Methods Box 1 for more information). Then, we used a mass univariate analysis, applying a linear mixed model to the structural connection values, and correcting p values for multiple comparison over the number of connections. We found a significant interaction between Time and Group for seven structural connections, showing both increases and decreases in the normalized values of structural connections (Figure 2.12A and Table 2.3). For the connections found to be significantly altered after space travel, we also performed a longitudinal analysis on the connection values, considering pre-flight, post-flight, and follow-up values just for the cosmonaut group. All the three connections that showed a decrease after space flight did not significantly change in the longitudinal analysis (linear mixed model considering Time as the fixed factor and subjects as random factors, R15-R21: χ^2=3.238, p_{FDR}=0.198, R33-R61: χ^2=5.861, p_{FDR}=0.053, and R83-R87: χ^2=0.998, p_{FDR}=0.607). Out of four connections which showed an increase in their value after space flight, two of them were normalized to the pre-flight value in the follow-up (R37-R52 and R83-R85) while the other two connections remained altered even at the follow-up scans (R34-R72 and R46-R96; Figure 2.12B and Table 2.3).

Effects of Space Travel on the Structural-Functional Relationship

Above we observed that space travel did not have a significant effect on the dynamic functional fluctuations but did affect structural connectivity. Therefore, we further asked how the structural-functional relationship is affected due to long-term travel to space. To investigate this question, we studied what regional alterations happen to the structural-functional coupling due to space travel. Using **graph signal processing (GSP)** framework, we represented the functional time series based on the **structural harmonics** calculated from an averaged

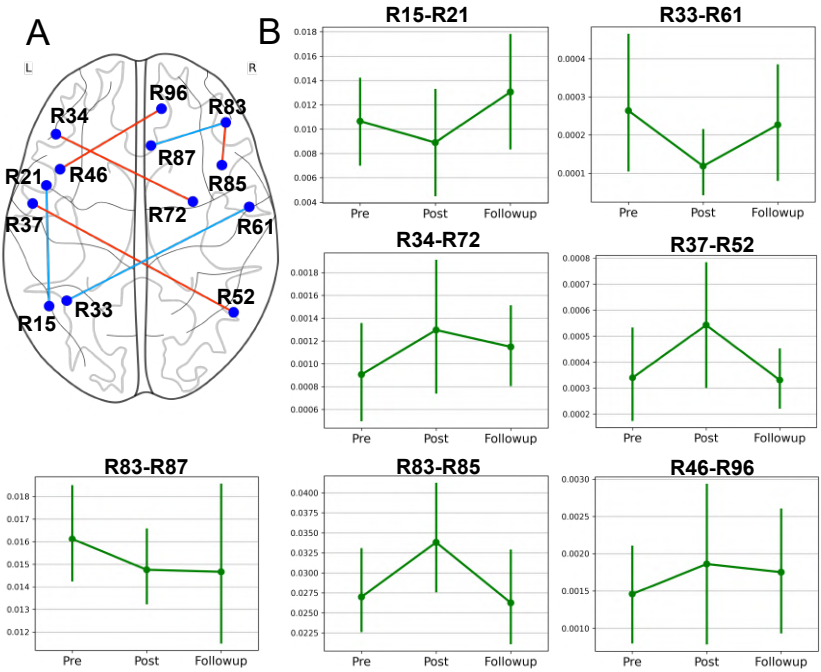

Figure 2.12 Structural connectivity alters after space flight. (A) Seven structural connections were found to be altered due to the long-term exposure to the microgravity, showing both decreasing and increasing values (Rxx is the region number xx in the Schaefer atlas, blue edges show a decrease, and red edges show an increase in the connection value after space flight). **(B)** Longitudinal analysis shows that some alterations in the structural connections are persistent while the others get normalized to the pre-flight values in the follow-up. Details of the statistical analysis are summarized in the Table 2.3.

version of the structural connectome. As we observed the structural connectivity changes after spaceflight, we calculated the average structural connectivity for each time point separately. By transforming the functional time series to the structural harmonics space, we calculated the coupling and decoupling index of each ROI time series to and from the underlying structure, as well as the **structural decoupling index** (**SDI**; Figure 2.13 and Method Box 1). A linear mixed model analysis revealed that the interaction between Time and Group has a significant effect on the SDI measure of the left insular cortex and right superior parietal lobule from the dorsal attentional network (Figure 2.14). While insular cortex activity showed more decoupling from the underlying structure, the posterior regions of dorsal attentional network showed more coupling to the

Table 2.3 Statistical analysis results of significantly altered structural connections after space flight. First a linear mixed model analysis was performed to investigate the interaction between time and group in the connection values considering pre- and post-flights for both groups of subjects. Then a linear mixed model was used in the cosmonaut group to explore the effect of time parameter on the connection values considering pre-flight, post-flight, and follow-up scans. In both analysis, subjects were considered as the random factors of the model.

		Post - Pre			Follow-up	
Connection	**Regions**	**Estimate**	χ^2	p_{FDR}	χ^2	p_{FDR}
R15-R21	LH_DAN_Post_1 – LH_DAN_PrCv_1	-0.001	21.174	0.010	3.238	0.198
R33-R61	LH_Cont_Par_1 – RH_SomMot_4	-0.0001	18.602	0.026	5.861	0.053
R34-R72	LH_Cont_PFCl_1 – RH_DAN_FEF_1	0.0004	22.080	0.009	17.047	<0.001
R37-R52	LH_DMN_Temp_1 – RH_Vis_3	0.0002	18.001	0.026	11.140	0.004
R46-R96	LH_DMN_PFC_6 – RH_DMN_PFCdPFCm_2	0.0005	26.836	0.002	6.285	0.043
R83-R85	RH_Cont_PFCl_2 – RH_Cont_PFCl_4	0.006	18.352	0.026	16.859	<0.001
R83-R87	RH_Cont_PFCl_2 – RH_PFCmp_1	-0.002	16.523	0.048	0.0998	0.607

LH: left hemisphere, RH: right hemisphere, DAN: dorsal attentional network, Post: posterior, PrCv: precentral ventral, Cont: executive control network, SomMot: somatomotor network, PFCl: lateral prefrontal cortex, FEF: frontal eye field, DMN: default mode network, Temp: temporal, Vis: visual network, PFCm: medial prefrontal cortex, PFCld: dorsolateral prefrontal cortex, PFCmp: medial posterior prefrontal cortex.

structure. As the SDI metric is a division of coupling and decoupling indices, we further investigated from which sources these alterations in the SDI measure are derived. Separate linear mixed model analysis on the coupling and decoupling measures showed that coupling measures change significantly for both the insular cortex (χ^2=16.659, p_{FDR}<0.001) and the superior parietal lobule (χ^2=21.849, p_{FDR}<0.001) while the decoupling index did not show any significant alteration after p-value FDR correction.

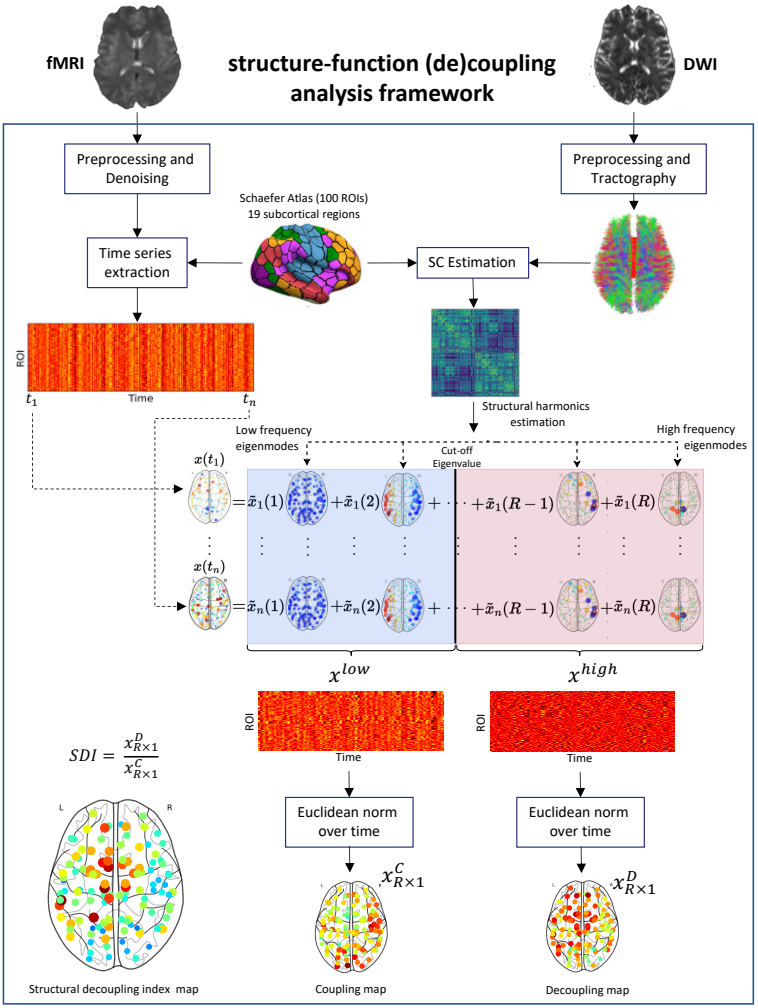

Figure 2.13 Structure-function (de)coupling analysis pipeline. Structural harmonics were estimated as the eigenvectors of the normalized Laplacian of the structural connectivity matrix. Then, functional activities at each time point were represented as linear combination of the structural harmonics. Since harmonic modes range from low frequency distributed to high frequency localized activities, functional data were filtered and decomposed into the low and high frequency components. Regional Euclidean norm of the lowpass filtered and high pass filtered versions of the signal resulted in coupled and decoupled maps respectively. (R: number of atlas regions, x^{low}: lowpass filtered version of the signal, x^{high}: high pass filtered version of the signal, x^C: coupling map, and x^D: decoupling map, SDI: structural decoupling index)

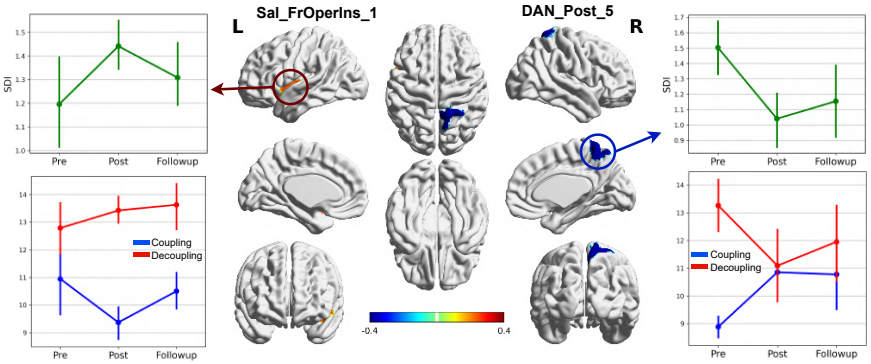

Figure 2.14 Regional structural decoupling index changes after space flight. While the structural decoupling index of the left insular cortex increases after space travel, this measure decreases in the right superior parietal lobule of dorsal attentional network. This alteration principally comes from the alterations in coupling index rather than the decoupling index, suggesting that the distributed activity of the region is affected more than its localized functioning. Sal: salience network, FrOperIns: frontal operculum insula, DAN: dorsal attentional network, Post: posterior.

2.4.2 Discussion

Traveling to space makes humans to confront newly non-experienced environmental conditions which affects both the body and the brain, namely microgravity, radiation, acceleration, social isolation, and stress (De la Torre, 2014). Thanks to neuroplasticity, when confronting new environmental circumstances, the brain changes its structure and function accordingly to adapt to the new conditions. Studying these structural and functional alterations helps us to better understand the relationship between the underlying brain mechanism of action and our mental characteristics. In this study, we investigated the influences of spaceflight on the brain's functional and structural networks and their coupling profile during rest. Using structural and functional MRI acquired before spaceflight, after return to the Earth, and after 8 months from the time of return of 18 cosmonauts, we showed that while functional dynamics were not affected, profound changes in the structural connectome were observed which led to regional alterations in the structural-functional coupling profile.

A separate analysis of structural and functional connectomes showed that dynamical FC patterns were not affected in terms of occurrence rate or mean dwell time, while several structural connections changed in both increasing and decreasing directions. One reason for structural connectivity changes can be

cortical volume alterations because of spaceflight. Since we estimated the structural connectivity as the number of white matter tracts between each pair of regions of interest normalized by the sum of volumes of those regions, changes in the volume of structurally connected cortical regions may lead to the alterations in the connectivity value of the link between them. In this regard, decreased cortical volumes lead to an increased structural connectivity value and an increased volume leads to decreased structural connectivity. Our findings of decreased structural connectivity between regions linked to the sensory motor areas (R61) and precentral cortex (R21) are in line with the previous reports that these cortical areas showed increased volume after a long-term spaceflight (Hupfeld et al., 2020; Koppelmans et al., 2016). We also found an increase in the connectivity measure of links connected to the prefrontal cortex. This region was also previously shown to be susceptible to environmental changes such as long Antarctic expeditions, demonstrating its alteration as volume reduction (Roy-O'Reilly et al., 2021; Stahn et al., 2019). Another reason for structural connectivity changes can be related to the microstructural changes in the white matter tracts. One set of tracts that have been shown to be affected in spaceflights are tracts connecting the occipital lobe with frontal and temporal lobes (Lee et al., 2019). We also showed that the structural connectivity between temporal regions of the default mode network and occipital regions of the visual network were significantly affected after spaceflight which is in line with those findings.

Since we found structural alterations due to long-term exposure to space-related conditions, but not any variation in the functional dynamics, we attempted to investigate how the structural-functional relationship is affected after facing such circumstances. We used the recently proposed SDI metric to quantify decoupling of cortical regions functional activity from the underlying structural connectome (Preti & Van De Ville, 2019). This metric has been shown to bear cognition related information (Preti & Van De Ville, 2019) and provides signatures to accurately classify different cognitive tasks and individual fingerprinting (Griffa et al., 2022). In particular, SDI has been shown to have higher values in the cortical regions related to higher-order cognition. On the other hand, it shows to have lower values in the cortical regions related to the low-order cognition (Preti & Van De Ville, 2019). An increased SDI value signifies a decoupling of functional activity from the underlying structure, meaning that the regions that are structurally connected have anti-correlated functional activity. On the other hand, a decreased SDI value signifies that the functional activity is coupled to the underlying structural connectome, meaning that regions

that are structurally connected show highly correlated activity. Here, we first found that the SDI measure increases in the left insular cortex. The insular cortex is a part of the salience network and has been related to a wide range of functional contexts, including sensory perception (Small, 2010), vestibular processing and interoception (Critchley et al., 2004), and motor function (Ackermann & Riecker, 2010). Previous studies on astronauts and cosmonauts reported a reduced resting state functional connectivity of the insular cortex with the rest of the brain after spaceflight (Demertzi et al., 2016; Jillings et al., 2023). Structural studies also reported a decreased volume of the left insular cortex due to spaceflight (Koppelmans et al., 2016). While the structural changes are mainly due to the brain's upward shift because of exposure to microgravity, we hypothesize that increased decoupling of functional activity from the structure in the insular cortex is an accommodating mechanism that keeps optimal functioning regardless of structural changes, which is vital in the new environment with conflicting and unfamiliar sensory stimuli (Jillings et al., 2023). On the other hand, we also found decreased SDI measure in the superior parietal lobule a region of dorsal attentional network. This region has been related to audio-visual multisensory integration and processing (Molholm et al., 2006). In typical conditions, a low value of SDI metric can be observed for sensory-motor and visual areas so that this higher coupling strength helps them to react fast and reliably to external and internal stimuli (Preti & Van De Ville, 2019). As a result, a decreased SDI measure of the superior parietal lobule can be related to the new need of the brain to integrate and process multisensory inputs faster than normal conditions in response to the non-experienced environmental circumstances.

Taken together, after space travel our brain faces new conditions that it has not experienced before. Prolonged exposure to microgravity causes structural alterations in the brain which can affect its cognitive performance. In order to keep its optimal functioning and to be adapted to the new conditions, the brain modifies its functional profile in relation to the underlying structure, potentially as a compensation mechanism. We showed that these modifications can be captured and investigated using regional measures of coupling and decoupling of functional activity to and from the underlying structure.

This study also posits specific limitations. First, as most other studies with space travelers, interpretation of results is limited due to the small sample size. In addition, as some cosmonauts did not attend the whole protocol, there are also missing data in different time points of the data acquisition which also limits the statistical approaches to infer results from the acquired data. To mitigate these problems, we used linear mixed model analysis that solves the problem of

missing data points. However, the small sample size remains a problem that prevents us from discovering small effects in this cohort of subjects. Second, cosmonauts usually go through intensive trainings to prepare for spaceflight. This fact restricts the result interpretation about how to check if the observed effect is due to spaceflight or a training effect. Further studies are needed to clarify this potential confound. Finally, our sample was limited to male subjects. This might induce an extra bias which can prevent us from generalizing our observations. These limitations are common among most of the studies conducted on the effects of spaceflight on the brain. Therefore, to have more robust explanations of what happens to the underlying mechanism of the brain during space travel, further experimental planning with higher number of cosmonauts and more gender diversity is required.

Methods Box 1

Participants

- **Mind Blanking:** Thirty-six healthy right-handed adults (27 women, 9 men, mean age: 23 y ± 2.9) participated in an fMRI experience-sampling task. All participants gave their written informed consent to take part in the experiment. The ethics committee of the University Hospital of Liège approved the study.
- **Psychedelics:** Data were collected from 49 healthy participants with previous experience with a psychedelic drug but not within the past 3 months of the experiment. Participants were randomized to receive a single dose of psilocybin (0.17 mg/kg, n=22 (12 men), age=23±2.9 y) or placebo (n=27 (15 men), age=23.1±3.8 y). This study was conducted according to the code of ethics on human experimentation established by the declaration of Helsinki (1964) and amended in Fortaleza (Brazil, October 2013) and in accordance with the Medical Research Involving Human Subjects Act (WMO) and was approved by the Academic Hospital and University's Medical Ethics committee (Maastricht University). All participants were fully informed of all procedures, possible adverse reactions, legal rights, responsibilities, expected benefits, and their right for voluntary termination without consequences.
- **Cosmonauts:** The data of 18 male Russian cosmonauts (mean age = 44.92 ± 5.64), engaged in long-duration space missions to the International Space Station, and thirteen healthy controls (mean age = 42.55 ± 6.11) matched for age, gender, and education were used in this study. The data acquisition was approved by the Institutional Review Board of the Antwerp University Hospital (13/38/357), the European Space Agency Medical Board, the Committee of Biomedicine Ethics of the Institute of Biomedical Problems of the Russian Academy of Science, and the Human Research Multilateral Review Board. All participants provided a signed informed consent, and all investigations were performed in accordance with the principles listed in the Declaration of Helsinki and its amendments.

Datasets

- **Mind Blanking:** Data were acquired during resting state while participants were lying inside the scanner with eyes open. At random times, they were interrupted by an auditory tone, probing them to report their immediate mental state via button presses (Fig. 1, Upper panel). The sampling probes were randomly distributed between 30 and 60 s. Each probe started with the appearance of an exclamation mark lasting for 1,000 ms, inviting the participants to review and characterize the cognitive events they just experienced. Then, on the screen four categories for a broad characterization of the cognitive experiences were shown: absence, perception, stimulus-dependent thought, and stimulus-independent thought. For reporting, participants used two response boxes, one in each hand. Participants used

an egocentric mental projection of their fingers onto the screen so that each finger corresponded to a specific mental category. Depending on the probes' trigger times and participants' reaction times, the duration of the recording session was variable (48–58 min). To minimize misclassification rates, participants had a training session outside the scanner at least 24 h before the actual session.

- **Psychedelics:** Six minutes of resting state fMRI were acquired from the participants with eyes open during peak subjective drug effect (102 minutes post treatment). In addition, the 5 Dimensions of Altered States of Consciousness (5D-ASC) scale and the Ego Dissolution Inventory (EDI) were evaluated 360 minutes after drug administration, as retrospective measures of drug effects.
- **Cosmonauts:** Ten minutes of resting state fMRI with eyes closed, DWI, and structural data were acquired in three time points: before the mission (pre-flight), shortly after (post-flight), and approximately 8 months later (follow-up).

Imaging Setup

- **Mind Blanking:** Experiments were carried out on a 3-T head-only scanner (Magnetom Allegra, Siemens Medical Solutions, Erlangen, Germany) operated with the standard transmit–receive quadrature head coil. fMRI data were acquired via a T2*-weighted gradient-echo echo-planar imaging sequence with the following parameters: TR = 2,040 ms, echo time = 30 ms, field of view = 192×192 mm^2, 64×64 matrix, 34 axial slices with 3 mm thickness and 25% interslice gap to cover most of the brain. A high-resolution T1-weighted magnetization-prepared rapid gradient echo image was acquired for anatomical reference (TR = 1,960 ms, echo time = 4.4 ms, inversion time = 1,100 ms, field of view = 230 ×173 mm, matrix size = 256×192×176, voxel size = 0.9×0.9×0.9 mm). The participant's head was restrained with a vacuum cushion to minimize head movement. Stimuli were displayed on a screen positioned at the rear of the scanner, which the participant could comfortably see via a head coil–mounted mirror.
- **Psychedelics:** Images were acquired on a MAGNETOM 7T MR scanner. 258 whole-brain EPI volumes were acquired at rest (TR = 1400 ms; TE = 21 ms; field of view=198 mm; flip angle = 60°; oblique acquisition orientation; interleaved slice acquisition; 72 slices; slice thickness = 1.5 mm; voxel size = 1.5 × 1.5 × 1.5 mm).
- **Cosmonauts:** Resting-state fMRI data were acquired on a 3T MRI scanner (Discovery MR750; GE Healthcare USA) located at the Federal Center of Treatment and Rehabilitation in Moscow, Russia. T2*-weighted echo planar imaging scans were acquired using a 16-channel head and neck array coil with the participants positioned head-first and supine. The following scanning parameters were used: echo time = 30 ms, repetition time = 2000ms, flip angle = 77°, voxel size = 3 × 3 × 3 mm^3, field of view = 192 × 192 × 126 mm (matrix dimension: 64 × 64, 42 axial slices). A total of 300 images per session were acquired after 4 dummy scans (8 s) to achieve steady-state conditions. In addition, a high-resolution fast-spoiled gradient echo (FSPGR) 3D T1-weighted image was acquired for the purpose of anatomical localization. The scanning parameters included: echo time = 3.06 ms, repetition time = 7.90 ms,

inversion time = 450 ms, flip angle = 12°, voxel size = 1 mm^3, field of view = 176 × 240 × 240 mm (matrix dimensions: 240 × 240, 176 sagittal slices). For DWI, an optimized multi-shell dMRI acquisition scheme was prescribed, containing diffusion weightings of b = 0, 700, 1200, and 2800 s/mm^2, applied in 8, 25, 45, and 75 directions, respectively. In addition, 3 b = 0 s/mm^2 images were acquired with reversed-phase encoding, for the purpose of correcting susceptibility-induced distortions. Other imaging parameters were repetition/echo time of 7800/100 ms, voxel size of 2.4 × 2.4 × 2.4 mm^3, matrix size of 100 × 100, 58 slices, and 1 excitation. Imaging was accelerated by a factor of 2 using the Array coil Spatial Sensitivity Encoding Technique.

Behavioral Analysis

- **Mind Blanking:** Paired t-tests were used to compare the number of reports of each mental state across participants (P values were FDR corrected with a significance level of α = 0.05). A generalized linear mixed model with a gamma distribution and inverse link function tested the relationship between reaction times and mental states. The choice of the generalized linear mixed model was because of positive tail in the distribution of reaction times and inhomogeneity of variance across mental states caused by an imbalanced number of reports. Mental state reports were considered as fixed effects, and participants were considered as the random effects, with sex and age as confound variables. In case of significant main effects, a post-hoc test was applied for pairwise comparisons. For that, we used the Tukey method to correct the type I error inflation that occurred in the multiple comparisons. To model dynamic transition between mental state reports, a Markov model was used to calculate the transition probabilities between participants' reports over the experiment. The uniformity of the distribution of each report over the acquisition duration was tested via χ2 test on the time point of reports across all participants. The acquisition duration of each subject was divided into 10 equal temporal bins, and the number of reports in each bin was counted. To calculate the effect size of the χ2 test, ϕ measure was used ($\varphi = \sqrt{\frac{\chi^2}{n}}$, where n is the number of observations).
- **Psychedelics:** A non-parametric Mann-Whitney U test was performed to compare the 5D-ASC and EDI scores between two groups. FDR correction was performed on the p-values of the 5D-ASC dimensions. The effect size was calculated based on the Cliff's delta measure: $d = \frac{2U}{mn} - 1$, where U is the test statistic, and m and n represent the size of each group (Cliff, 1993).

Neuroimaging Data Preprocessing

- **Mind Blanking:** Preprocessing and denoising were performed via a locally developed pipeline written in Python [nipype package (Gorgolewski et al., 2011)] encompassing toolboxes from Statistical Parametric Mapping 12 (Penny et al., 2011), FSL 6.0 (Jenkinson et al., 2012), AFNI (Cox, 1996), and ART

(http://web.mit.edu/swg/software.htm). In this pipeline, all the functional volumes were realigned to the first volume and then, in a second pass, to their average. Estimated motion parameters were then used for artifact detection. An image was defined as an outlier or artifact image if the head displacement in the x, y, or z direction was greater than 3 mm from the previous frame, if the rotational displacement was greater than 0.05 rad from the previous frame, or if the global mean intensity in the image was more than 3 SD from the mean image intensity for the entire scans. After skull-stripping of structural data [using FSL BET (S. M. Smith, 2002) with fractional intensity of 0.3], realigned functional images were registered to the bias-corrected structural image in the subject space (rigid body transformation with normalized mutual information cost function). After white matter (WM), gray matter (GM), and cerebrospinal fluid (CSF) masks were extracted, all the data and masks were transformed into the standard stereotaxic Montreal Neurological Institute space (MNI152 with 2-mm resolution). WM and CSF masks were further eroded by one voxel. For noise reduction, we modelled the influence of noise as a voxel-specific linear combination of multiple empirically estimated noise sources by deriving the first five principal components from WM and CSF masked functional data separately. These nuisance regressors together with detected outlier volumes, motion parameters, and their first-order derivative were used to create a design matrix in the first-level general linear model (GLM). After the functional data were smoothed with a Gaussian kernel of 6 mm full width at half-maximum, the designed GLM was fitted to the data. Before GLM was applied, functional data were demeaned and detrended and all the motion-related and tissue-based regressors were first normalized and then demeaned and detrended via the approach explained in (Power et al., 2014). A temporal causal bandpass filter of 0.008–0.09 Hz was then applied on the residuals of the model to extract low-frequency fluctuations of the BOLD signal. Schaefer atlases (Schaefer et al., 2018) with 100 ROIs were then used to parcellate each individual brain. The average of voxel time series in each region was considered as the extracted ROI time series and was used for further analysis. All eventual connectivity analyses were performed with both the inclusion and the removal of GS.

- **Psychedelics:** The fMRI was preprocessed using locally developed pipeline based on SPM12 (Penny et al., 2011). In this pipeline, after susceptibility distortion correction and realignment, functional data were registered to the high resolution T1 image, then normalized to the standard MNI space, and finally was smoothed using a Gaussian kernel with a full width at half maximum (FWHM) of 6. After segmentation of structural T1 image into grey matter (GM), white mater (WM), and CSF masks, the bias corrected structural image and all the extracted masks were normalized to the MNI space. Further, WM and CSF masks were eroded by one voxel to remove any overlapping between these tissues and the GM voxels. To denoise functional time series, we used a locally developed pipeline written in Python [nipype package (Gorgolewski et al., 2011)]. In this pipeline, a general linear model (GLM) was fitted to each voxel data separately, regressing out the effect of six movement parameters

(translation in x, y, and z directions, and rotation in yaw, roll, and pitch directions), constant and linear trends using zero-order and first-order Legendre polynomials, 5 principal components of signals in the WM and CSF masks, physiological data, and outlier data points. Outlier detection was performed using ART toolbox (http://web.mit.edu/swg/software.htm). Any volume with a movement value of greater than 3 mm, rotation value of greater than 0.05 radians, and z-normalized global signal intensity of greater than 3 was considered as an outlier. After regressing out these nuisance regressors, the remaining signal was filtered in the range of [0.008, 0.09] Hz and was used for further analysis. Schaefer atlas with a resolution of 100 ROIs (Schaefer et al., 2018) together with additional 19 subcortical regions was used to extract the averaged BOLD signals inside each ROI.

- **Cosmonauts:** The fMRI was preprocessed and denoised using locally developed pipeline based on SPM12 (Penny et al., 2011). In this pipeline, after realignment, functional data were registered to the high resolution T1 image, then normalized to the standard MNI space, and finally was smoothed using a Gaussian kernel with a full width at half maximum (FWHM) of 6. After segmentation of structural T1 image into grey matter (GM), white mater (WM), and CSF masks, the bias corrected structural image and all the extracted masks were normalized to the MNI space. Further, WM and CSF masks were eroded by one voxel to remove any overlapping between these tissues and the GM voxels. To denoise functional time series, a general linear model (GLM) was fitted to each voxel data separately, regressing out the effect of six movement parameters (translation in x, y, and z directions, and rotation in yaw, roll, and pitch directions), constant and linear trends using zero-order and first-order Legendre polynomials, 5 principal components of signals in the WM and CSF masks, physiological data, and outlier data points. Outlier detection was performed using ART toolbox (http://web.mit.edu/swg/software.htm). Any volume with a movement value of greater than 3 mm, rotation value of greater than 0.05 radians, and z-normalized global signal intensity of greater than 3 was considered as an outlier. After regressing out these nuisance regressors, the remaining signal was filtered in the range of [0.008, 0.09] Hz and was used for further analysis. Schaefer atlas with a resolution of 100 ROIs (Schaefer et al., 2018) together with additional 19 subcortical regions was used to extract the averaged BOLD signals inside each ROI. DWI data were preprocessed using MRTrix3 (https://www.mrtrix.org). Preprocessing steps included denoising (Veraart et al., 2016), Rician bias correction, Gibbs ringing correction (Kellner et al., 2016), Susceptibility-induced and Eddy current distortion correction (Andersson et al., 2016; Andersson & Sotiropoulos, 2016a), movement (including between-slice movement) correction (Andersson et al., 2017), and bias field correction (Tustison, Avants, Cook, Yuanjie Zheng, et al., 2010). The anatomical image was registered with the DWI (b=0) image and was segmented into five tissue type masks related to cortical grey matter, white matter, CSF, subcortical grey matter, and unknown tissue types (R. E. Smith et al., 2012). Response functions were estimated using the Tournier algorithm (J. D. Tournier et al., 2013) and fiber orientation distributions

were estimated using multi-shell multi-tissue constrained spherical deconvolution (Jeurissen et al., 2014a). Finally, 1 million tracts were generated for each acquisition session using anatomically constrained tractography and second-order Integration over fiber orientation distributions (J. D. Tournier et al., 2010) followed by spherical-deconvolution informed filtering of the tractogram (SIFT) to remove the spurious connections (R. E. Smith et al., 2013). Considering a Schaefer atlas with 100 ROIs and 19 attached subcortical regions, a structural connectivity matrix was created by counting the number of streamlines between each pair of regions normalized by the sum of the related regions volumes.

Neuroimaging Data Analysis

- **Dynamic FC Estimation:** We used the phase-based coherence analysis to extract between-region connectivity patterns at each time point of the scanning session (Demertzi et al., 2019). For each participant i, after z-normalization of time series at each region r (i.e., $x_{i,r}[t]$), the instantaneous phase of each time series was calculated via Hilbert transform as:

$$\hat{x}_{i,r}(t) = \frac{1}{\pi t} * x_{i,r}(t)$$

where * indicates a convolution operator. Using this transformation, we produced an analytical signal for each regional time series as:

$$x^{a}_{i,r}(t) = x_{i,r}(t) + j\hat{x}_{i,r}(t)$$

where $j = \sqrt{-1}$. From this analytical signal, the instantaneous phase of each time series can be estimated as:

$$\varphi_{i,r}(t) = \tan^{-1}\left(\frac{\hat{x}_{i,r}(t)}{x_{i,r}(t)}\right)$$

After wrapping each instantaneous phase signal of $\varphi_{i,r}(t)$ to the $[-\pi, \pi]$ interval and naming the obtained signal as $\theta_{i,r}(t)$, we calculated a connectivity measure for each pair of regions as the cosine of their phase difference. For example, the connectivity measure between regions r and s in subject i was defined as:

$$conn_{i,r,s}(t) \triangleq \cos\left(\theta_{i,r}(t) - \theta_{i,s}(t)\right)$$

By this definition, completely synchronized time series lead to a connectivity value of 1, completely desynchronized time series produce a connectivity value of zero, and anticorrelated time series produce a connectivity measure of -1. Using this approach, we created a connectivity matrix of 100×100 at each time point t for each subject i that we called $C_i(t)$:

$$C_i(t) \triangleq \left[conn_{i,r,s}(t)\right]_{r,s}$$

After collecting connectivity matrices of all time points of all participants, we applied k-means clustering on all estimated connectivity matrices. With this technique, four robust and reproducible patterns were extracted as the centroids of the clusters, and each resting connectivity matrix was assigned to one of the extracted patterns. We chose to extract four patterns to compare our results with previous researches (Demertzi et al., 2019). We calculated the occurrence rate of each pattern simply by

counting the number of matrices that were assigned to each specific pattern at each subject separately. In each study, significant differences between pattern occurrence rates were analyzed via paired t-test and FDR correction of p values over possible pairwise comparisons.

- **Classification of MB Based on Time-Varying Connectivity Matrices:** Phase-based coherence matrices within the analysis windows were considered as the feature vectors and the related mental state reports as the class labels. First, an SVM model for binary classification was designed to classify MB reports from all the other reports. As the dataset was imbalanced, we calculated precision, recall, and balanced accuracy as the efficiency parameters of the classifier (MB reports were defined as positive class. See Appendix B). As the cross-validation strategy, a five-fold stratified cross-validation with 10 repeats was applied. This classification strategy was also repeated for a one-versus-one classification of MB versus each of the other reports separately. To compare the results with an empirical chance level, a dummy classifier was also used to classify MB from other reports. This dummy classifier generated random predictions by respecting the training set class distribution.

- **GS Effect on the MB:** We calculated the GS for each subject after applying the atlas and time series extraction, by averaging time series of all the ROIs. To study the effect of the GS on the analysis results, we subtracted it once from the time series related to each ROI (GSS):

$$x'_{i,r}(t) = x_{i,r}(t) - g_i(t)$$

where i identifies the subject, r identifies the ROI, and $g_i(t)$ is the GS of the subject i, and regressed it out once from the ROI time series (GSR):

$$x'_{i,r}(t) = x_{i,r}(t) - \frac{\left|\left|x_{i,r}(t)\right|\right|}{||g_i(t)||} corr\left(x_{i,r}(t), g_i(t)\right) g_i(t)$$

To study the relationship between GS and mental states, the GS amplitude was calculated for each mental state. The GS amplitude was defined as the sum of the absolute value of the five GS time points related to the functional repertoire of each mental state. A generalized mixed effect model with gamma distribution and inverse link function was fitted to the GS amplitude values, considering mental states as main effect and subjects as random effect of the model. In case of finding a significant effect, a Tukey post-hoc test was performed to compare each pair of the mental states in terms of their related GS amplitude.

- **Static Functional Connectivity Analysis of Psychedelic Data:** Pearson correlations were calculated between the BOLD time series of each pair of ROIs and a connectivity matrix was created for each participant. For each participant, the average of the connectivity values over the whole brain was considered as the

overall connectivity value of the brain. An independent t-test was performed to compare the overall connectivity values between psilocybin and placebo groups. Average of the connectivity values between the regions of each network was considered as the within network connectivity values for each subject. Independent t-test was performed to compare the within-network connectivity values between two groups. As there were 7 networks, FDR correction was performed to correct for multiple comparison. Between-network connectivity was calculated as the average of the connectivity values between regions of any pair of networks. After performing an independent t-test to compare the between-network connectivity values of placebo and psilocybin groups, FDR correction was applied to correct for the 21 between-network comparisons.

- **Dynamic FC Analysis of Psychedelic Data:** After FC state estimation, we calculated the occurrence rate of each pattern and the transitions probabilities between each pair of states as dynamic features of the system. Occurrence rate of each pattern was defined as the proportion of connectivity matrices assigned to that pattern and was calculated for each subject separately. Independent t-test was used to compare the occurrence rate of each FC pattern between psychedelics and placebo groups. Bonferroni correction was used to correct the p-values for multiple comparison. Markov model was used to model the transition probabilities between each FC pattern for each subject. To detect any significantly different transition probability between two groups, Wilcoxon rank-sum test was performed on each transition and p-values were FDR-corrected.

- **Regional GS Analysis of Psychedelic Data:** Euclidean norm of the BOLD signals were calculated at each ROI as a measure of power of the signal. Independent t-test was used to compare the regional GS power between two groups and p-values were FDR-corrected due to multiple comparison.

- **Dynamic FC Analysis of Cosmonauts Data:** After FC state estimation, we calculated the occurrence rate and mean dwell time of each pattern and the transitions probabilities between each pair of states as dynamic features of the system. Occurrence rate of each pattern was defined as the proportion of connectivity matrices assigned to that pattern and mean dwell time was defined as the average time brain spent at each pattern in consecutive transitions. Both measures were calculated for each subject separately. Linear mixed model, considering dynamic variables as a function of time and group interaction and subjects as random factor, was used to compare the occurrence rate and mean dwell time of each FC pattern before and after spaceflight in two groups of cosmonauts and controls. FDR correction was used to correct the p-values for multiple comparison. Markov model was used to model the transition probabilities between each FC pattern for each subject. To detect any significantly different transition probability between two

groups, Wilcoxon rank-sum test was performed on each transition and p-values were FDR-corrected.

- **SC Analysis of Cosmonauts Data:** After estimation of tractograms for each subject and each data acquisition session, structural connectome was estimated by applying Schaefer atlas with 100 regions of interest and counting the number of tracts between each pair of regions and normalizing it by the sum of volumes of the connected regions. A univariate mass analysis using linear mixed models was performed considering the values of each connection as the dependent variable, the interaction of time and group as the independent variable, and subjects as random factors for pre- and post-flights and two groups of subjects. P-values were corrected using FDR method. For the significantly altered connections, we also analyzed the longitudinal changes of the connection values by fitting a linear mixed model considering time (preflight, postflight, and follow-up) as fixed effect and subjects as random effect to the connection values of cosmonauts group.

Structural-Functional Relationship Analysis of Cosmonauts Data: Considering GSP (Ortega et al., 2018) as the main analysis framework, the main idea here was to span a multi-dimensional space using orthonormal structural connectome harmonics and represent all the functional time series in that space. This transformation led to the possibility of studying regional coupling and decoupling of functional data to and from the underlying structure and how they can be used to predict ongoing mental states. Considering a structural connectivity matrix $S_{R\times R}$ where R is the number of ROIs, the normalized Laplacian of this matrix can be computed as $L(S) = D^{-\frac{1}{2}}(D-S)D^{-\frac{1}{2}}$, where D is a diagonal matrix representing the degree of each node in the S matrix: $D_{ii} = \sum_{j=1}^{R} S_{ij}$. Eigen decomposition of this normalized Laplacian matrix will lead to a set of orthonormal bases with a notion of spatial frequency (higher eigen value, higher spatial frequency) which are called structural harmonics: $L = U\Lambda U^{-1}$ where U is the matrix containing eigenvectors and Λ is a diagonal matrix containing corresponding eigen values. To create a common space for all the subjects, average of all the structural connectivity matrices of all the subjects will be calculated to estimate the S matrix (In this study, as significant changes in the structural connectome were detected due to space travel, separate average structural connectomes were calculated for pre and post flight acquisitions). Considering functional time series matrix $X_{R\times T}$ where R is the number of ROIs and T is the number of BOLD signal time points, we can transform this matrix to the structural harmonics space and transform back from this space to the original space as:

$$\begin{cases} \tilde{X} = U^{-1}X \\ X = U\tilde{X} \end{cases}$$

where $\tilde{X}$ is the corresponding representation of matrix X in the structural harmonics space. Keeping the first C eigenvectors ($1 \leq C \leq R$) and setting the rest to zero will

lead to a matrix with low frequency eigenmodes and we can name it as $\mathrm{U}^{\mathrm{low}}$. In the same manner, we can keep the highest R-C eigen vectors and set the others to create a matrix with high frequency eigenmodes and call it $\mathrm{U}^{\mathrm{high}}$. Reconstructing the signal in the original space with $\mathrm{U}^{\mathrm{low}}$ will lead to a spatially lowpass filtered version of the signal called $\mathrm{X}^{\mathrm{low}}$. The same transformation using $\mathrm{U}^{\mathrm{high}}$ will lead to a highpass filtered version of the signal called $\mathrm{X}^{\mathrm{high}}$:

$$\begin{cases} X^{low} = U^{low}U^{-1}X \\ X^{high} = U^{high}U^{-1}X \end{cases}$$

In this manner, $\mathrm{X}^{\mathrm{low}}$ will contain the portion of the signal aligned with the underlying structure and $\mathrm{X}^{\mathrm{high}}$ will contain the portion of the signal liberal from the underlying structure. Calculating the Euclidean norm of each row in the $\mathrm{X}^{\mathrm{low}}$ matrix will lead to a regional measure of functional-structural coupling called $\mathrm{X}^{\mathrm{C}}_{\mathrm{R}\times 1}$and calculating this norm in the rows of $\mathrm{X}^{\mathrm{high}}$ will lead to a regional measure of functional-structural decoupling called $\mathrm{X}^{\mathrm{D}}_{\mathrm{R}\times 1}$. Element-wise division of the decoupled signal by the coupled signal will result in a parameter called structural decoupling index (SDI):

$$SDI_{R\times 1} = \frac{X^{D}_{R\times 1}}{X^{C}_{R\times 1}}$$

SDI is an R-element vector containing information about the regional decoupling of functional data from the underlying structure. To analyze spaceflight related changes in the SDI measure, a linear mixed model was applied considering interaction of time and group as fixed effect and subjects as random effect for pre- and post-flight data of two groups of subjects. For significantly altered regions a longitudinal analysis was also performed by fitting a linear mixed model to the SDI values of cosmonauts group considering time (preflight, postflight, and follow-up) as fixed effect and subjects as random effect. In all cases, p-values were corrected using FDR method.

Neurobehavioral Analysis

- **Mind Blanking.** To evaluate the similarity between mental states' functional connectivity patterns and the main resting state recurrent functional configurations, we extracted the five connectivity matrices preceding each probe as the functional repertoire of each specific mental state and then calculated their cosine similarity to the main resting state patterns. To consider the effect of hemodynamic response, all analyses were performed on the shifted versions of the connectivity matrices with time lags ranging from zero (five matrices before the probe) to three (two preprobe and three postprobe matrices). The selection of this time window was justified by the fact that ongoing experience can fluctuate slowly with a period of ~10 s (Van Calster et al., 2017), as well as by the nature of the hemodynamic response that reaches its maximum after three post-event

scans (Aizenstein et al., 2004). Cosine similarity between two sample matrices of A and B can be calculated as:

$$dist(A,B) = \frac{Tr(A^T B)}{\sqrt{Tr(A^T A)Tr(B^T B)}}$$

where Tr(.) indicates trace of a matrix. Cosine similarity determines how similar two matrices/vectors are irrespective of their norm. It can be considered as the normalized version of the Euclidean distance (i.e., projecting the vectors onto the unit sphere and calculating Euclidean distance, which is then effectively the cosine of the angle between those vectors). Subsequently, for each mental state the distribution of distances to all four centroids was created. A generalized linear mixed effect model with gamma distribution and log link function was applied to test the relationship between the distances to each pattern and the mental states. In this model, all mental state reports were considered as fixed effects and participants as random effects, with sex and age as confound variables. To correct for the multiple comparison problem due to fitting the model to the distance values of different patterns separately, an effect was considered significant if its p value was less than 0.05/K, where K is the number of patterns. In the case of a significant effect, a Tukey post hoc test was applied to compare each pair of mental states separately and to correct the type I error inflation due to multiple comparisons.

- **Psychedelics:** A canonical correlation analysis was conducted using the sixteen transition probability variables as predictors of the 5D-ASC and EDI variables, to evaluate the multivariate shared relationship between the two variable sets.

3

Toward Mental State Decoding at Rest

This chapter is based on:

Mortaheb, S., Liégeois, R., Raimondo, F., Boulakis, P. A., Fort, L. D., Moallemian, S., Sharifpour R., Karapanagiotidis, T., Van De Ville, D., and Demertzi, A., **2023**. Regional functional-structural coupling and decoupling can decode ongoing mental states during task-free conditions. OSF Preregistration, https://doi.org/10.17605/OSF.IO/TK3UW

3.1 Introduction

Ongoing experience is dynamic and rich in content, taking the form of mental states. Taking this view, a traditional challenge in computational neuroscience is to infer mental contents based on the functional and structural characteristics of the brain, which is known as "*mental state decoding*" or "*brain reading*" (Haynes & Rees, 2006; Poldrack, 2006; Poldrack, 2011). The development of brain reading algorithms can not only advance our understanding of brain-mind interactions, but can also be used for the cognitive evaluation of individuals who are unable to communicate directly (Monti et al., 2010).

Put simply, mental state decoders are **classification models** whose parameters are estimated based on the neural patterns to predict variant mental states. After estimation of the model parameters (training phase), decoders can take new neural patterns as inputs and predict in which mental state an individual is. In order to identify and investigate mental states, one can design a variety of highly controlled experimental paradigms characterized by a series of distinct states induced by a temporally constrained experimental design (Haynes & Rees, 2006; Schrouff et al., 2012). For example, using specific cognitive tasks some studies have attempted to decode particular mental states, such as mental imagery (Monti et al., 2010; Schrouff et al., 2012), lie detection (Davatzikos et al., 2005), and object recognition (Hanson & Halchenko, 2008). These studies considered functional activation patterns inferred from **general linear models (GLM)** fitting to fMRI signals as neural features of their designed decoder. The main challenge of decoding, though, comes for task-free conditions where ongoing experience is spontaneous and dynamic, forming a sequence of different mental states (i.e., thoughts, stimuli perception, and mind blanking as explained in Chapter 1; Van Calster et al., 2017).

As the resting paradigm precludes the use of cognitive tasks, one needs to resort to appropriate proxies to quantify spontaneous mental state contents as objectively as possible. Experience-sampling facilitates this endeavor using quantification of participants' mental states by providing them with options which best describe their state, either self-caught or via probing (Reed & Mihaly, 2014; Van Calster et al., 2017). While self-catching is suitable to study occurrences of pre-defined mental states, probing can capture various spontaneously occurring mental states. In that sense, during rest individuals are interrupted in random time points to report their immediate mental state.

After the definition of mental states during task-free conditions using experience-sampling, one can also characterize spontaneous brain activity

fluctuations over time to design relevant decoders. While during task-related conditions cognitive states are usually predicted using brain's functional activation patterns, in task-free conditions different mental states can be linked to the brain's functional and structural networks (Gonzalez-Castillo et al., 2019; Karapanagiotidis et al., 2017). For example, different aspects of ongoing thoughts have been linked to the different regions of the DMN (Karapanagiotidis et al., 2017; Smallwood et al., 2021), sensory perception has been associated with parts of VAN and DAN (Van Calster et al., 2017), and mind blanking has been shown to be linked to a globally coherent functional topology (Mortaheb et al., 2022). Resting state can also be viewed as a sequence of spontaneous "*cognitive-task-like*" processes (Gonzalez-Castillo et al., 2019; Shirer et al., 2012) such as working memory, visual or auditory attention, episodic or autobiographical memory, mathematical calculations, etc. Considering this model, one can learn the underlying functional organization of the related processes by performing specific cognitive tasks and using them to predict and decode those processes during rest (Gonzalez-Castillo et al., 2019).

While so far studies have used either the brain's functional or structural connectome as the input of their designed decoding model, recent studies argue that taking both functional and structural information into account and studying their regional interdependence can lead to more insight about cognitive states arising from the brain (Griffa et al., 2022; Preti & Van De Ville, 2019). Importantly, it has been shown that coupling of structure and function occurs in the regions related to lower-order cognition, such as visual and somatosensory cortices, while decoupling occurs in the regions related to higher-order cognition, such as emotion, autobiographical memory, and social cognition (Preti & Van De Ville, 2019). It has been shown that such features can be used to efficiently decode various cognitive states during task performance (Griffa et al., 2022). The question is whether these structural-functional signatures are also predictors of ongoing mental states during task-free conditions.

With the aim to predict ongoing mental states in task-free conditions, we developed a model which uses region-wise coupling and decoupling of the brain's functional activity to and from the underlying structural connectome. As task-free conditions span a wide range of mental states with their various dimensions, we here focused on the dominant dimensions of ongoing experience. Using **principal component analysis (PCA)**, previous studies have shown that when participants report their ongoing thoughts, the temporal (past vs future) and referent (self vs others) dimensions contribute the most into the principal components of their reports (Karapanagiotidis et al., 2017). At the same time,

when participants lay in the scanner with eyes open, they still have auditory and visual percepts which directs their mind temporal dimension to the present. As a result, the goal was to develop a decoder to predict the temporal and referent dimensions of ongoing thinking, and spontaneous occurrences of mind blanking during task free conditions.

3.2 Study Overview

Three different scenarios were defined for mental state decoding: i) decoding cognitive tasks that simulate mental states happening during rest, ii) decoding individual reports in an experience-sampling paradigm during rest, and iii) decoding individual reports in the experience-sampling paradigm based on the features extracted from the cognitive tasks (Figure 3.1A, B). In each scenario, we used structural-functional relationship features to train and test the designed decoder model (Methods Box 2). To this end, functional and structural data were acquired in two separate sessions. At the first session, data acquisition started by acquiring structural T1-weighted MPRAGE images, followed by functional MRI while participants were at rest with eyes open. Then, participants were invited to perform five cognitive tasks that simulated the principal mental states happening during rest. After a 30-minute pause, at the second session an experience sampling paradigm was performed to probe the actual mental states happening during rest (Figure 3.1C).

3.2.1 Cognitive Tasks

In the first session, five cognitive tasks were used: 1) remembering the past/imagining the future about self (PF-S), 2) remembering the past/imagining the future about others (PF-O), 3) auditory oddball (A-OB), 4) visual oddball (V-OB), and 5) self-caught mind blanking (MB; Figure 3.2, Methods Box 2). These tasks can be considered as proxies to the mental states happening during rest. The order of the tasks was random across participants, except for the mind blanking task, which was always presented first to avoid effects of accumulated fatigue.

3.2.2 Experience-Sampling during Rest

In the second session, we used an adaptation of novel experience-sampling paradigms to probe participants' ongoing experience (Van Calster et al., 2017). In this paradigm, participants were lying in the scanner with eyes open and at random times they were interrupted by an auditory probe inviting them to report their immediate mental state by button press (Figure 3.3). In the first step, they

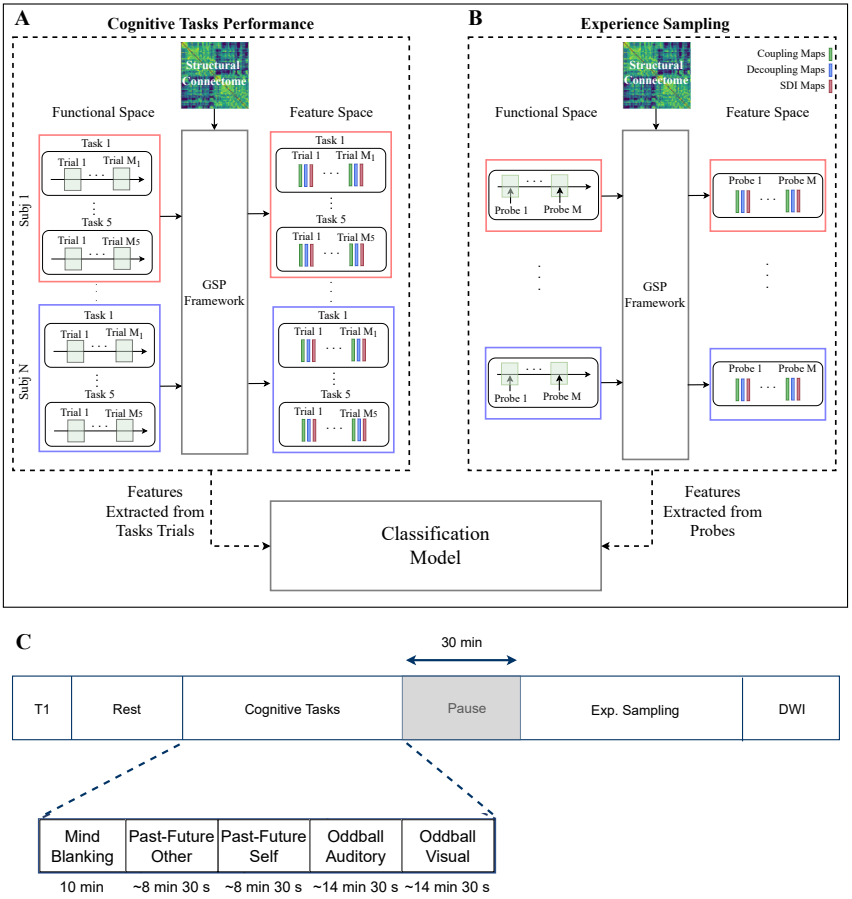

Figure 3.1. Study overview. A) Participants performed five cognitive tasks which simulated the mental states happening in the task-free conditions. Coupling, decoupling, and structural decoupling index (SDI) maps were extracted at the trial level for each subject and were used to train and test a classifier to classify corresponding cognitive tasks. **B)** In the second session participants performed an experience sampling task to report their actual mental states during rest. The same set of features were extracted at the probe level and a classifier model was used to predict the participants' responses. **C)** In the acquisition paradigm, the order of cognitive tasks was random across the participants. For each participant, the data acquisition was performed on the same day but in two sessions, between which 30 minutes pause took place in order to i) prevent the participants becoming drowsy, and ii) account for signal attenuation which takes place in the scanner after one hour of acquisition.

were asked to report whether their thought was in the "past", "future", "present", or simply "nowhere" (i.e., mind blanking). Based on their report, a

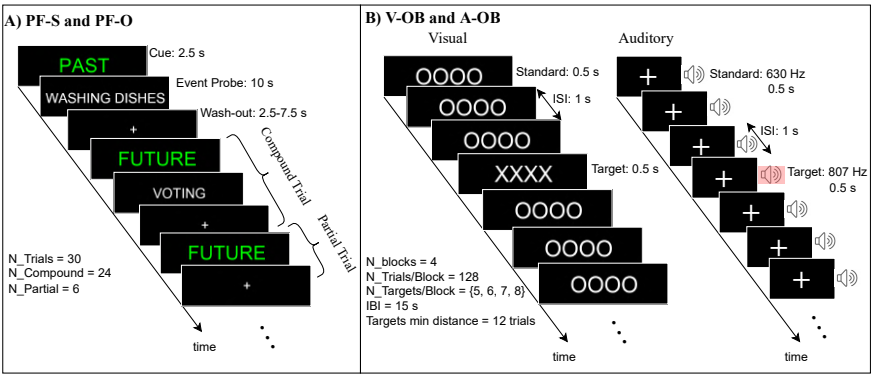

Figure 3.2 Cognitive tasks. **A)** In the Past-Future Self (PF-S) and Past-Future Other (PF-O) tasks, participants either remembered a specific event in the past or imagined it in the future based on the orientation cue at the beginning of each trial. This task was performed twice, once the event was related to the self, and the other time related to another person. Using these two tasks, the temporal and referent dimensions of the thoughts were studied. **B)** Classic oddball tasks were used to study attention to the deviant visual or auditory stimuli. We used two versions of oddball task, one visual (V-OB) and one auditory (A-OB). Each oddball task was performed in 4 separate blocks each containing 128 trials. (IBI: inter-block interval, ISI: inter-stimulus interval)

second question was asked. If their report was the “past” or the “future”, the second question asked whether this thought was about “yourself” or “others”, leading to four categories of responses as “Past-Self”, “Past-Other”, “Future-Self”, and “Future-Other”. If their report was the “present”, the second question asked whether they had a “sensory perception” or a “stimulus-dependent thought”, leading to two more categories of “Present-Sens”, and “Present-SDep”. If their report was “nowhere”, no further question was asked. In general, each participant was probed 25 times and the interval between each two probes was chosen randomly between 30 and 60 seconds. For each participant, the responses that took longer than 10 seconds were considered as the erroneous responses and were excluded from the analysis. The data acquisition of this session was finished by acquiring diffusion weighted images.

3.2.3 Feature Extraction

Regional structural-functional (de)coupling measures were estimated at the trial-level using graph signal processing (GSP; Ortega et al., 2018), explained in Chapter 2. In this framework, the idea is to span an algebraic space using structural harmonics estimated from the structural connectivity matrix, and

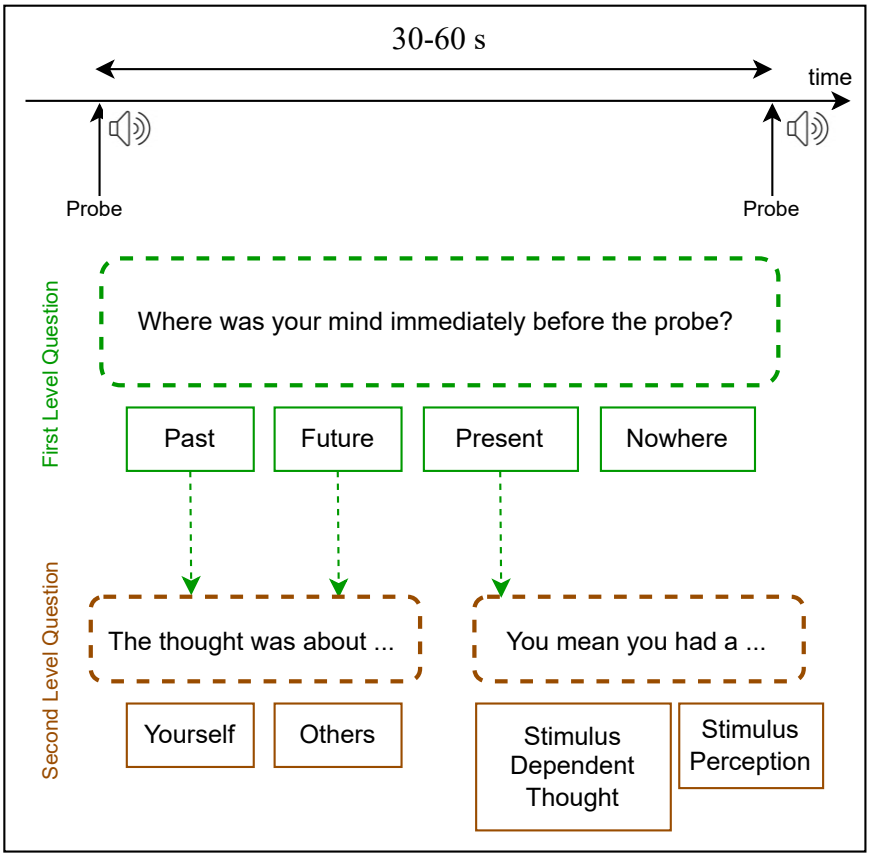

Figure 3.3 Experience-sampling. During experience-sampling, participants were at rest and their mind was free to wander. At random time points they were probed to report their mental state. At the first step, they reported the temporal dimension of their mental state by pressing corresponding buttons. If their mind was in the past or in the future, they answered a second question about the referent of their thought (i.e., the thought was about themselves or the others). If their mind was at present, they were asked to report whether they had a stimulus-dependent thought or a stimuli perception. If they reported their mind was nowhere, reports were considered as mind blanking and no further questions were asked.

represent each time point of functional data as the linear combination of estimated harmonics (See Methods box 1). We used the averaged structural connectome across all subjects as the representative anatomical connectivity of the group. Structural harmonics can be divided into low frequency and high frequency modes showing respectively distributed slow variation and localized

fast variation over the brain. The representation of functional data as the linear combination of structural harmonics allows the filtering of functional data at each time point into low frequency and high frequency components showing their slow and fast spatial variations respectively (Methods Box 1). Using this concept, one can introduce the so-called coupled and decoupled components of the functional data to and from the underlying structural connectome. In fact, region-wise Euclidean norm of low-pass filtered, and high-pass filtered versions of the functional leads to coupling and decoupling maps, respectively (Method Box 1). Further, division of decoupling by the coupling maps results in structural decoupling index (SDI) maps. These features were calculated for each trial of cognitive tasks and each probe of experience-sampling. For the experience-sampling probes feature extraction, an analysis window of 10 seconds length was considered before each probe. The selection of this time window was justified by the fact that ongoing experience can fluctuate slowly with a period of ~10 s (Van Calster et al., 2017). To account for hemodynamic effects, all the analysis windows were lagged by 5 time points for either cognitive tasks trials or experience-sampling probes. In fact, previous studies have shown that the peak effect of hemodynamic response function happens after ~6 seconds (Aizenstein et al., 2004), which is equivalent to 5 volumes considering the repetition time in our study (TR=1.17 seconds).

3.3 Results

Preliminary results are based on participation of eight healthy adults (5 women, 3 men, age: 29.5y ±3.9). All participants gave their written informed consent to take part in the experiment. The study was approved by the local ethics committee of the ULiège University Hospital (CHU Liège).

3.3.1 Structural Harmonics Estimation

The averaged structural connectome was used to estimate the structural harmonics (Figure 3.4A). The eigen decomposition of normalized Laplacian of structural connectome led to a set of **orthonormal** eigenvectors and their corresponding eigenvalues (Methods box 2). Eigenvalues increased from zero to 1.54 (Figure 3.4B) and had a notion of spatial frequency. It was shown by zeros-crossing rate of corresponding eigenvectors which counted the number of edges in the structural connectome whose nodes had values with the opposite sign in the eigenvector (Figure 3.4C). This notion was better understood by visualizing different structural harmonics corresponding to low and high eigenvalues (Figure 3.4D). Structural harmonics related to the low eigenvalues were characterized by

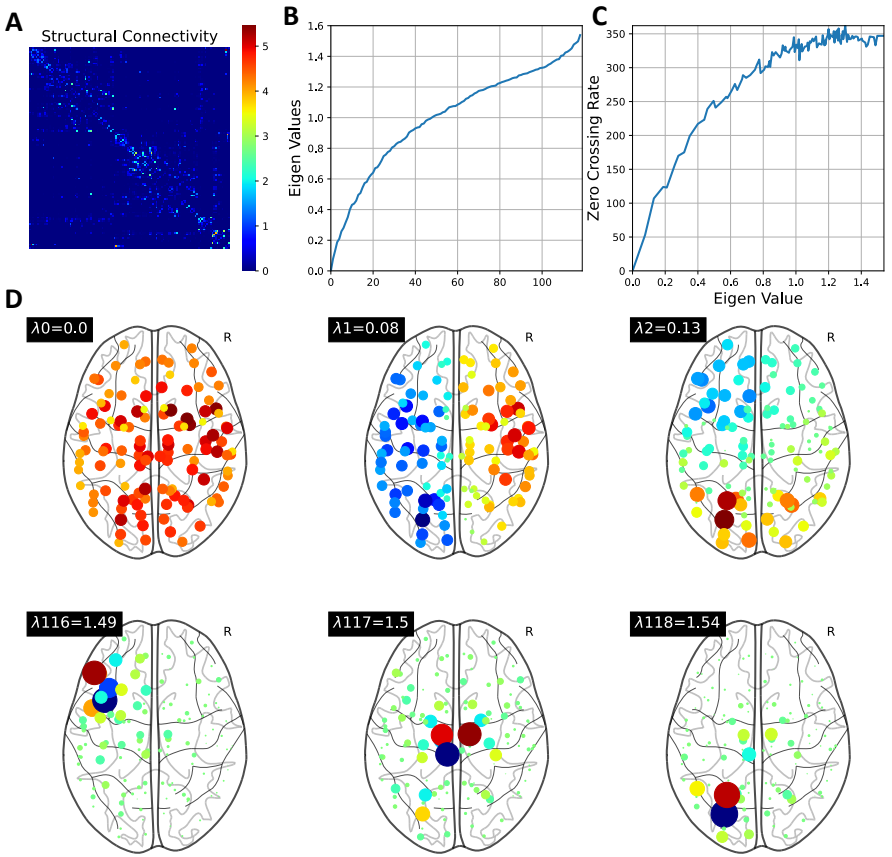

Figure 3.4 Structural harmonics estimation. A) The averaged structural connectome was calculated across all subjects to create a common space for structural-functional analysis. **B)** The eigenvalues of the normalized Laplacian of structural connectome are increasing from zero to 1.54. **C)** These eigenvalues have the notion of frequency as the zero-crossing rate of their corresponding eigenvectors are also increasing. **D)** The eigenvectors corresponding to the lower eigenvalues show a slow and distributed variation over the brain structure, while the eigenvectors corresponding to the higher eigenvalues show a fast and localized variation.

slow variations across the brain structure while the harmonics related to the higher eigenvalues were characterized by localized and fast variations. In order to define low and high frequency harmonic modes for further analyses, a cut-off eigenvalue should be chosen. Instead of choosing a fixed value, we performed feature extraction and decoding based on a wide range of cut-off eigenvalues.

3.3.2 Decoding Cognitive Tasks

We used a support vector machine (SVM) classifier with a linear kernel to classify cognitive tasks trials based on the extracted features. The classification model was trained and tested using a stratified 4-fold cross validation with 10 repeats and a one-vs-all classification approach. Because of the low number of participants, decoding was performed at the trial level. Z-score normalization and PCA were applied on the extracted features prior model training and test. Due to the variability in the number of different mental state reports, this dataset was highly imbalanced. To evaluate the classifier's performance for imbalanced datasets, specific measures such as *precision*, *recall*, and *balanced accuracy* can be used. While precision is defined as the ability of the classifier not to label as positive a sample that is negative, recall is the ability of the classifier to classify positive samples correctly. In that sense, balanced accuracy can be defined as the average of the recall values across the classes. This is equivalent of calculating classifier accuracy while each sample is weighted according to the inverse prevalence of its true class which accordingly will avoid inflated performance estimates on imbalanced datasets (refer to Appendix B for more details). These metrics were calculated for different feature vectors and cut-off eigenvalues and the one with the highest balanced accuracy was considered as the best decoder. The following results are based on the best decoder performance.

Temporal dimensions of cognitive tasks were decoded higher than chance-level. We first categorized the task trials into four groups related to their temporal dimension, i.e., Past, Present, Future, and Nowhere. While PF-O and PF-S tasks were directly related to the Past and Future, A-OB and V-OB trials were assigned to the Present, and MB trials were considered as the mind was nowhere. Trials related to the Present time were classified with higher balanced accuracy than the other temporal dimensions, while MB reports showed lower performance (Figure 3.5). The best performance of decoder for each temporal dimension achieved by decoupling maps as feature vectors (Table 3.1).

Reference dimensions of cognitive tasks were decoded higher than chance-level. The PF-S and PF-O tasks also examined the reference dimensions, namely thoughts about self vs. thoughts about others. We also tested if the designed decoder is capable of differentiating the referent of our thoughts at different temporal dimensions. Classification results showed that the balanced accuracy was higher than the chance level (i.e., 0.5) for both Past and Future thoughts (Appendix C, Figure C1). The highest balanced accuracy for referent of thoughts in the Past was achieved while using coupling feature vectors with a cut-off

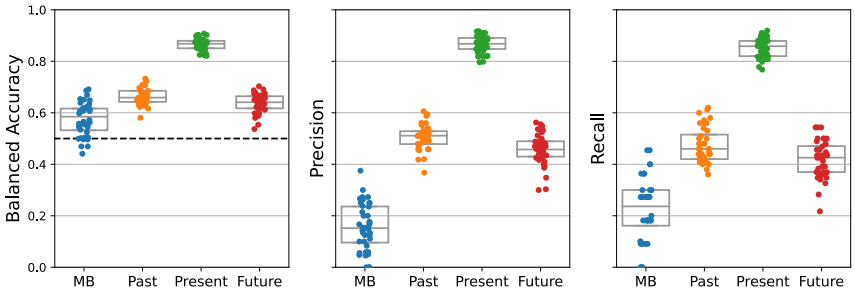

Figure 3.5 The temporal dimensions of cognitive tasks could be decoded higher than chance-level. Classifying the tasks' temporal dimensions using a one-vs-all approach showed that these were decoded higher than chance-level. The decoupling measure calculated based on medial cut-off frequencies showed the highest performance among the feature vectors. While Present was decoded with the highest decoding accuracy, the MB reports showed the lowest.

Table 3.1. The best averaged performance of decoder for each temporal dimension.

Classifier	Feature	Cut-off Eigenvalue	Balanced Accuracy	Precision	Recall
Past vs all	Decoupling map	50	0.66	0.50	0.47
Present vs all	Decoupling map	80	0.87	0.87	0.85
Future vs all	Decoupling map	70	0.64	0.46	0.42
MB vs all	Decoupling map	70	0.58	0.16	0.23

eigenvalue of 20 (mean balanced accuracy=0.58, mean precision=0.57, mean recall=0.56; Appendix C, Table C1). On the other hand, the best balanced accuracy for referent of thoughts in the Future was achieved while using SDI feature vectors with a cut-off eigenvalue of 80 (mean balanced accuracy=0.55, mean precision=0.56, mean recall=0.56; Appendix C, Table C1).

3.3.3 Decoding Experience-Sampling Reports During Rest

The same decoding approach that was designed for the cognitive tasks' classification was also used to predict the subjective reports during experience-sampling.

Behavioral analysis. During the experience sampling, MB was reported fewer times (median=3, IQR=3.5, min=0, max=7) and future-oriented thoughts were reported more often than any other mental state (median=11, IQR=4.5, min=4, max=15). Pair-wise comparisons showed that just the number of future thoughts

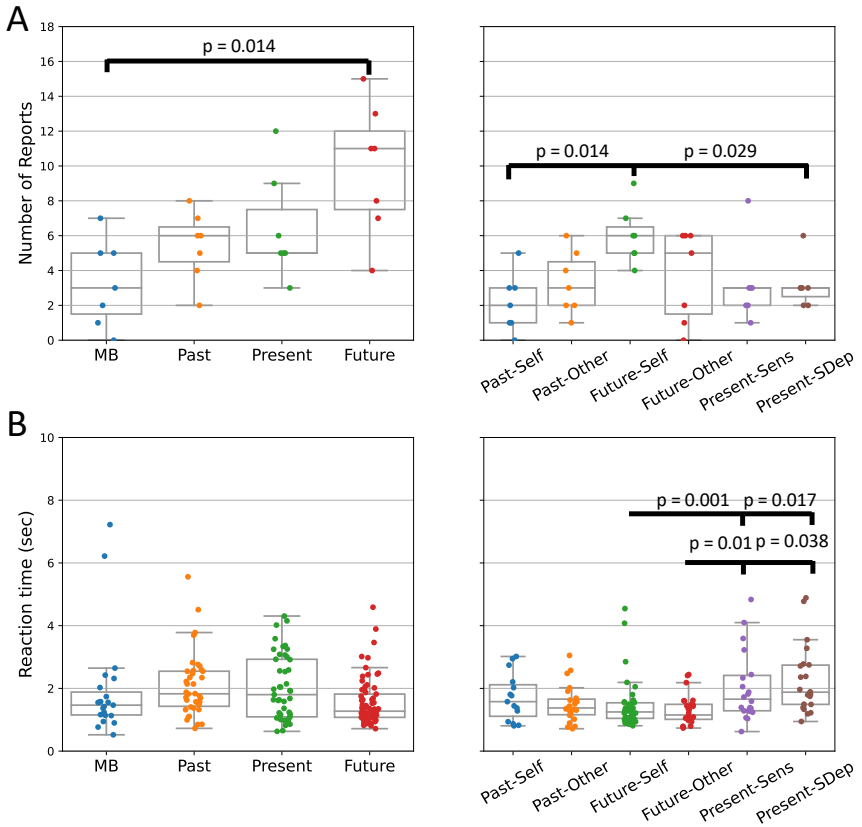

Figure 3.6. Behavioral characteristics of experience-sampling paradigm. (A) *left.* Ongoing mental states are characterized by a high number of reports about Future thinking and by a low number of reports about mind blanking. *right*. In addition, these future thoughts were mainly self-focused. **(B)** *left.* In terms of reaction times, no significant effect of temporal dimensions of mental states on reaction times was observed. *Right*. On the other hand, a significant effect of reference dimension of mental states was observed showing that Future-Self and Future-Other were reported faster than Present-Sens and Present-SDep.

and MB reports are significantly different (paired t-test, t=3.851, p=0.014, FDR-corrected; Figure 3.6A left panel). This high number of future thoughts were mainly related to the Self (median=6, IQR=1.5, min=4, max=9; Figure 3.6A right panel). Also, Future-Self thoughts were significantly higher in occurrence than Past-Self (paired t-test, t=4.361, p=0.001, FDR-corrected), and Present-SDep thoughts (paired t-test, t=3.573, p=0.004). Considering reaction times, there

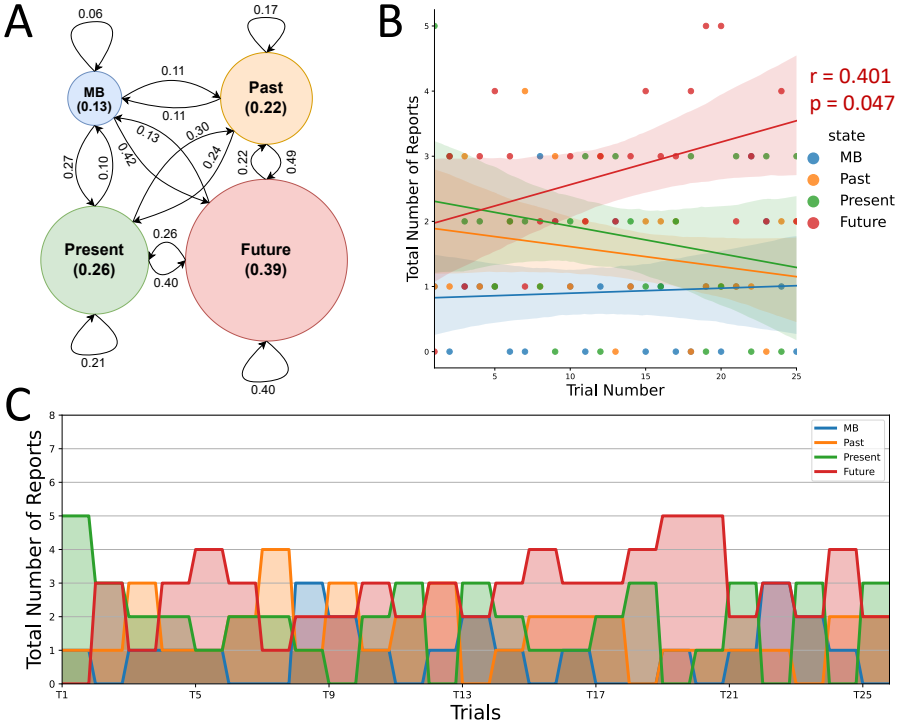

Figure 3.7. There is high tendency towards the Future Thought state with the passage of time. (A) Transition dynamics over the course of experience-sampling shows that there is a high probability of going into Future Thought state after any other mental state reports. All probability measures are the averaged values across subjects. Diameter of the circles are proportional to the probability of each mental state report. **(B, C)** Calculating the total number of reports over all subjects and over the acquisition time shows that with the passage of time the number of Future thought reports also increases significantly.

were no significant effect of mental states on the temporal dimensions of mental states ($\chi2[3]=6.644$, p=0.084, generalized linear mixed model analysis; Figure 3.6B left panel). However, in terms of reference dimension of mental states, there was a significant effect of mental state ($\chi2[5]=23.347$, p=0.0003; generalized linear mixed model analysis; Figure 3.6B right panel), with Future-Self being reported faster than Present-Sens (z=3.886, P=0.001) and Present-SDep (z=3.203, P=0.017), and Future-Other being faster than Present-Sens (z=3.362, p=0.010) and Present-SDep (z=2.942, p=0.038; post-hoc Tukey test).

Dynamic transitions between mental state reports showed an overall high tendency to go into the Future-Thought state and an overall low tendency to go into the MB state (Figure 3.7A). Finally, in terms of distribution of reports over the acquisition time, there was a positive correlation between the total number of Future Thoughts over all the subjects and probe number (r=0.401, p=0.047; Figure 3.7B), which shows an increase in the number of Future Thoughts as the experiment continues (Figure 3.8C). On the other hand, no significant correlation was found for MB (r=0.062, p=0.767), Past (r=-0.225, p=0.279), and Present (r=-0.241, p=0.245) mental states.

Temporal dimensions of thoughts were decoded higher than chance-level. Considering participant responses to the first-level question, we categorized experience-sampling probes into four classes related to the temporal dimensions of the thoughts: Past, Present, Future, and Nowhere. Different combination of features and cut-off frequencies led to higher than chance-level balanced

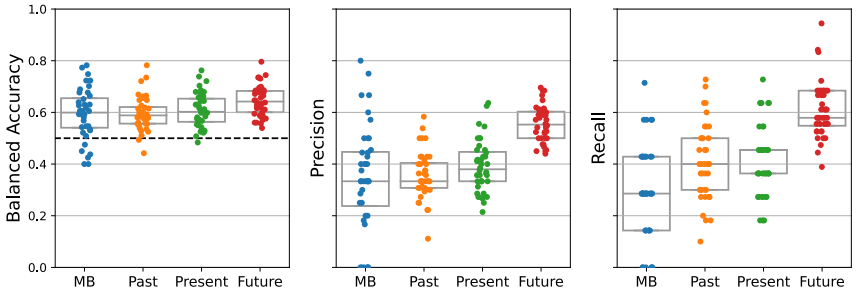

Figure 3.8. The temporal dimensions of thoughts during rest could be decoded higher than chance-level. Decoding of thoughts temporal dimensions using a one-vs-all approach showed that they could be decoded higher than chance-level. While Future time was decoded with the highest decoding accuracy, MB reports showed the lowest.

Table 3.2. The best performance of decoder for each temporal dimension of thoughts during rest.

Classifier	**Feature**	**Cut-off Eigenvalue**	**Balanced Accuracy**	**Precision**	**Recall**
Past vs all	Decoupling map	70	0.60	0.36	0.41
Present vs all	Coupling map	40	0.61	0.39	0.42
Future vs all	SDI map	110	0.65	0.56	0.61
MB vs all	Decoupling map	40	0.60	0.35	0.29

accuracy for thought temporal dimension prediction (Figure 3.8). The classifier's best performance measures are summarized in Table 3.2.

Reference dimensions of thoughts were decoded higher than chance-level. If the mind of participants were at the Past or in the Future, in the second question they had to response whether their thought was about themselves or another person. Different combination of features and cut-off frequencies were shown to be able to classify self-related and other-related reports at each temporal dimension higher than chance-level (Appendix C, Figure C2 and Table C2).

3.3.4 Decoding Experience-Sampling Reports based on Tasks Features

In the third scenario, we trained the classifier based on the features extracted from the cognitive tasks and tested its performance based on the features extracted from the experience-sampling paradigm.

Temporal dimensions of thoughts were decoded higher than chance-level. Evaluating performance of the decoder in classifying the experience sampling probes showed that all temporal dimensions of thoughts can be decoded higher than chance level (Figure 3.9 and Table 3.3). Particularly, the best performance was achieved for the Past thoughts using SDI maps (balanced accuracy=0.64, precision=0.33, and recall=0.72), while MB reports were successfully decoded using decoupling maps (balanced accuracy=0.60, precision=0.22, recall=0.54).

Reference dimensions of thoughts were decoded higher than chance-level. Considering the Past and the Future thought reports, classification of self-related and other-related probes at each temporal dimension showed that the performance of decoding is higher in the Past thoughts when compared to the Future thoughts (Balanced Accuracy=0.62, precision=0.58, and recall=0.58; Appendix C, Figure C3 and Table C3). While the coupling feature vectors showed higher performance in reference classification of the Past thoughts, decoupling feature vectors showed higher performance for the Future thoughts (Appendix C, Table C3).

3.4 Discussion

During resting state, the mind freely wanders through time and space and gets occupied with different contents (Smallwood et al., 2021). In this study, we investigated the decodability of the ongoing mental states based on the brain's

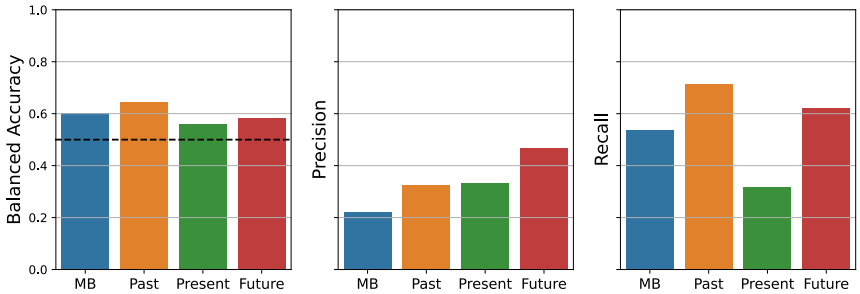

Figure 3.9 Temporal dimensions of thoughts during rest can be decoded higher than chance-level from the temporal dimensions of tasks. Decoding of temporal dimensions of thoughts during rest using a one-vs-all classifier trained on task data shows that they can be decoded higher than chance-level in specific combinations of features and cut-off eigenvalues.

Table 3.3. The best performance of decoder for each temporal dimension of thoughts during rest.

Classifier	**Feature**	**Cut-off Eigenvalue**	**Balanced Accuracy**	**Precision**	**Recall**
Past vs all	SDI map	20	0.64	0.33	0.72
Present vs all	Coupling map	10	0.56	0.33	0.32
Future vs all	SDI map	20	0.58	0.47	0.62
MB vs all	Decoupling map	80	0.60	0.22	0.54

underlying neural mechanism. As resting state is an unconstrained condition, the ongoing mental states can be highly variable across time that makes their decoding a challenging problem in neuroscience.

We used a modified version of experience-sampling paradigm together with fMRI acquisition to quantify the dynamism of ongoing mental states, as well as the underlying neuronal activity. Behaviorally, we found that ongoing cognition is composed of low probable occurrences of mind blanking (13%), accompanied by environmental thoughts or perceptual events (26%), and highly probable wandering of mind through time, also known as mental time travel (61%; Karapanagiotidis et al., 2017). These findings are in line with previous studies which also tried to formulate different ongoing mental states during rest (Kane et al., 2007; Van Calster et al., 2017; Ward & Wegner, 2013). We also found that the most common reported mental state was self-focused future thoughts (39%). This is also in line with previous studies in which used principal component

analysis to show that the first principal component of ongoing thoughts is related to the future and self (Karapanagiotidis et al., 2017). We also found that these Future thoughts have higher occurrence probabilities at the end of the acquisition, while other mental states are uniformly distributed across the time course of the data acquisition. In fact, when participants get familiar with the scanner environment and learn how to perform the experience-sampling task, their mind gets less engaged to the environment and fills with stimulus independent thoughts, showing themselves mainly as future self-focused thoughts. We should notice that this mental dynamic formulation is not directly related to the ongoing mental spontaneity as in the experience-sampling paradigm the subjective reports are gathered every 30-60 seconds. However, investigating different aspects of this dynamism is important as it is the source of imbalanced mental state reports which affects any decoding approach (Ramyachitra & Manikandan, 2014).

When subjects are at rest, they often engage in a series of self-paced cognitive processes including visual imagery, episodic memory recall, future planning, somatosensory sensation, etc. (Delamillieure et al., 2010; Van Calster et al., 2017). As a result, one can describe the resting state as short periods of "spontaneous cognitive-task-like processes" (Gonzalez-Castillo et al., 2019). Considering this, we performed mental state decoding in three different scenarios: i) train and test the decoder using specific cognitive tasks that simulate mental states during rest, ii) train and test the decoder using actual mental state reports in an experience-sampling paradigm, and iii) train the decoder based on the features extracted from the cognitive tasks and test its performance on predicting experience-sampling reports. In the first scenario, we used specific tasks to orient participants' minds into different temporal dimensions and to manipulate the referent of their thought contents. The advantage of this approach is that the tasks are controlled, and their occurrence rate and duration can be designed. However, these constraints also make the situation not completely similar to what happens during rest. The second scenario is more realistic. Participants report their actual mental states, and their mind is not constrained. The disadvantage of this scenario is that the number of mental state reports can be highly imbalanced, and no information exists regarding duration of each mental state. This can affect the decoder training efficiency. As a result, we proposed the third scenario, in which the decoder is trained on a more controlled and balanced dataset gathered from task performance and is used to decode the mental states during rest. Our decoding model performed higher than chance-level in all three scenarios. Although higher than chance-level, the

decoder performance was different for various mental states in each scenario. This was further shown to be affected by the extracted feature vectors used to train and test the decoder.

In this study, we used feature vectors explaining regional coupling or decoupling of functional activity to and from the underlying structural connectome to decode the mental states. While the coupling index is related to the low variation and distributed spatial functional activity, decoupling mainly describes fast changing local functional activity over the structure of the brain (Medaglia et al., 2018). The division of the decoupling index by coupling index infuses the information contained in these two indices into a single index called the structural decoupling index (SDI; Preti & Van De Ville, 2019). All these neural indices have been shown to have cognitive relevance, and can be used to decode cognitive tasks and fingerprinting (Griffa et al., 2022). In this study, we showed that these indices can also be used to decode ongoing mental states. Particularly, we showed that temporal dimensions of cognitive tasks were decoded using decoupling indices, indicating that more localized functional activity supports the temporal dimensions of cognitive tasks. On the other hand, the temporal dimensions of the experience-sampling reports were more heterogenous, meaning that different features of coupling, decoupling, and SDI could be used to decode them efficiently. This observation comes from the fact that during the resting state the mind is less constrained and more distributed functional activity can be observed.

Taken together, we showed that the underlying dynamic coupling and decoupling profile of functional activity to and from the brain can support the ongoing mental states during rest. This study also has several limitations. First, using self-reports to characterize the ongoing mental states could be unreliable. This is because self-reports are usually subject to contextual and motivational biases (Nisbett & Wilson, 1977), which limits the experience-sampling data to reveal real ongoing cognition. Second, the ongoing mental state reports are highly variable across participants, leading to highly imbalanced datasets. This not only limits the ability of mental state decoders, but also leads to imprecise performance evaluations. In this study, we used balanced accuracy together with precision and recall trying to reduce the effect of an imbalanced dataset in performance evaluation. In addition, recruiting young healthy participants for the study was another source of having imbalanced dataset, leading to higher number of future thought reports than the other mental states. Adding older participants to the study not only leads to the development of more general decoders, but also can lead to a less imbalanced dataset. Third, regarding self-

catch paradigm, with the current design, it is not possible to distinguish between the time participants have a specific mental state and the time they decide to report that. More advanced designs are required in future studies to overcome this issue. Finally, small sample size limited our study's ability to generalize results and prevented us from using more realistic models (e.g., multi-class multi-label classification). With higher power from a larger sample size, more generalizable results and more realistic models can be achieved.

Methods Box 2

Mind blanking task. To simulate the spontaneous occurrences of mind blanking, we used a self-catching paradigm (Ward & Wegner, 2013). In this task, participants were at rest with eyes open, fixating on a black screen. Participants were asked to press a button whenever they felt they had a mind blanking state, defined as a state where participants were not able to remember what they had in their mind. The task total duration was 10 minutes.

Remembering past/imagining future (self/other-focused) tasks. The aim in this task was to simulate remembering a topic in the past or imagining it in the future using the variations of currently published tasks (Gilmore et al., 2018). Participants were asked to envision a specific scenario in response to one of the two task orientation cues (Figure 3.2A). The orientation cues directed the participants to either remember a specific event in the past or imagine a specific event that might occur in the future. There were two different versions of this task: a) a "self-related" version, in which participants had to remember or imagine the events about themselves, and b) an "other-related" version, in which this had to be about other people. At each trial of the task, participants were shown an orientation cue for 2.5 seconds, during which they were instructed whether they should remember an event or imagine it in the future. Thirty randomly distributed trials were used, of which 15 were related to remembering the past and 15 were related to imagining the future. In 80% of the trials (24 trials), the orientation cue was followed by a word or phrase (showing a topic) which lasted for 10 seconds. These trials are called compound trials. The other 20% of the trials (6 trials) ended after the orientation cue and no topic was shown to the participants. They are called partial trials. The order in which compound and partial trials were shown to the participants was random. Inter-trial interval was chosen randomly between 2.5 and 7.5 seconds during which participants were looking at a fixation cross and they had to clear their mind and wait for the next orientation cue. In this experiment, topics were chosen from 32 words and short phrases (see Appendix A). The task total duration was about 8minutes and 30 seconds.

Oddball (auditory and visual) tasks. To simulate the external stimuli perception conditions, we used the standard auditory and visual oddball paradigms that have been adapted to the fMRI acquisitions (Stevens et al., 2000). Each oddball paradigm consisted of 4 blocks. Each block was made of 128 trials of which 5 to 8 were rare target trials and the rest were frequent standard trials (Figure 3.2B). Participants were asked to count the number of target trials and report at the end of each block. To account for the hemodynamic activity resulting from the rare target trials, there were at least 12 standard trials between each two target trials. In the visual oddball paradigm, the standard stimuli were "OOOO", and the target stimuli were "XXXX", while in the auditory paradigm, the standard stimuli were presented as a beep with a

frequency of 630 Hz, and the target stimuli were presented as a beep with a frequency of 807 Hz. In both paradigms, each stimulus lasted for 500 ms with an inter-stimulus interval of 1000 ms. Blocks were separated with an interval of 15 seconds. The task total duration was about 14 minutes and 30 seconds.

Imaging Setup. All MR images were acquired on a whole-body 3T scanner (Magnetom Prisma, Siemens Medical Solutions, Erlangen, Germany) operating with a 20-channel receiver head coil. For anatomical reference at each session, a high-resolution T1-weighted image was acquired for each subject (T1-weighted 3D magnetization-prepared rapid gradient echo (MPRAGE) sequence, TR = 1900 ms, TE = 2.19 ms, inversion time (TI) = 900 ms, FoV = 256x240 mm^2, matrix size = 256x240x224, voxel size = 1x1x1 mm^3, acceleration factor in phase-encoding direction R=2).

Multi-slice T2*-weighted functional images were acquired with the multi-band gradient-echo echo-planar imaging sequence (CMRR, University of Minnesota) using axial slice orientation and covering the whole brain (36 slices, multiband factor = 2, FoV = 216x216 mm^2, voxel size 3x3x3 mm^3, 25% interslice gap, matrix size 72x72x36, TR = 1133 ms, TE = 30 ms, FA = 90°). The five initial volumes were discarded to avoid T1 saturation effects. To remove the physiological noise, respiration and cardiac pulsation signals were also recorded.

Diffusion-weighted (DW) data were acquired using a multiband SE-EPI sequence (Center for Magnetic Resonance Research (CMRR), University of Minnesota), with 2mm isotropic spatial resolution. Acquisition parameters include TR = 4030 ms, TE = 69.80 ms, 70 transverse slices, slice thickness = 2 mm and slice acceleration factor = 2, in-plane resolution 2x2 mm^2 (FoV = 192x216 mm^2, matrix = 96x108) and acceleration factor 2, bandwidth per pixel = 2264 Hz/Px. The multi-shell diffusion-weighted imaging (DWI) scheme included 118 volumes. The first volume was discarded to avoid T1 saturation effect. The remaining 117 volumes corresponded to a total of 105 DW images interleaved with 12 b=0 images. The set of diffusion directions which was created using electrostatic repulsion (Slater et al., 2019) was defined over three shells (b = 650, 1000 & 2000). For the purpose of susceptibility-induced distortion correction, 5 additional b=0 volumes was acquired with the same acquisition parameters as above, but inverted phase encoding (PE) direction (Andersson et al., 2003).

Data Preprocessing. The fMRI data were preprocessed and denoised using locally developed pipeline based on SPM12 (Penny et al., 2011). In this pipeline, after susceptibility distortion correction and realignment, functional data were registered to the high resolution T1 image, then normalized to the standard MNI space, and finally was smoothed using a Gaussian kernel with a full width at half maximum (FWHM) of 6. After segmentation of structural T1 image into grey matter (GM), white mater (WM), and CSF masks, the bias corrected structural image and all the extracted masks were normalized to the MNI space. Further, WM and CSF masks were eroded

by one voxel to remove any overlapping between these tissues and the GM voxels. To denoise functional time series, a general linear model (GLM) was fitted to each voxel data separately, regressing out the effect of six movement parameters (translation in x, y, and z directions, and rotation in yaw, roll, and pitch directions), constant and linear trends using zero-order and first-order Legendre polynomials, 5 principal components of signals in the WM and CSF masks, physiological data (i.e., respiration and cardiac pulsation), and outlier data points. Outlier detection was performed using ART toolbox (http://web.mit.edu/swg/software.htm). Any volume with a movement value of greater than 3 mm, rotation value of greater than 0.05 radians, and z-normalized global signal intensity of greater than 3 was considered as an outlier. After regressing out these nuisance regressors, the remaining signal was used for further analysis. Schaefer atlas with a resolution of 100 ROIs (Schaefer et al., 2018) together with additional 19 subcortical regions was used to extract the averaged BOLD signals inside each ROI.

For the DWI images, all the preprocessing, denoising, and structural connectivity (SC) estimation steps were performed in MRTrix3 (J.-D. Tournier et al., 2019). Susceptibility-induced and eddy current-induced distortions, as well as movements were estimated and corrected using topup (Andersson et al., 2003) and eddy(Andersson & Sotiropoulos, 2016b) in FSL 6.0.4. Further, the denoised images were bias corrected using ANTs (Tustison, Avants, Cook, Zheng, et al., 2010). After registering the structural T1 image to the DWI image, it was segmented into 5 tissue types using FSL. Response functions of GM, WM, and CSF were estimated using Dhollander algorithm (Dhollander et al., 2019). A multi-shell multi-tissue constrained spherical deconvolution approach was used to estimate fiber orientation distributions at each voxel (Jeurissen et al., 2014b, p.) and further, they were normalized (Raffelt et al., 2017). One million tracts were generated using probabilistic iFOD2 algorithm (J.-D. Tournier et al., 2010). Considering a Schaefer atlas with 100 ROIs and 19 attached subcortical regions, a structural connectivity matrix was created by counting the number of streamlines between each pair of regions normalized by the sum of the related regions volumes.

Behavioral Analysis. Paired t-tests were used to compare the number of reports of each mental state across participants (P-values were FDR-corrected with a significance level of $\alpha = 0.05$). A generalized linear mixed model with a gamma distribution and inverse link function tested the relationship between reaction times and mental states. The choice of the generalized linear mixed model was because of a positive tail in the distribution of reaction times and inhomogeneity of variance across mental states caused by an imbalanced number of reports. Mental state reports were considered as fixed effects, and participants were considered as the random effects. In case of significant main effects, a post-hoc test was applied for pairwise comparisons. For that, we used the Tukey method to correct the type I error inflation that occurred in the multiple comparisons. To model dynamic transition between mental state reports, a Markov model was used to calculate the transition

probabilities between participants' reports over the experiment. To detect any possible trend in the mental state reports during over the acquisition time, the sum of mental state reports at each trial number was calculated across the subjects for each mental state and the Pearson correlation between this value and trial numbers were estimated.

Decoder Design. Considering the graph signal processing framework explained in Methods Box 1, coupling, decoupling, and SDI vectors were calculated for each trial of each task and each probe of the experience-sampling paradigm, for each subject separately. A support vector machine (SVM) classifier with linear kernel was used as the decoder. The classifier was trained and tested considering: i) coupling vectors as feature, ii) decoupling vectors as features, and iii) SDI vectors as features. Each feature vector was estimated based on different cut-off eigenvalues from 10th to 110th eigenvalue with incrementing steps of 10. The decoder was trained and tested in three different scenarios: 1) train and test using features of cognitive tasks, 2) train and test using features of experience-sampling task, and 3) train based on the task features and test on the experience-sampling features. At each scenario, different feature vectors calculated using different cut-off eigenvalues were used for decoding and the best decoding performance was reported. Due to the highly imbalanced dataset of mental state reports, balanced-accuracy, recall, and precision metrics were used to assess the decoder performance at each scenario (See Appendix B). For cross-validation, a stratified 4-fold strategy with 10 repetitions was used and the performance of each repetition was considered in the performance analysis. To implement the decoder, we used the locally developed codes which use Julearn python package, designed for high-level machine learning applications (https://juaml.github.io/julearn/main/index.html).

4 Final Discussion and Conclusion

4.1 General Discussion

Current noninvasive imaging techniques, together with mathematical frameworks, have helped researchers to model the human brain as a complex network of interacting neuronal elements. This modeling approach led to the definition of structural and functional networks that support diverse cognitive functions and ongoing mentation. Specifically, during rest the functional network alters dynamically which can be characterized at the system level by a finite set of functional connectivity patterns; considering that, the underlying brain dynamics can be modeled as spontaneous transitions between those FC states. In addition, the functional organization that the brain takes at each state can be constrained to or completely liberal from the structural network. This makes the brain's structural-functional relationship also a dynamic phenomenon. The question I asked in this thesis was how these spontaneous changes in the brain's configuration are associated with our ongoing subjective experience during resting state.

We investigated this question from different perspectives: neural correlates of spontaneous occurrences of mind blanking, effects of external pharmacological perturbations on the brain and mind, effects of environmental changes on the brain dynamics, and mental state decoding at normal wakeful rest conditions. During resting state, there are spontaneous occurrences of mind blanking which have not been widely investigated so far. We found that a combination of highly integrated FC state and high global signal amplitude leads to mind blanking periods. On the other hand, administration of psilocybin as an external perturbation factor makes the highly integrated FC state an attractor state in the brain's dynamical landscape but accompanied with a low global signal amplitude. Further, long-term exposure to microgravity showed that structural-functional coupling profiles play as a specific compensatory mechanism which adapts brain functioning in confronting with new environmental circumstances. In an attempt to decode mental states during rest, we also found that such structural-functional (de)coupling profiles are associated with the ongoing cognition.

We can summarize the main findings of this thesis into three main concepts: i) a spontaneously occurring functionally hyper-connected state affects our experience of self and environment during rest, ii) global signal as a proxy of physiological state plays an important role in our ongoing subjective experience during rest, and iii) regional structural-functional (de)coupling during rest is a signature of our ongoing mentation. In this chapter we discuss these three

findings in more detail and based on the results of the thesis we suggest future perspectives to continue this research.

4.1.1 Functionally Hyper-Connected State during Rest

Ongoing cognition is a dynamic interaction between integration and segregation (Shine, 2019). In this regard, fluctuations of the functional connectome during rest can be characterized using a finite set of spontaneously occurring connectivity patterns defined by specific integration and segregation profiles. Among them, a specific pattern characterized by overall positive inter-areal coherence, showing maximal integration and efficiency and minimal segregation and modularity, plays an important role in human cognition. This FC state has been reported in various studies, appearing during NREM sleep (El-Baba et al., 2019), mind-blanking instances (Mortaheb et al., 2022), epileptic episodes (Glynn & Detre, 2013), and administration of psychedelic drugs (Lord et al., 2019; Tagliazucchi et al., 2016). Unique network-level features of this FC pattern and its presence in a wide range of neurobehavioral studies poses the question about the role of this state in the dynamical landscape of functional patterns. Investigation of behavioral and neurophysiological counterparts of this connectivity pattern can help us to better understand this connectivity profile.

From the behavioral perspective, as this hyper-connectivity pattern appears in various states across the wakefulness-arousal axis (from sleep to psychedelic state), it is difficult to establish a coherent, overlapping behavioral pattern associated with its presence. However, the most homogeneous feature appears to be an overall detachment of perception of internal/external stimuli from awareness and altered conscious experience. In this thesis, we first observed that hyper-connectivity was predictive of mind blanking, a unique phenomenological state of inability to recover the content of our mind into the awareness (Mortaheb et al., 2022). While it is still unclear whether mind blanking has cognitive (Andrillon et al., 2021) or metacognitive (Efklides, 2014) origins, it appears that presence of hyper-connectivity pattern inhibits access to conscious experience, resulting in experiences of mental absences, usually accompanied by a decline in performance in attentional tasks (Andrillon et al., 2021; Ward & Wegner, 2013). This has been related to decrease of arousal and presence of local sleeps during wakefulness (Andrillon et al., 2021). In the same line, this pattern was also reported to be prevalent during NREM sleep which is also characterized by lowest levels of arousal (El-Baba et al., 2019). On the other hand, in this thesis, in line with other studies (Lord et al., 2019; Tagliazucchi et al., 2016), we found that this hyper-connectivity can also be dominant as a result of psychedelic drugs

intake, leading to profound shift in awareness levels, without a noticeable change in wakefulness levels. This state is categorized by the "diffusion" of the boundaries between the self and the environment, experiencing a lack of differentiation between self and external representations and a holistic sensation (Nour et al., 2016). Observing this FC state in two different arousal and awareness levels with completely different behavioral counterparts allows us to investigate more deeply the neurophysiological substrates of this pattern.

From the neurophysiological perspective, when this connectivity pattern is accompanied by high global signal amplitude, it can be act as a signature of low arousal and presence of slow-wave activity in the brain. In fact, presence of periods of neural silencing during wakefulness shows itself as slow-wave activity which further leads to local sleeps (Vyazovskiy et al., 2011). Slow-wave activity and local sleeps in parietal regions were shown to be signatures of mind blanking (Andrillon et al., 2021). In addition, studies on rats using administration of isoflurane showed that progressive decrease in arousal is associated with increased intensity of slow wave activity and increased strength of functional connectivity (Aedo-Jury et al., 2020), possibly by disrupting clustering of regions into clearly demarcated and competitive networks (Bukhari et al., 2018). In general, these neural characteristics show that wakefulness is not supported just by constant active neural states. In fact, our brains during wakefulness can also show instances of synchronized neural down states, possibly for homeostatic reasons (Bridi et al., 2020). On the other hand, when this hyper-connectivity pattern is accompanied by low global signal amplitude, it is representative of high arousal levels in the psychedelic state which is associated with accessing and integrating higher amount of information at the same time leading to hallucinations and alterations in feeling of self.

The fact that a single connectivity pattern when accompanied by two different global signal amplitude profiles leads to different subjective experience highlights the importance of the global signal as a proxy of underlying physiological state in interpretation of neuroimaging studies.

4.1.2 Global Signal at Rest

While dealing with resting state fMRI signals, FC measures can be influenced by the presence of a strong global component called the global signal (Wong et al., 2013). A common pre-processing step to remove the effects of this signal component from the BOLD time series is global signal regression, also known as orthogonalization to the global signal (Murphy et al., 2009; Wong et al., 2013). In

this step, the global signal is calculated as the average of BOLD signals across all the voxels of whole brain or all the voxels of grey matter (Liu et al., 2017) and is used as a nuisance regressor in a general linear model to remove the associated variance from the observed BOLD signals (Desjardins et al., 2001). However, whether to use global signal regression or not is still controversial because studies have shown that it can bias in correlation values to have a zero mean, leading to spurious anticorrelations (Anderson et al., 2011; Fox et al., 2009; Murphy et al., 2009). In addition, while some studies consider the global signal having non-neural sources such as motion, scanner artifacts, respiration (Power et al., 2017), cardiac rate (Chang & Glover, 2010), and vascular activity (Colenbier et al., 2020; Zhu et al., 2015), other studies suggest that the global signal may contain significant neural correlates (Schölvinck et al., 2010; Wong et al., 2013; Xu et al., 2018). As a result, there is still no consensus on keeping the global signal in the analysis or regressing it out before starting any kind of analysis. Both approaches can reveal complementary inferences about the brain's functional organisation (Murphy & Fox, 2017).

To better understand the global signal and its effect on the brain's functional organization analysis, it is important to investigate to what extent and how neural sources contribute in the global signal formation and what the physiological relevance of this global signal is (Wong et al., 2013; Zhang & Northoff, 2022). Previous studies have provided a neural-based explanation of global signal by finding correlations between local field potential power fluctuations in different frequency bands and resting state BOLD signal across the cortex, suggesting that GS is strongly driven by slow frequency fluctuations (Leopold, 2003; Schölvinck et al., 2010). Sleep studies also have shown that the amplitude and variance of the global signal increases by a transition from wakefulness to the sleep state (Fukunaga et al., 2006; He & Liu, 2012; Larson-Prior et al., 2009) which is characterized by slow-wave activity (El-Baba et al., 2019). Considering that global signal amplitude was also shown to be associated with vigilance scores (Wong et al., 2013), an important potential function of the global signal can be suggested as meditating the level of arousal (Zhang & Northoff, 2022). This can be further supported by close relationship between the global signal and physiological counterparts of metabolic consumption, such as respiration and cardiac activity (Chen et al., 2020), and recent findings that respiration drives the fluctuations of arousal (Raut et al., 2021).

In addition to meditating the level of arousal, recent studies also suggest behavioral roles for the global signal (Li, Bolt, et al., 2019; Zhang & Northoff, 2022). By exploring the individual differences in global signal topography and a

battery of phenotypes, Li and colleagues found that the global signal contains information related to trait-level cognition and behavior (Li, Bolt, et al., 2019). This notion was further approved by examining the occurrence rate of the co-activation patterns at the peak of the global signal during rest compared to task states which showed that the global signal bears cognitive information (Zhang et al., 2020). Our finding in this thesis that the global signal amplitude is different across the ongoing mental states, having the highest amplitude for the mind blanking reports, is in line with both arousal-meditating role of the global signal and its association with ongoing cognition.

Together, the global signal contains both neural and non-neural nuisance components. Regressing the global signal completely out from the BOLD signal leads to the loss of valuable cognitive information and keeping it may lead to incorrect inferences about the cognitive origin of experimental observations. Some methods have been developed to selectively remove the noise in the global signal while preserving its neural contents (Glasser et al., 2018) and research in this area is still continuing.

4.1.3 Structural-Functional relationships and Ongoing Cognition

The brain's large-scale white matter connections shape the way cerebral areas functionally interact, leading to formation of functional networks (Mišić et al., 2016; Wang et al., 2015). Neuroimaging studies have shown that the brain's structural and functional connectomes are similar in different topological aspects such as small-worldness, modularity, and having highly connected hubs (Bullmore & Sporns, 2012; Filippi et al., 2013; He & Evans, 2010; Wang et al., 2015). These findings suggest that in a general view, structure and function are closely related to each other and regions that are linked structurally tend to also be connected functionally (Koch et al., 2002). However, recent studies have shown that coupling of functional activity to the underlying brain's structure can be regionally heterogeneous (Griffa et al., 2022; Gu et al., 2020; Preti & Van De Ville, 2019; Suárez et al., 2020). In fact, during the wakeful resting state a high coupling of functional activity to the structural connectivity can be observed in the unimodal regions such as sensory-motor and visual areas (Popp et al., 2023; Preti & Van De Ville, 2019) while a high functional-structural decoupling can be observed in the multimodal areas and frontal, parietal, and temporal regions related to the higher-level cognition (Popp et al., 2023; Preti & Van De Ville, 2019), and sub-cortical areas (Medaglia et al., 2018). These characteristics have been shown to be heritable (Gu et al., 2020), variable across age and sex (Gu et

al., 2020; Hagmann et al., 2010), and directly related to the cognitive ability (Popp et al., 2023; Wang et al., 2018).

The direct association of structural-functional relationship profiles with ongoing cognition was further approved in pathological conditions. In this regard, abnormalities or disruptions in structural-functional relationship were reported in cognitive disorders such as schizophrenia (Cocchi et al., 2014; Collin et al., 2017; Skudlarski et al., 2010), idiopathic generalized epilepsy (Zhang et al., 2011), psychogenic nonepileptic seizures (Ding et al., 2013), bipolar disorder (Collin et al., 2017), cognitive impairments in multiple sclerosis (Ye et al., 2022), attention deficit hyperactivity disorder (Lee et al., 2021), and even in altered states of consciousness (Luppi et al., 2023; Panda et al., 2022). In addition, the role of structural-functional coupling alterations in Parkinson's dementia, which is characterized by changes in perception and thoughts, showed the direct association of structural-functional relationship profiles with ongoing mental states. These results highlight the significance of the underlying interaction between structural and functional connectomes to shape our daily life conscious experience.

Our daily life can be defined as continuously facing changing environmental and internal demands. The capacity to adapt in a flexible way to suit changing demands is a fundamental aspect of cognitive control, known as cognitive and behavioral flexibility (Monsell, 2003). Cognitive flexibility is an essential component of executive functioning, and permits the efficient adaptation of thoughts and behaviors in response to changing environmental demands (Medaglia et al., 2018; Uddin, 2021). Both structural and functional connectomes were shown to play an important role in supporting cognitive flexibility (Uddin, 2021). For example, modification of structural and functional connections using cognitive training and physical exercises were shown to improve cognitive flexibility (Gomez-Pinilla & Hillman, 2013). More importantly, the structural-functional relationship has been suggested as a signature of mental flexibility. Considering task switching cost as a measure of mental flexibility, it has been shown that higher liberality of functional activity from the underlying structure in a whole-brain level is associated with higher switching cost and so less mental flexibility (Medaglia et al., 2018). In confronting new environmental conditions such as space, we found that the regional structural-functional relationship alters in multi-sensory integration and processing areas. We hypothesize that this observation is exactly related to the adaptation of mental flexibility to the new environmental circumstances. Being in space requires an adaptation to the new set of environmental demands and so a different cognitive flexibility profile. In

addition, structural changes due to exposure to microgravity also affects specific regional structural-functional relationships. As a result, a new structural-functional coupling configuration will be adapted to both compensate the structural changes and adapt the cognitive flexibility to the new environmental demands.

All the mentioned studies used a static measure to infer the relationship between the functional and structural connectomes either during task or resting state. There are recent studies which try to unveil the dynamic alterations in the structural-functional relationship to find out how the structure supports the functional dynamism by integrating the time-resolved functional map corresponding to a given functional network with a whole-brain tractogram (Basile et al., 2022; Calamante et al., 2017). Structural-functional features extracted in this framework were shown to be predictive of higher-order cognition such as fluid intelligence, sustained attention, and cognitive flexibility (Basile et al., 2022). In this thesis, we also showed that the structural-functional coupling and decoupling maps change dynamically during resting state and these time-varying features can be predictive of ongoing mental states.

Taken together, combining information from both structure and dynamic fluctuations of the functional connectome helps us to make a general inclusive framework which bridges neural space to the dynamically changing mental space, specifically in resting conditions. Additionally, considering the role of global signal as a proxy of physiological state in characterization of cognitive and mental states, we can think about more general brain-body interactions to investigate the ongoing mentation.

4.2 Future Perspectives: A brain-body characterization of mental states

So far, a vast area of research about brain-mind relationships has investigated the brain in isolation from the rest of the body. However, research findings propose that physiological pathways influence brain function in direct and indirect ways (Critchley & Harrison, 2013). In addition, in this thesis our findings about cognitive and behavioral roles of the global signal as an indirect measure of physiological states highlights the importance of considering bodily signals in cognitive and behavioral studies. Therefore, combined assessment of brain-body

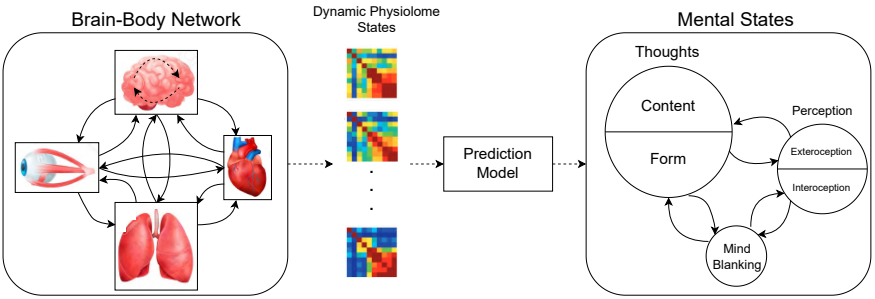

Figure 4.1 Using the Network Physiology framework, the dynamic interactions between brain regions, and between brain and other bodily organs (i.e., heart, lungs, eyes) can be described and then summarized into a finite number of time-varying brain-body connectivity states (i.e., physiolome states). Based on that one can develop a mathematical model that makes use of physiolomes to infer ongoing mental states in task-free conditions.

signals can be critical to advance our understanding of how individuals solve the fundamental issue of continuously evaluating, reacting, and adapting to a dynamically changing environment (Criscuolo et al., 2022). At a system-level point of view, a network of interactions sub-serving the regulation of the homeostatic function encompasses physiological rhythms, such as respiratory drive, cardiovascular, and ocular activities (Pernice et al., 2021). In that perspective, instead of investigating brain network in isolation, we can define a brain-body physiological network considering activities in the brain and other bodily organs such as respiration, heartbeat, and pupil diameter.

My future plan is to develop such brain-body networks under the framework of "Network Physiology" (Bartsch et al., 2015; Bashan et al., 2012; Ivanov, 2021), in which the dynamic interaction between brain and other bodily organs is modeled as a dynamic network. In this network, nodes represent various organs (i.e., brain, heart, lungs, eyes) with physiological activities coming from the organ's dynamical system and whose links represent the coordination and synchronization between organ systems and sub-systems exhibiting transient characteristics. These networks can be represented by connectivity matrices called "physiolomes" (Ivanov, 2021). It has been shown that the physiolome works as an appropriate solution to characterize the dynamic nature of brain-body interactions in different conditions such as sleep stages (Bashan et al., 2012), exercising (Balagué et al., 2022), focused attention (Marzbanrad et al., 2020), and mental stress (Pernice et al., 2021). Therefore, estimating physiolomes states during rest can be a new approach to examine brain, body, and mind and their dynamical interactions at resting state. As a result, a

suggestion for future research is to develop a mental state decoder based on a dynamic brain-body physiolome interaction model (Figure 4.1).

The main factors affecting the performance of mental state decoders are variability in individuals, physiological and neural changes over time, and level of consciousness. Decoding models not only should be generalizable across time and individuals, but also need to be implemented in the lower levels of consciousness. To get one step closer to this goal, another suggestion for future research would be to design the mentioned mental state decoders in light anesthesia, when participants are still responsive and able to report their mental state (Ghoneim & Weiskopf, 2000). This approach results in finding consciousness-level-related features which can be used to predict ongoing mental states specific to each level of consciousness.

These suggestions for future research are in line with our final goal to better understand ongoing cognition during rest to benefit individuals with neuropsychiatric disorders (where mental states can be destabilized) as well as individuals with compromised communication abilities (whose mental state evaluation can be vital for their survival).

Appendices

Appendix A: Collection of Words for the PF Tasks

for the "*Remembering Past/Imagining Future (Self/Other-related)*" tasks, we used a collection of general words and phrases containing 32 different items, events, or situations. We chose this set from a bigger collection introduced in (Gilmore et al., 2018).

BEACH	EMAIL	NAPPING	STAYING UP ALL NIGHT
BEDROOM	FLOWERS	PACKING LUGGAGE	TELLING A LIE
BIRTHDAY	FUNERAL	PHONE CALL	TEXT MESSAGING
BRUSHING TEETH	GETTING LOST	PIZZA	TRAIN RIDE
BUYING A DRINK	HAIR CUT	PUBLIC SPEECH	VACATION
COOKING	HAMBURGER	RECEIVING A LETTER	VALENTINE'S DAY
DOCTOR	HAVING A COLD	RESTAURANT	VISITING RELATIVES
DRINKING COFFEE/TEA	KITCHEN	SHOWERING	WAITING IN A LINE

Appendix B: Classifier Performance Measures for Imbalanced Datasets

Considering a K-class classification, the precision, recall, and balanced accuracy is defined as:

Precision: A parameter between 0 and 1 also defined as the ability of the classifier not to label as positive a sample that is negative. This parameter can be defined for each class C_k $(1 < k < K)$ separately:

$$Precision_{C_k} = \frac{TP_k}{TP_k + FP_k}$$

A high precision shows that classifier is not biased toward larger classes.

Recall: A parameter between 0 and 1 defined as the ability of the classifier to classify positive samples correctly. This parameter can be defined for each class C_k $(1 < k < K)$ separately:

$$Recall_{C_k} = \frac{TP_k}{TP_k + FN_k}$$

a high recall score shows that the classifier is not biased toward the larger classes.

Balanced Accuracy: To compute balanced accuracy, each sample is weighted according to the inverse prevalence of its true class which accordingly will avoid inflated performance estimates on imbalanced datasets. In a multi-class classification, the balanced accuracy is defined as the average of the Recall values across the classes:

$$Balanced\ Accuracy = \frac{1}{K}\sum_{k=1}^{K} Recall_{C_k}$$

In the above-mentioned definitions: TP=True Positive, FP=False Positive, TN=True Negative, and FN=False Negative.

Appendix C: Supplementary Results for Mental State Decoding

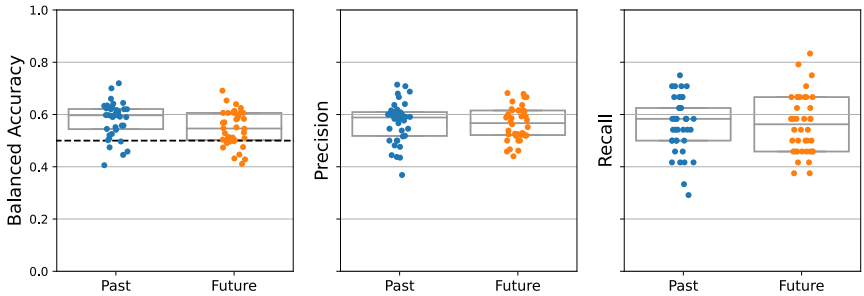

Figure C1. Referent dimensions of cognitive tasks were decoded higher than chance-level. Decoding the thought referents in different temporal dimensions showed a higher than chance-level performance.

Table C1. The best performance of decoder for reference dimensions of cognitive tasks.

Temporal Dimension	**Feature**	**Cut-off Eigenvalue**	**Balanced Accuracy**	**Precision**	**Recall**
Past	Coupling map	20	0.58	0.57	0.56
Future	SDI map	80	0.55	0.56	0.56

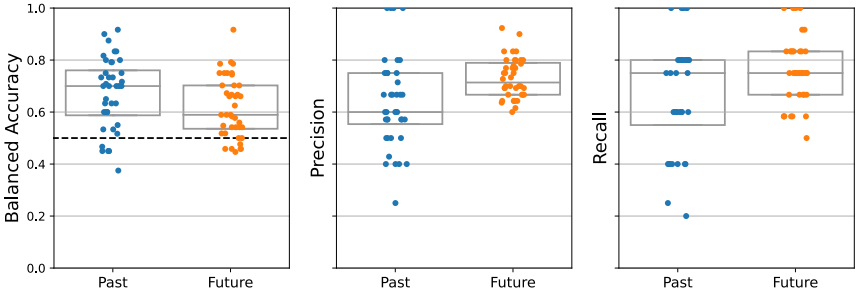

Figure C2. Referent dimensions of thoughts during rest were decoded higher than chance-level. Decoding the thought referents in different temporal dimensions showed a higher than chance-level performance.

Table C2. The best performance of decoder for reference dimensions of cognitive tasks.

Temporal Dimension	**Feature**	**Cut-off Eigenvalue**	**Balanced Accuracy**	**Precision**	**Recall**
Past	Coupling map	20	0.67	0.64	0.67
Future	SDI map	90	0.62	0.73	0.76

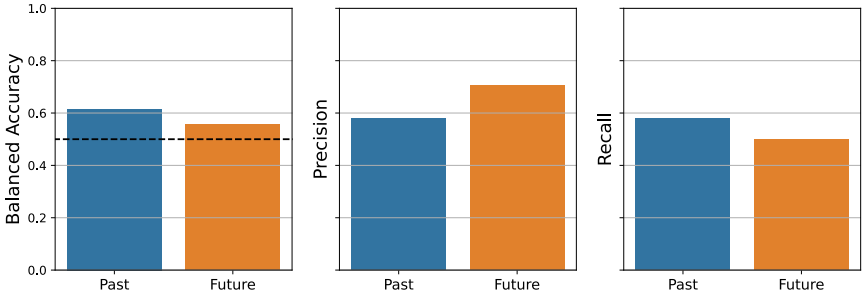

Figure C3. Referent dimensions of ongoing thoughts were decoded higher than chance-level. Decoding the thought referents in different temporal dimensions showed a higher than chance-level performance.

Table C3. The best performance of decoder for reference dimensions of ongoing thoughts based on cognitive tasks features.

Temporal Dimension	**Feature**	**Cut-off Eigenvalue**	**Balanced Accuracy**	**Precision**	**Recall**
Past	Coupling map	30	0.62	0.58	0.58
Future	Decoupling map	40	0.56	0.71	0.50

Appendix D: Supplementary Results for Mind Blanking Analysis

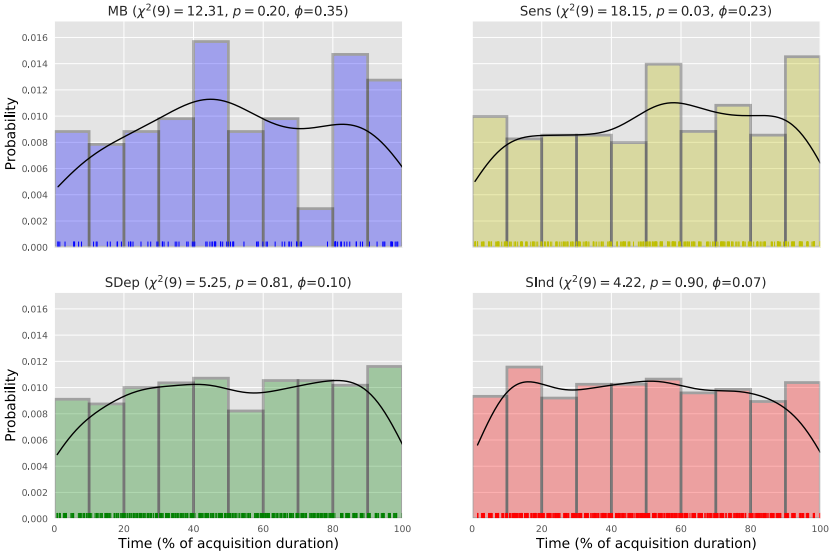

Figure D1. Mind blanking reports are uniformly distributed across the acquisition time. By dividing the acquisition period into 10% bins and counting the number of MB reports at each bin for all the subjects, the distribution of reports was found to be uniform (χ^2 test). The same results were found for SDep and SInd reports but the hypothesis of uniformity was rejected for the Sens reports.

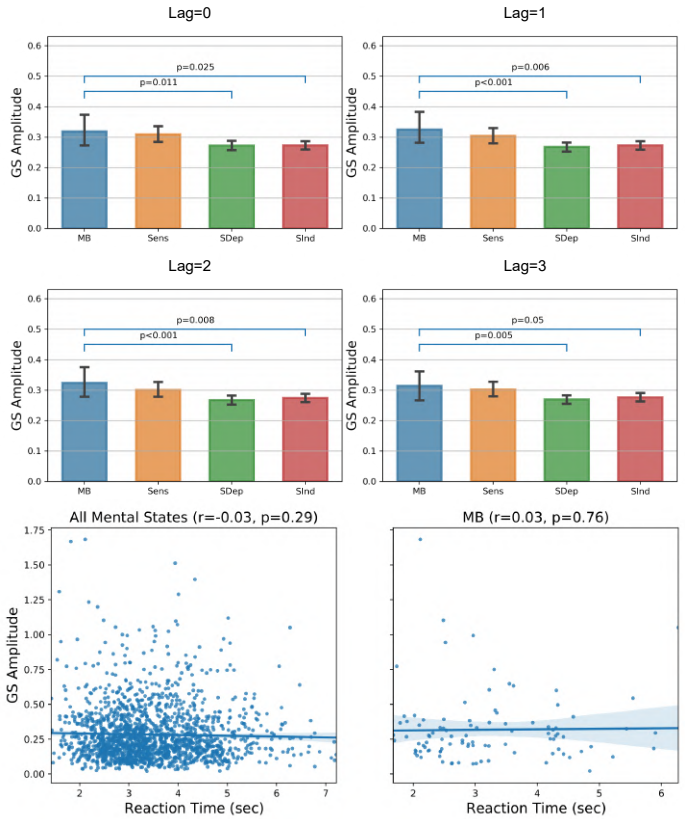

Figure D2. Mind blanking is characterized by high cortical global signal amplitude. Average absolute value of the global signal of the 5 scans prior each mental state report shows that the global signal amplitude is significantly higher for MB reports compared to the content-oriented states. These results are replicated considering different pre-probe window lags (related to the hemodynamic response peak time). Bars show the mean of the magnitude and error bars are 95% confidence interval.

Table D1. Performance of SVM classifier when predicting MB reports based on phase coherence matrices (lag = 0)

	Balanced Accuracy	Recall	Precision
MB VS. SENS	0.97	0.94	0.99
MB VS. SDEP	0.95	0.91	1
MB VS. SIND	0.94	0.87	1
MB VS. OTHERS	0.90	0.79	1
MB VS. OTHERS (DUMMY)	0.50	0.05	0.06

Table D2. Performance of SVM classifier when predicting MB reports based on phase coherence matrices (lag = 1)

	Balanced Accuracy	Recall	Precision
MB VS. SENS	0.97	0.94	0.99
MB VS. SDEP	0.95	0.91	1
MB VS. SIND	0.94	0.87	1
MB VS. OTHERS	0.90	0.79	1
MB VS. OTHERS (DUMMY)	0.50	0.05	0.06

Table D3. Performance of SVM classifier when predicting MB reports based on phase coherence matrices (lag = 2)

	Balanced Accuracy	Recall	Precision
MB VS. SENS	0.98	0.95	0.99
MB VS. SDEP	0.96	0.91	1
MB VS. SIND	0.94	0.88	1
MB VS. OTHERS	0.90	0.81	1
MB VS. OTHERS (DUMMY)	0.50	0.05	0.06

Table D4. Performance of SVM classifier when predicting MB reports based on phase coherence matrices (lag = 3)

	Balanced Accuracy	Recall	Precision
MB VS. SENS	0.97	0.95	0.99
MB VS. SDEP	0.96	0.92	1
MB VS. SIND	0.94	0.88	1
MB VS. OTHERS	0.90	0.81	1
MB VS. OTHERS (DUMMY)	0.50	0.05	0.06

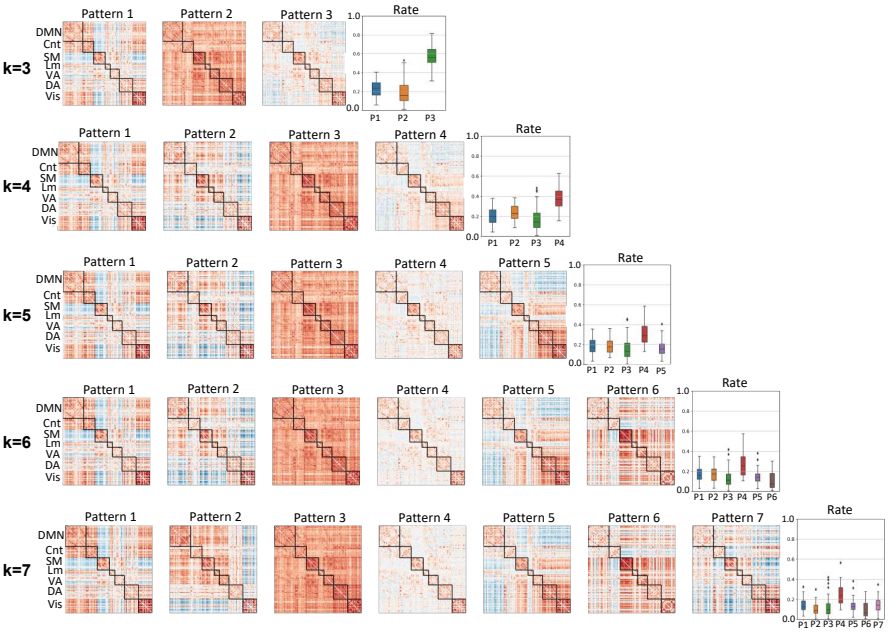

Figure D3. Four main recurrent functional configurations characterize the resting periods of the experience-sampling paradigm (lag = 0). K-means clustering on the connectivity matrices related to the resting periods and 5 pre-probe matrices related to the reported mental states shows that four patterns recurrently appear during these periods of the experience-sampling even up to k=7 clusters.

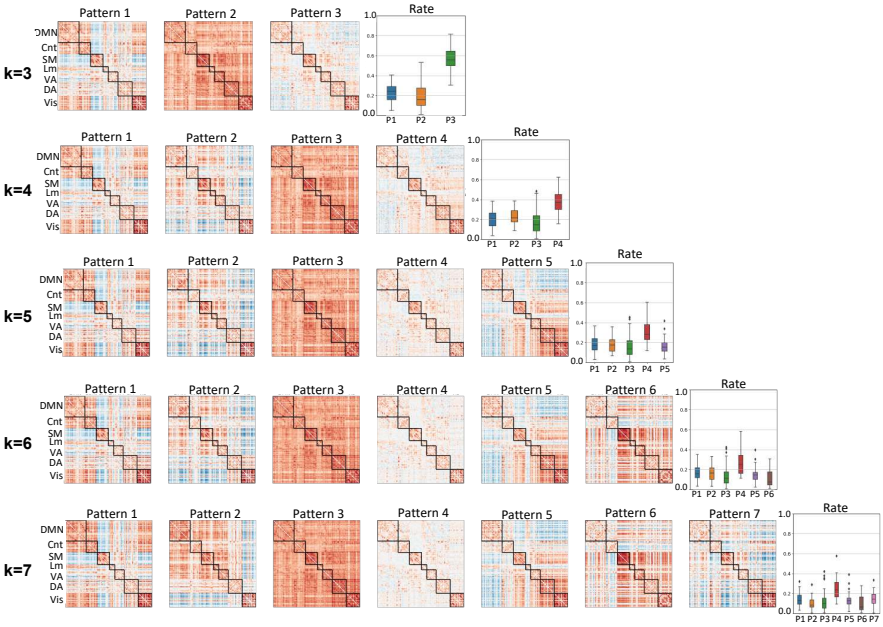

Figure D4. Four main recurrent functional configurations characterize the resting periods of the experience-sampling paradigm (lag = 1). K-means clustering on the connectivity matrices related to the resting periods and 5 pre-probe matrices related to the reported mental states shows that four patterns recurrently appear during these periods of the experience-sampling even up to k=7 clusters.

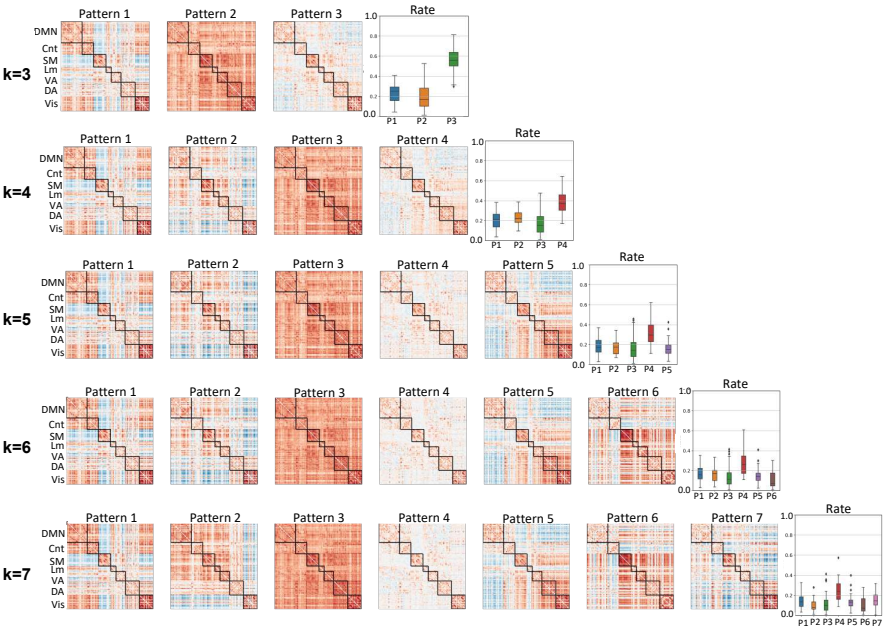

Figure D5. Four main recurrent functional configurations characterize the resting periods of the experience-sampling paradigm (lag = 2). K-means clustering on the connectivity matrices related to the resting periods and 5 pre-probe matrices related to the reported mental states shows that four patterns recurrently appear during these periods of the experience-sampling even up to k=7 clusters.

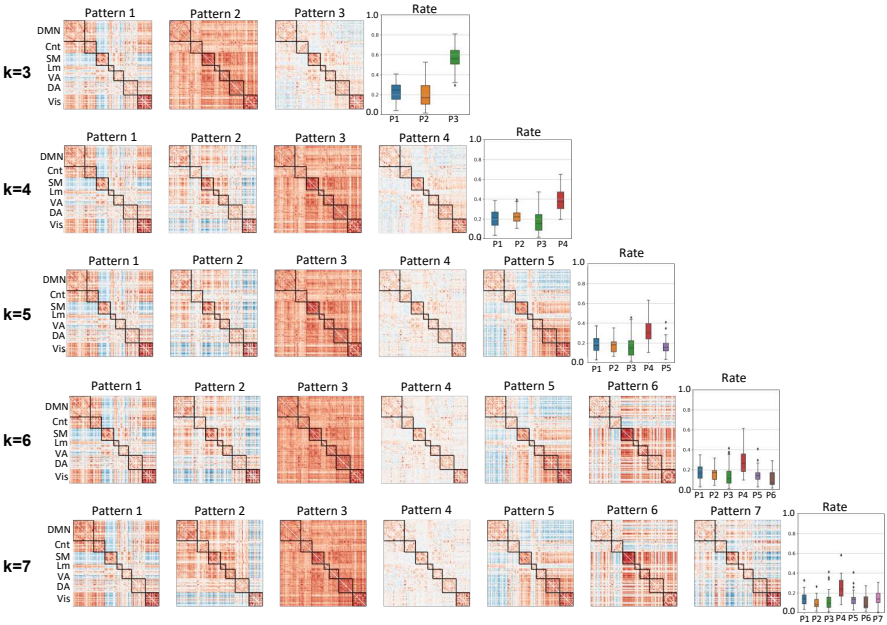

Figure D6. Four main recurrent functional configurations characterize the resting periods of the experience-sampling paradigm (lag = 3). K-means clustering on the connectivity matrices related to the resting periods and 5 pre-probe matrices related to the reported mental states shows that four patterns recurrently appear during these periods of the experience-sampling even up to k=7 clusters.

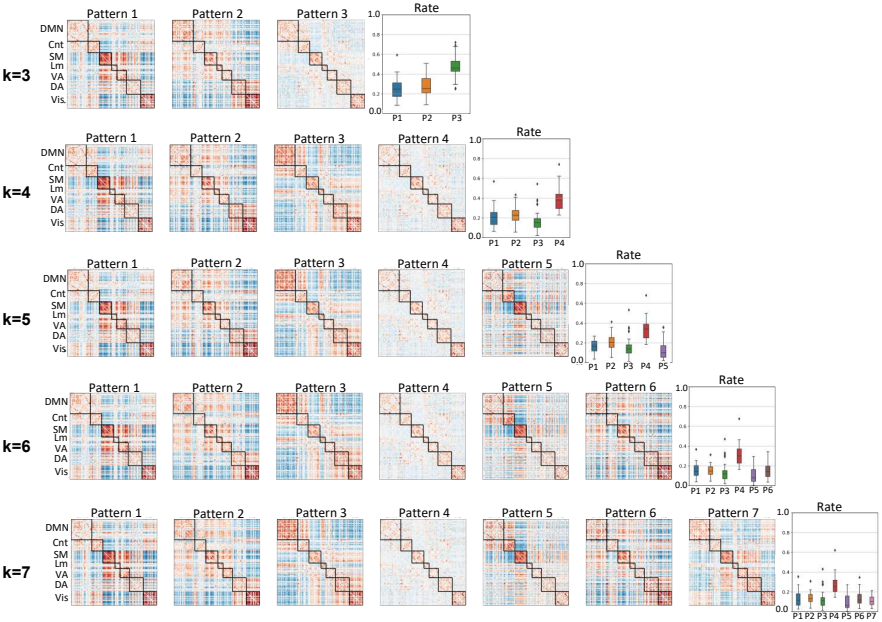

Figure D7. Effect of <u>global signal subtraction</u> on the extracted brain patterns (lag = 0). After subtracting the global signal from regional time series, the resting periods of the experience-sampling paradigm fail to show the overall positive connectivity configuration, suggesting an important contribution of the global signal on this brain pattern. Notes: recurrent functional configurations are extracted using k-means clustering with number of clusters ranging from 3 to 7, considering 5 pre-probe connectivity matrices related to the reported mental state.

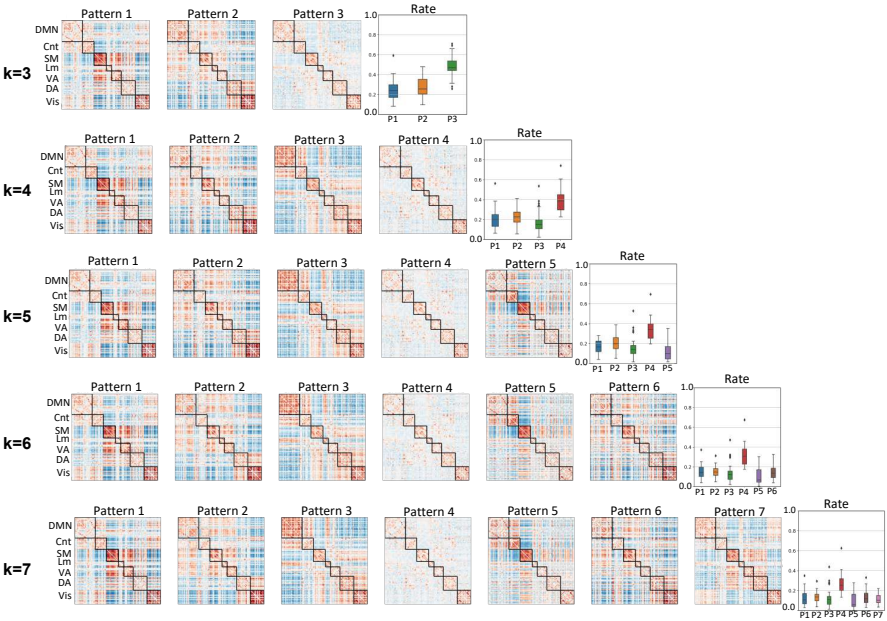

Figure D8. Effect of <u>global signal subtraction</u> on the extracted brain patterns (lag = 1). After subtracting the global signal from regional time series, the resting periods of the experience-sampling paradigm fail to show the overall positive connectivity configuration, suggesting an important contribution of the global signal on this brain pattern. Notes: recurrent functional configurations are extracted using k-means clustering with number of clusters ranging from 3 to 7, considering 5 pre-probe connectivity matrices related to the reported mental state.

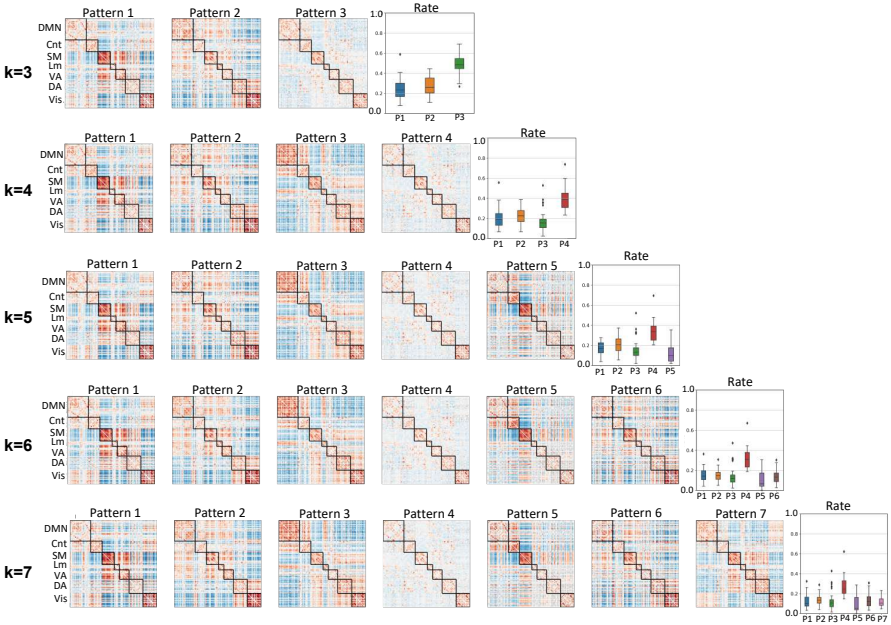

Figure D9. Effect of <u>global signal subtraction</u> on the extracted brain patterns (lag = 2). After subtracting the global signal from regional time series, the resting periods of the experience-sampling paradigm fail to show the overall positive connectivity configuration, suggesting an important contribution of the global signal on this brain pattern. Notes: recurrent functional configurations are extracted using k-means clustering with number of clusters ranging from 3 to 7, considering 5 pre-probe connectivity matrices related to the reported mental state.

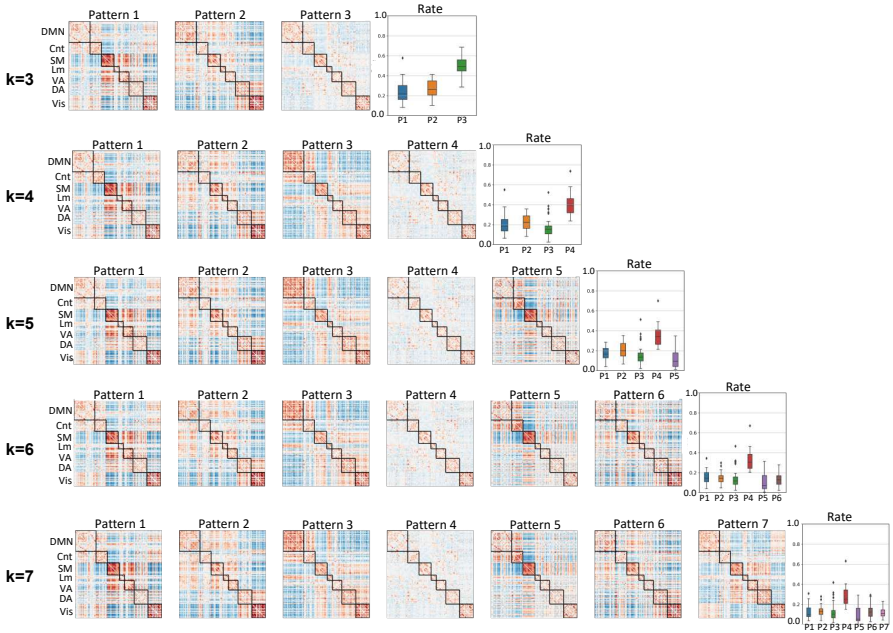

Figure D10. Effect of <u>global signal subtraction</u> on the extracted brain patterns (lag = 3). After subtracting the global signal from regional time series, the resting periods of the experience-sampling paradigm fail to show the overall positive connectivity configuration, suggesting an important contribution of the global signal on this brain pattern. Notes: recurrent functional configurations are extracted using *k*-means clustering with number of clusters ranging from 3 to 7, considering 5 pre-probe connectivity matrices related to the reported mental state.

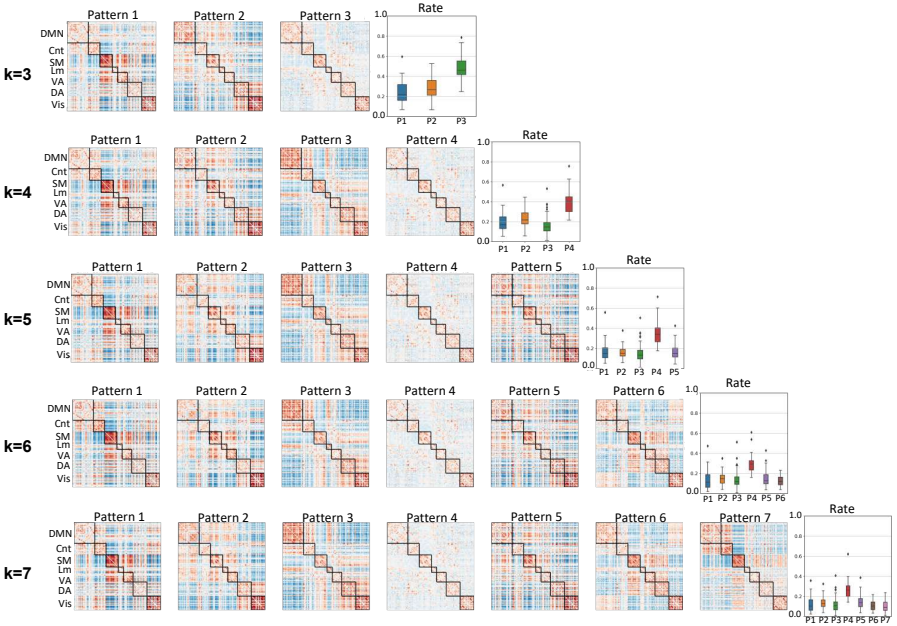

Figure D11. Effect of <u>global signal regression</u> on the extracted brain patterns (lag = 0). After regressing out the global signal from regional time series, the resting periods of the experience-sampling paradigm fail to show the overall positive connectivity configuration, suggesting an important contribution of the global signal on this brain pattern. Notes: recurrent functional configurations are extracted using k-means clustering with number of clusters ranging from 3 to 7, considering 5 pre-probe connectivity matrices related to the reported mental state.

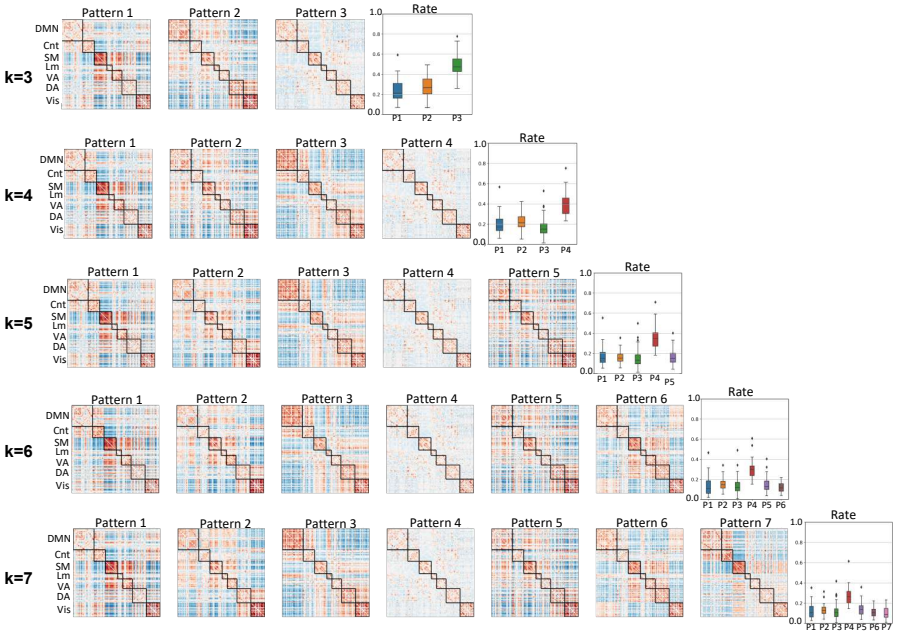

Figure D12. Effect of <u>global signal regression</u> on the extracted brain patterns (lag = 1). After regressing out the global signal from regional time series, the resting periods of the experience-sampling paradigm fail to show the overall positive connectivity configuration, suggesting an important contribution of the global signal on this brain pattern. Notes: recurrent functional configurations are extracted using k-means clustering with number of clusters ranging from 3 to 7, considering 5 pre-probe connectivity matrices related to the reported mental state.

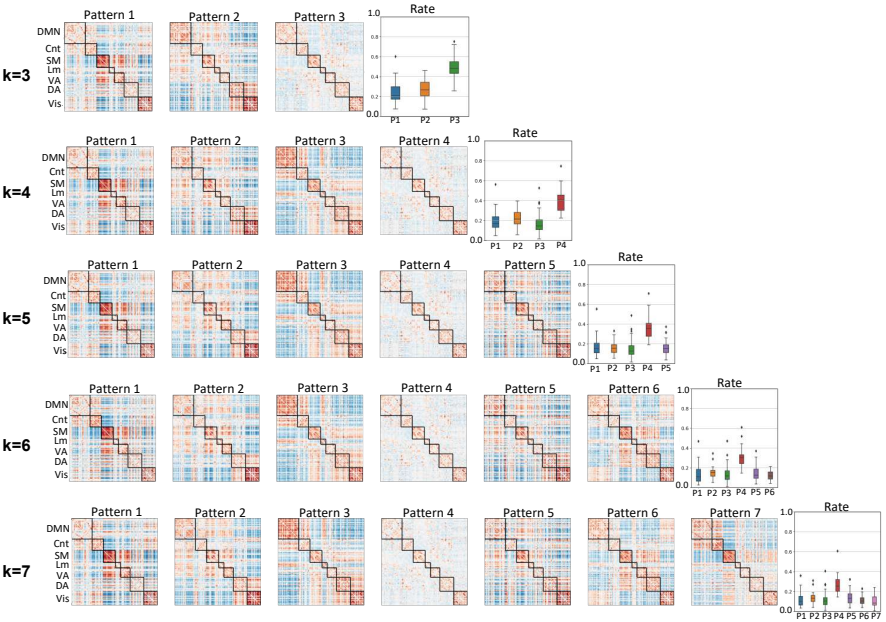

Figure D13. Effect of <u>global signal regression</u> on the extracted brain patterns (lag = 2). After regressing out the global signal from regional time series, the resting periods of the experience-sampling paradigm fail to show the overall positive connectivity configuration, suggesting an important contribution of the global signal on this brain pattern. Notes: recurrent functional configurations are extracted using k-means clustering with number of clusters ranging from 3 to 7, considering 5 pre-probe connectivity matrices related to the reported mental state.

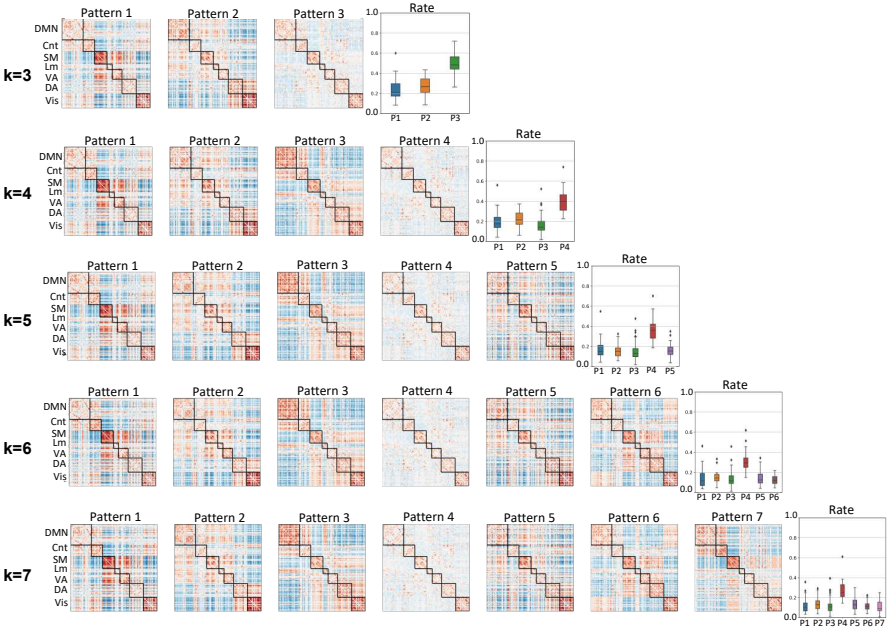

Figure D14. Effect of <u>global signal regression</u> on the extracted brain patterns (lag = 3). After regressing out the global signal from regional time series, the resting periods of the experience-sampling paradigm fail to show the overall positive connectivity configuration, suggesting an important contribution of the global signal on this brain pattern. Notes: recurrent functional configurations are extracted using k-means clustering with number of clusters ranging from 3 to 7, considering 5 pre-probe connectivity matrices related to the reported mental state.

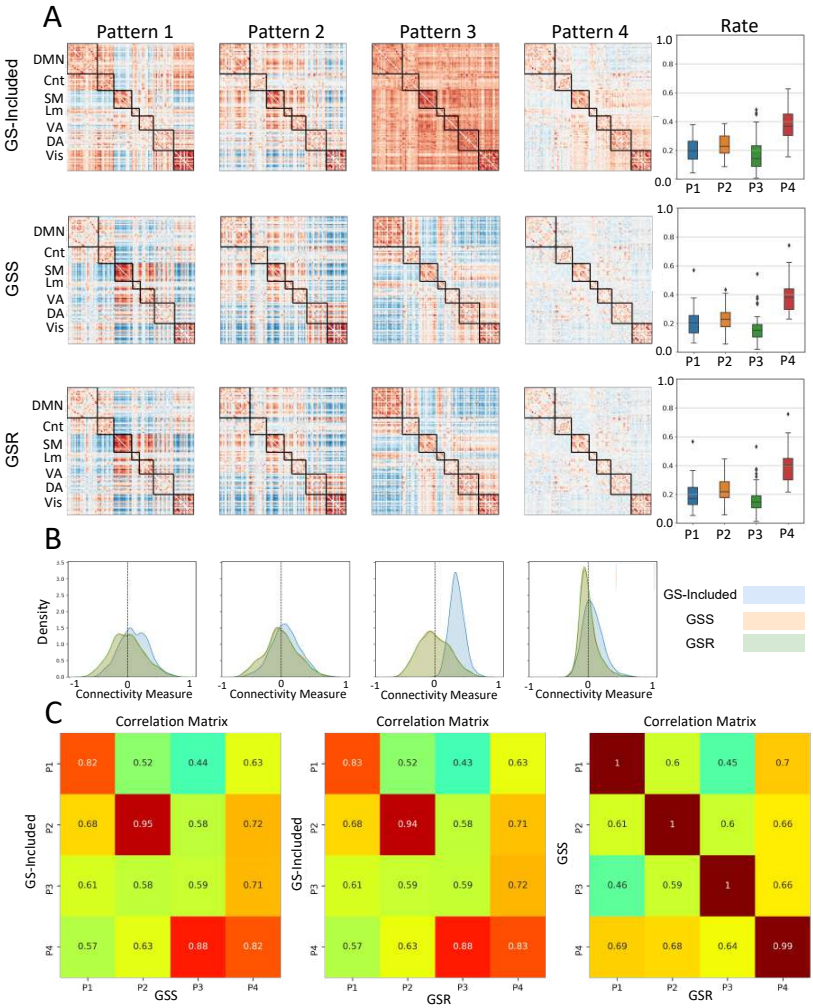

Figure D15. The overall positive coherence configuration (Pattern 3) is mediated by the cortical global signal (GS). A) When subtracting (GSS)/regressing out (GSR) the global signal from the ROI time series, Pattern 3 positive connectivity reduces significantly. As the occurrence rate of Pattern 3 is relative to the occurrence rates of the other patterns its appearance is not influenced either when the GS is included in the analysis or removed by subtraction or regression. B) GSS/GSR shifts the connectivity distribution to more negative values and this effect is more prominent for Pattern 3. C) The similarity of Pattern 3 to itself is no longer significant after GSS-GSR whereas for the other patterns the GS removal strategies do not affect their intra-correlation values.

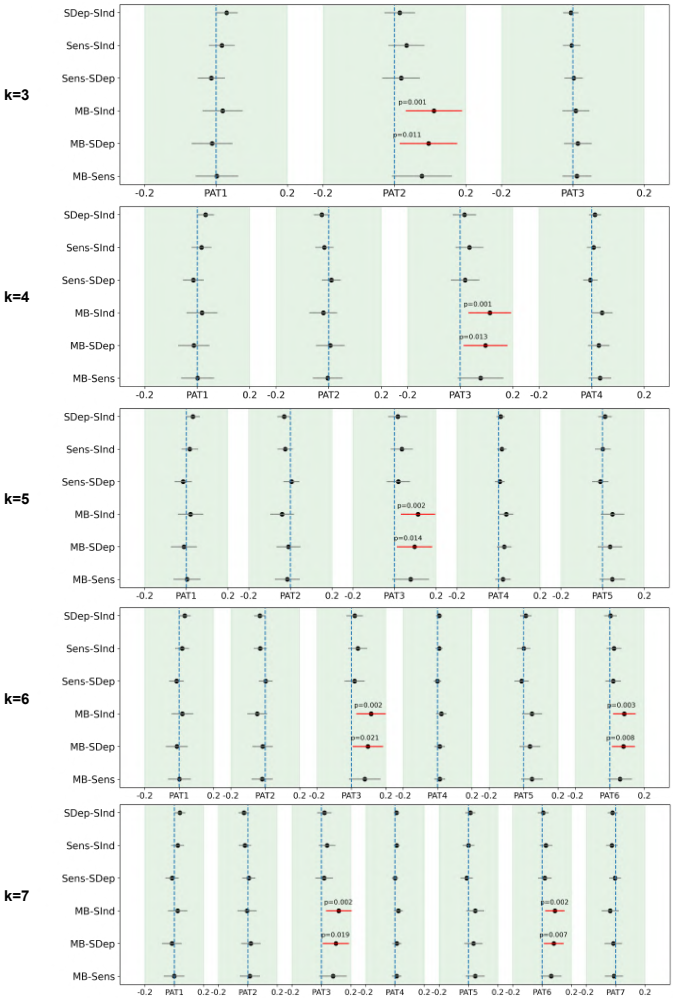

Figure D16. The overall positive coherence Pattern 3 shows the highest similarity to connectivity patterns of the Mind Blanking (MB) reports even at high number of clusters (lag = 0). Considering a mental state analysis window with lag=0, a generalized linear mixed model analysis for each pattern separately shows the highest similarity of the overall positive coherence Pattern 3 to the connectivity matrices related to the MB reports. The results are replicated with different number of clusters (k=3-7). For each cluster number k, a model fit is considered significant if its p-value is lower than 0.05 k to correct for multiple tests. In case of significant fit, a post-hoc Tukey test was performed for contrast analysis between different mental state pairs. Notes: SDep = Stimulus Dependent Thought, SInd = Stimulus Independent Thought, Sens: Sensory Perception.

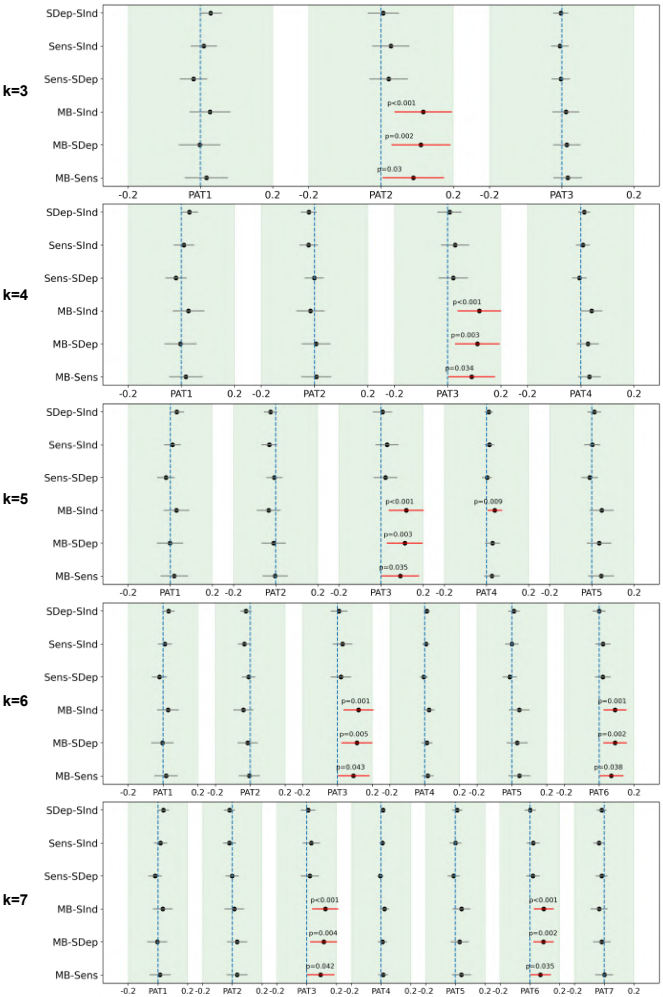

Figure D17. The overall positive coherence Pattern 3 shows the highest similarity to connectivity patterns of the Mind Blanking (MB) reports even at high number of clusters (lag = 1). Considering a mental state analysis window with lag=1, a generalized linear mixed model analysis for each pattern separately shows the highest similarity of the overall positive coherence Pattern 3 to the connectivity matrices related to the MB reports. The results are replicated with different number of clusters (k=3-7). For each cluster number k, a model fit is considered significant if its p-value is lower than 0.05 k to correct for multiple tests. In case of significant fit, a post-hoc Tukey test was performed for contrast analysis between different mental state pairs. Notes: SDep = Stimulus Dependent Thought, SInd = Stimulus Independent Thought, Sens: Sensory Perception.

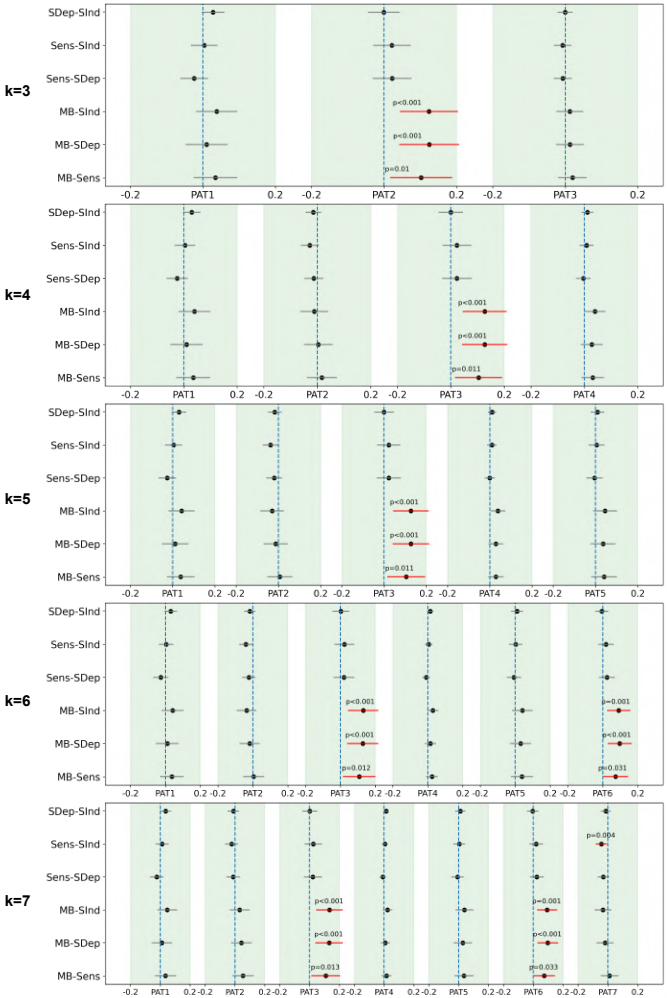

Figure D18. The overall positive coherence Pattern 3 shows the highest similarity to connectivity patterns of the Mind Blanking (MB) reports even at high number of clusters (lag = 2). Considering a mental state analysis window with lag=2, a generalized linear mixed model analysis for each pattern separately shows the highest similarity of the overall positive coherence Pattern 3 to the connectivity matrices related to the MB reports. The results are replicated with different number of clusters (k=3-7). For each cluster number k, a model fit is considered significant if its p-value is lower than 0.05 k to correct for multiple tests. In case of significant fit, a post-hoc Tukey test was performed for contrast analysis between different mental state pairs. Notes: SDep = Stimulus Dependent Thought, SInd = Stimulus Independent Thought, Sens: Sensory Perception.

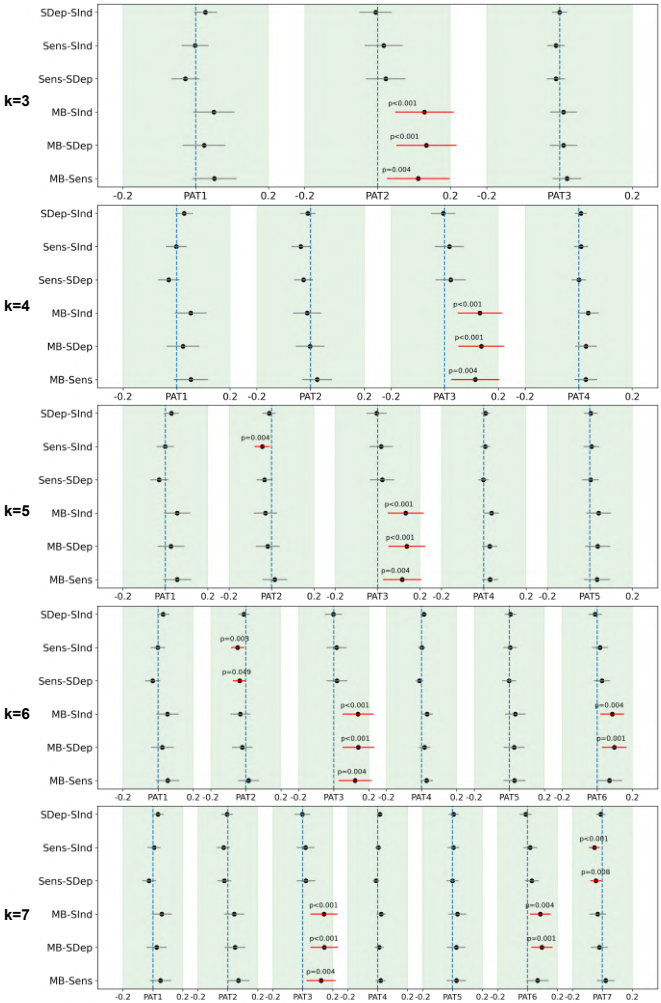

Figure D19. The overall positive coherence Pattern 3 shows the highest similarity to connectivity patterns of the Mind Blanking (MB) reports even at high number of clusters (lag = 3). Considering a mental state analysis window with lag=3, a generalized linear mixed model analysis for each pattern separately shows the highest similarity of the overall positive coherence Pattern 3 to the connectivity matrices related to the MB reports. The results are replicated with different number of clusters (k=3-7). For each cluster number k, a model fit is considered significant if its p-value is lower than 0.05 k to correct for multiple tests. In case of significant fit, a post-hoc Tukey test was performed for contrast analysis between different mental state pairs. Notes: SDep = Stimulus Dependent Thought, SInd = Stimulus Independent Thought, Sens: Sensory Perception.

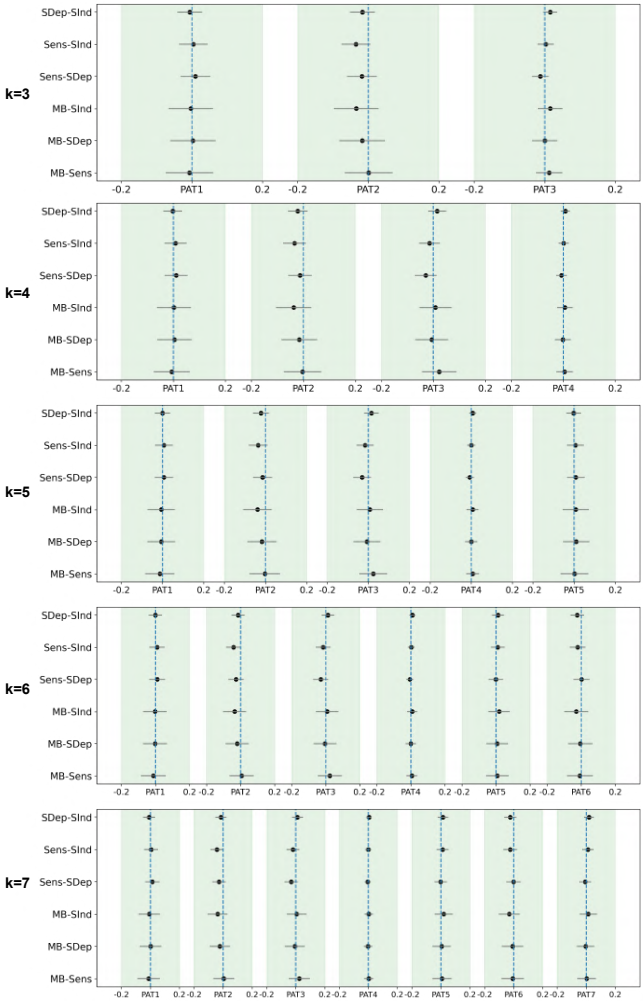

Figure D20. After <u>global signal subtraction</u>, none of the functional connectivity patterns can be meaningfully assigned to MB (lag = 0). Considering a mental state analysis window with lag=0, a generalized linear mixed model analysis for each pattern separately could not result in significant similarity of any pattern to the connectivity matrices related to the MB reports. The results are replicated with different number of clusters (k=3-7). For each cluster number k, a model fit is considered significant if its p-value is lower than 0.05 k to correct for multiple tests. In case of significant fit, a post-hoc Tukey test was performed for contrast analysis between different mental state pairs.

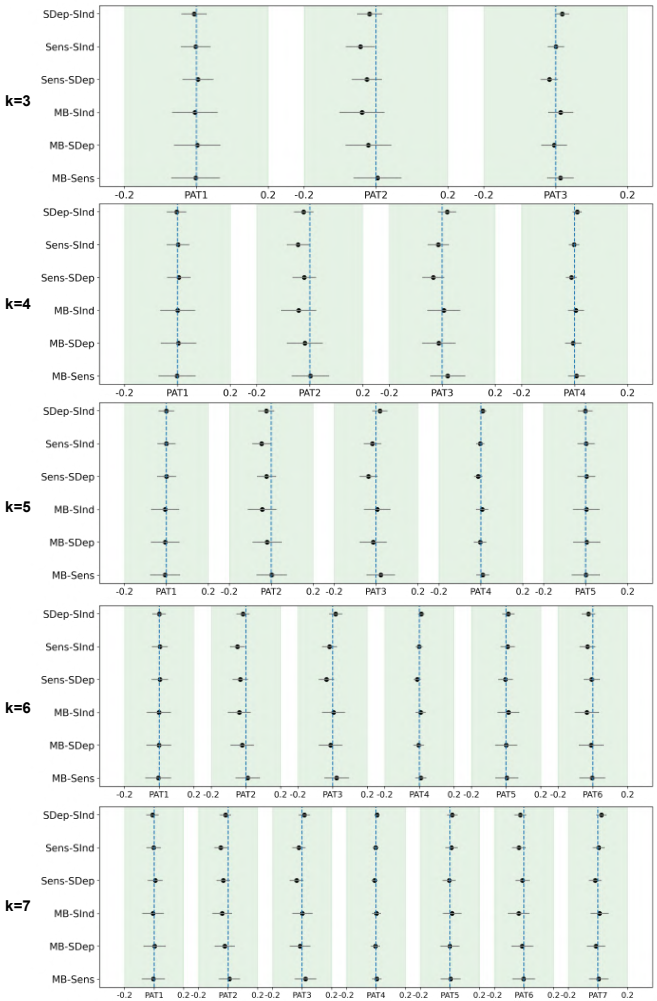

Figure D21. After <u>global signal subtraction</u>, none of the functional connectivity patterns can be meaningfully assigned to MB (lag = 1). Considering a mental state analysis window with lag=1, a generalized linear mixed model analysis for each pattern separately could not result in significant similarity of any pattern to the connectivity matrices related to the MB reports. The results are replicated with different number of clusters (k=3-7). For each cluster number k, a model fit is considered significant if its p-value is lower than 0.05 k to correct for multiple tests. In case of significant fit, a post-hoc Tukey test was performed for contrast analysis between different mental state pairs.

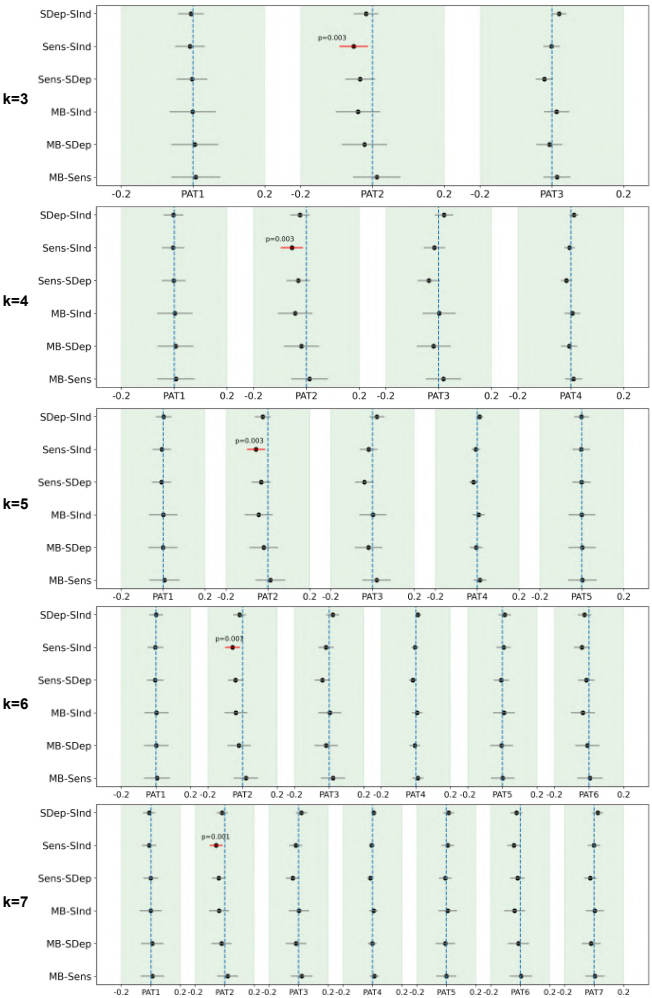

Figure D22. After <u>global signal subtraction</u>, none of the functional connectivity patterns can be meaningfully assigned to MB (lag = 2). Considering a mental state analysis window with lag=2, a generalized linear mixed model analysis for each pattern separately could not result in significant similarity of any pattern to the connectivity matrices related to the MB reports. The results are replicated with different number of clusters (k=3-7). For each cluster number k, a model fit is considered significant if its p-value is lower than 0.05 k to correct for multiple tests. In case of significant fit, a post-hoc Tukey test was performed for contrast analysis between different mental state pairs.

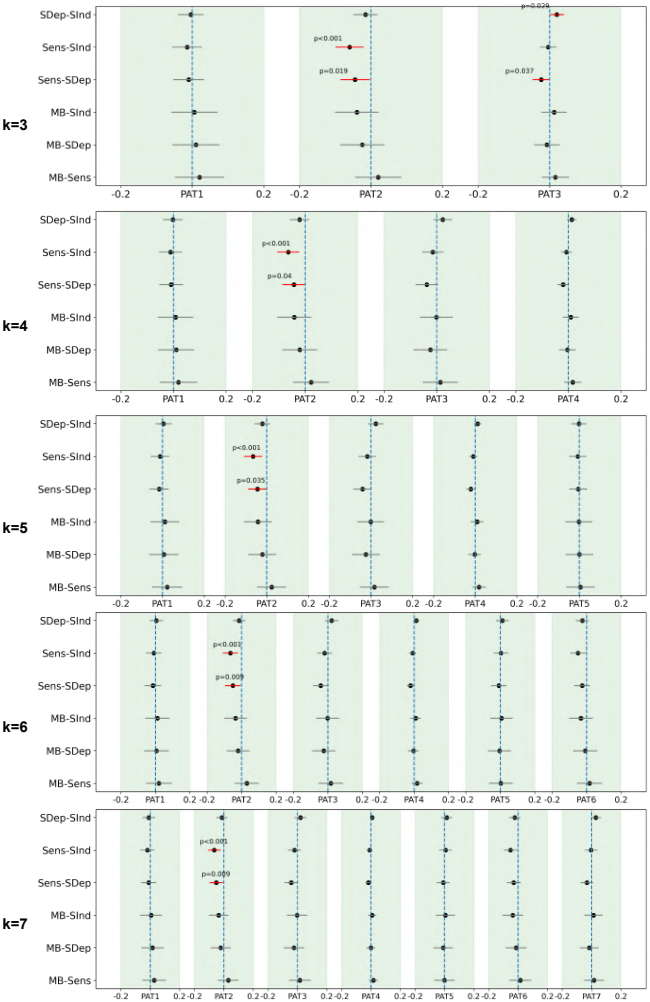

Figure D23. After <u>global signal subtraction</u>, none of the functional connectivity patterns can be meaningfully assigned to MB (lag = 3). Considering a mental state analysis window with lag=3, a generalized linear mixed model analysis for each pattern separately could not result in significant similarity of any pattern to the connectivity matrices related to the MB reports. The results are replicated with different number of clusters (k=3-7). For each cluster number k, a model fit is considered significant if its p-value is lower than 0.05 k to correct for multiple tests. In case of significant fit, a post-hoc Tukey test was performed for contrast analysis between different mental state pairs.

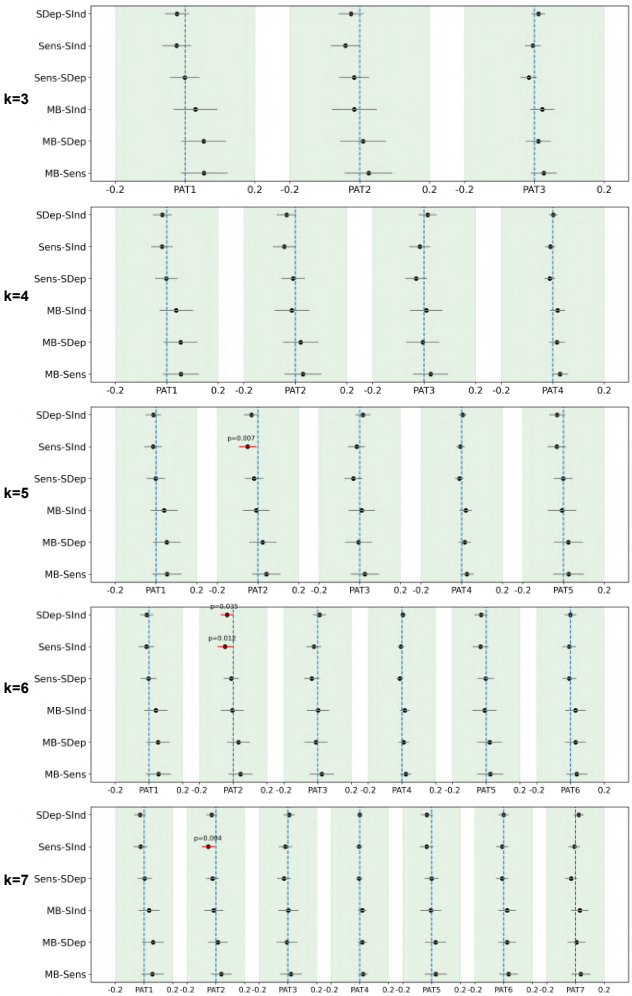

Figure D24. After <u>global signal regression</u>, none of the functional connectivity patterns can be meaningfully assigned to MB (lag = 0). Considering a mental state analysis window with lag=0, a generalized linear mixed model analysis for each pattern separately could not result in significant similarity of any pattern to the connectivity matrices related to the MB reports. The results are replicated with different number of clusters (k=3-7). For each cluster number k, a model fit is considered significant if its p-value is lower than 0.05 k to correct for multiple tests. In case of significant fit, a post-hoc Tukey test was performed for contrast analysis between different mental state pairs.

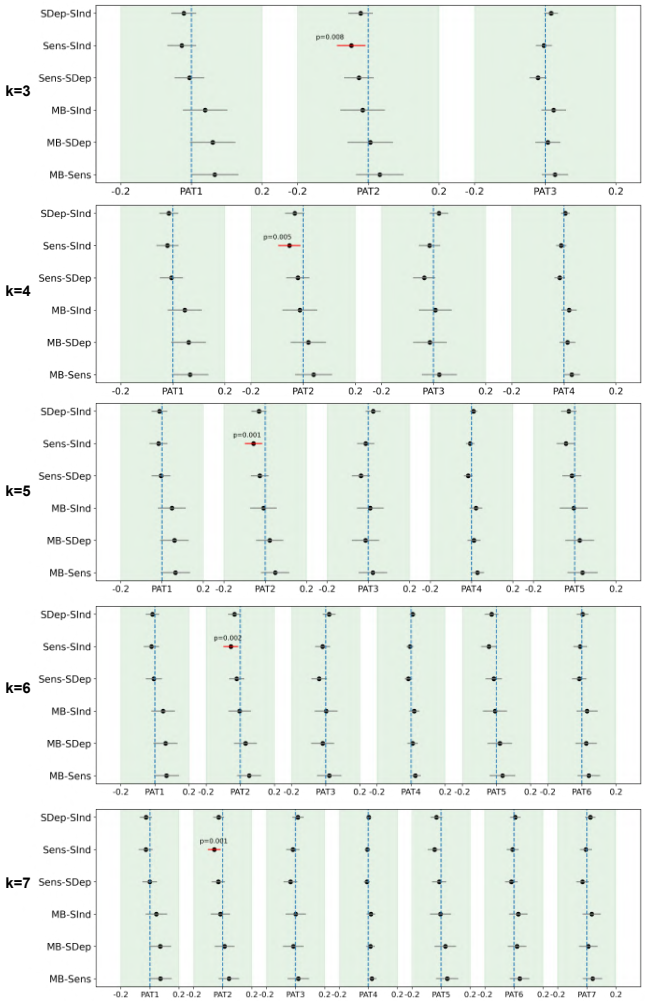

Figure D25. After <u>global signal regression</u>, none of the functional connectivity patterns can be meaningfully assigned to MB (lag = 1). Considering a mental state analysis window with lag=1, a generalized linear mixed model analysis for each pattern separately could not result in significant similarity of any pattern to the connectivity matrices related to the MB reports. The results are replicated with different number of clusters (k=3-7). For each cluster number k, a model fit is considered significant if its p-value is lower than 0.05 k to correct for multiple tests. In case of significant fit, a post-hoc Tukey test was performed for contrast analysis between different mental state pairs.

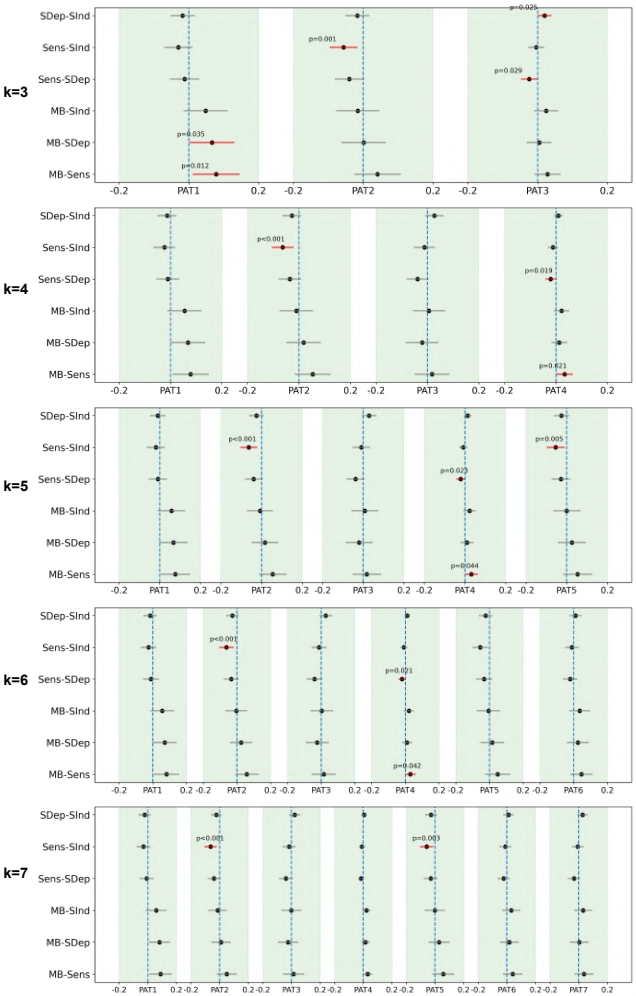

Figure D26. After <u>global signal regression</u>, none of the functional connectivity patterns can be meaningfully assigned to MB (lag = 2). Considering a mental state analysis window with lag=2, a generalized linear mixed model analysis for each pattern separately could not result in significant similarity of any pattern to the connectivity matrices related to the MB reports. The results are replicated with different number of clusters (k=3-7). For each cluster number k, a model fit is considered significant if its p-value is lower than 0.05 k to correct for multiple tests. In case of significant fit, a post-hoc Tukey test was performed for contrast analysis between different mental state pairs.

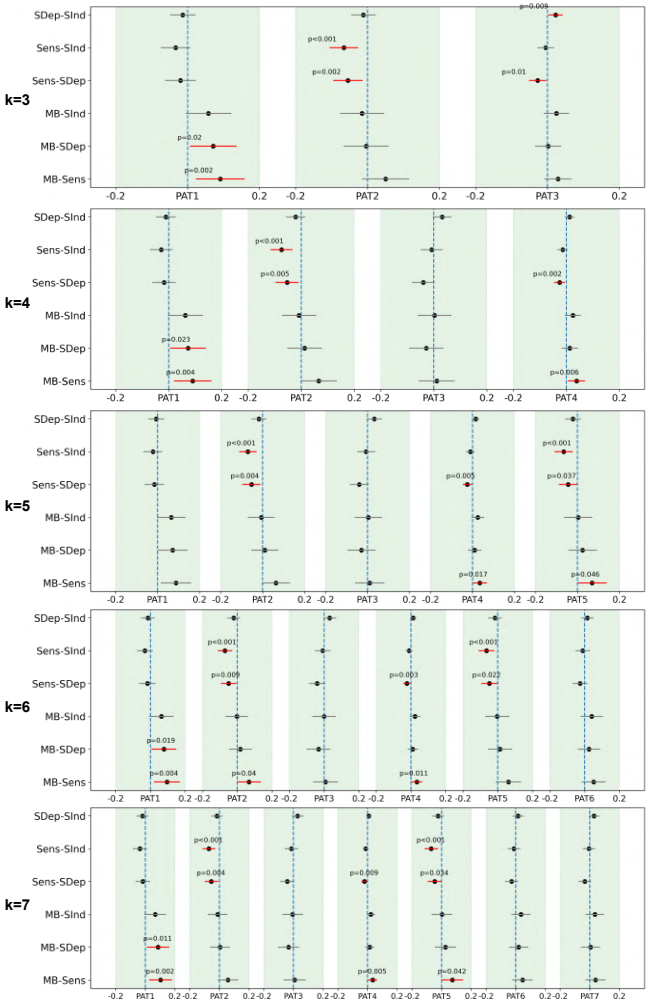

Figure D27. After <u>global signal regression</u>, none of the functional connectivity patterns can be meaningfully assigned to MB (lag = 3). Considering a mental state analysis window with lag=3, a generalized linear mixed model analysis for each pattern separately could not result in significant similarity of any pattern to the connectivity matrices related to the MB reports. The results are replicated with different number of clusters (k=3-7). For each cluster number k, a model fit is considered significant if its p-value is lower than 0.05 k to correct for multiple tests. In case of significant fit, a post-hoc Tukey test was performed for contrast analysis between different mental state pairs.

References

Ackermann, H., & Riecker, A. (2010). The contribution(s) of the insula to speech production: A review of the clinical and functional imaging literature. *Brain Structure and Function*, *214*(5–6), 419–433. https://doi.org/10.1007/s00429-010-0257-x

Aedo-Jury, F., Schwalm, M., Hamzehpour, L., & Stroh, A. (2020). Brain states govern the spatio-temporal dynamics of resting-state functional connectivity. *ELife*, *9*, e53186. https://doi.org/10.7554/eLife.53186

Aguilera, M., & Di Paolo, E. A. (2021). Critical integration in neural and cognitive systems: Beyond power-law scaling as the hallmark of soft assembly. *Neuroscience & Biobehavioral Reviews*, *123*, 230–237. https://doi.org/10.1016/j.neubiorev.2021.01.009

Aizenstein, H. J., Clark, K. A., Butters, M. A., Cochran, J., Stenger, V. A., Meltzer, C. C., Reynolds, C. F., & Carter, C. S. (2004). The BOLD Hemodynamic Response in Healthy Aging. *Journal of Cognitive Neuroscience*, *16*(5), 786–793. https://doi.org/10.1162/089892904970681

Allen, E. A., Damaraju, E., Plis, S. M., Erhardt, E. B., Eichele, T., & Calhoun, V. D. (2014). Tracking Whole-Brain Connectivity Dynamics in the Resting State. *Cerebral Cortex*, *24*(3), 663–676. https://doi.org/10.1093/cercor/bhs352

Alperin, N., Bagci, A. M., & Lee, S. H. (2017). Spaceflight-induced changes in white matter hyperintensity burden in astronauts. *Neurology*, *89*(21), 2187–2191. https://doi.org/10.1212/WNL.0000000000004475

Andersen, K. A. A., Carhart-Harris, R., Nutt, D. J., & Erritzoe, D. (2021). Therapeutic effects of classic serotonergic psychedelics: A systematic review of modern-era clinical studies. *Acta Psychiatrica Scandinavica*, *143*(2), 101–118. https://doi.org/10.1111/acps.13249

Anderson, B. T., Danforth, A., Daroff, P. R., Stauffer, C., Ekman, E., Agin-Liebes, G., Trope, A., Boden, M. T., Dilley, P. J., Mitchell, J., & Woolley, J. (2020). Psilocybin-assisted group therapy for demoralized older long-term AIDS survivor men: An open-label safety and feasibility pilot study. *EClinicalMedicine*, *27*, 100538. https://doi.org/10.1016/j.eclinm.2020.100538

Anderson, J. S., Druzgal, T. J., Lopez-Larson, M., Jeong, E.-K., Desai, K., & Yurgelun-Todd, D. (2011). Network anticorrelations, global regression, and phase-shifted soft tissue correction. *Human Brain Mapping*, *32*(6), 919–934. https://doi.org/10.1002/hbm.21079

Andersson, J. L. R., Graham, M. S., Drobnjak, I., Zhang, H., Filippini, N., & Bastiani, M. (2017). Towards a comprehensive framework for movement and distortion

correction of diffusion MR images: Within volume movement. *NeuroImage*, *152*, 450–466. https://doi.org/10.1016/j.neuroimage.2017.02.085

Andersson, J. L. R., Graham, M. S., Zsoldos, E., & Sotiropoulos, S. N. (2016). Incorporating outlier detection and replacement into a non-parametric framework for movement and distortion correction of diffusion MR images. *NeuroImage*, *141*, 556–572. https://doi.org/10.1016/j.neuroimage.2016.06.058

Andersson, J. L. R., Skare, S., & Ashburner, J. (2003). How to correct susceptibility distortions in spin-echo echo-planar images: Application to diffusion tensor imaging. *NeuroImage*, *20*(2), 870–888. https://doi.org/10.1016/S1053-8119(03)00336-7

Andersson, J. L. R., & Sotiropoulos, S. N. (2016a). An integrated approach to correction for off-resonance effects and subject movement in diffusion MR imaging. *NeuroImage*, *125*, 1063–1078. https://doi.org/10.1016/j.neuroimage.2015.10.019

Andersson, J. L. R., & Sotiropoulos, S. N. (2016b). An integrated approach to correction for off-resonance effects and subject movement in diffusion MR imaging. *NeuroImage*, *125*, 1063–1078. https://doi.org/10.1016/j.neuroimage.2015.10.019

Andrillon, T., Burns, A., Mackay, T., Windt, J., & Tsuchiya, N. (2021). Predicting lapses of attention with sleep-like slow waves. *Nature Communications*, *12*(1), 3657. https://doi.org/10.1038/s41467-021-23890-7

Andrillon, T., Windt, J., Silk, T., Drummond, S. P. A., Bellgrove, M. A., & Tsuchiya, N. (2019). Does the Mind Wander When the Brain Takes a Break? Local Sleep in Wakefulness, Attentional Lapses and Mind-Wandering. *Frontiers in Neuroscience*, *13*. https://www.frontiersin.org/articles/10.3389/fnins.2019.00949

Balagué, N., Hristovski, R., Almarcha, M., Garcia-Retortillo, S., & Ivanov, P. Ch. (2022). Network Physiology of Exercise: Beyond Molecular and Omics Perspectives. *Sports Medicine - Open*, *8*(1), 119. https://doi.org/10.1186/s40798-022-00512-0

Barisano, G., Sepehrband, F., Collins, H. R., Jillings, S., Jeurissen, B., Taylor, J. A., Schoenmaekers, C., De Laet, C., Rukavishnikov, I., Nosikova, I., Litvinova, L., Rumshiskaya, A., Annen, J., Sijbers, J., Laureys, S., Van Ombergen, A., Petrovichev, V., Sinitsyn, V., Pechenkova, E., … Wuyts, F. L. (2022). The effect of prolonged spaceflight on cerebrospinal fluid and perivascular spaces of astronauts and cosmonauts. *Proceedings of the National Academy of Sciences*, *119*(17), e2120439119. https://doi.org/10.1073/pnas.2120439119

Barrett, F. S., Krimmel, S. R., Griffiths, R. R., Seminowicz, D. A., & Mathur, B. N. (2020). Psilocybin acutely alters the functional connectivity of the claustrum with brain networks that support perception, memory, and attention. *NeuroImage*, *218*, 116980. https://doi.org/10.1016/j.neuroimage.2020.116980

Bartsch, R. P., Liu, K. K. L., Bashan, A., & Ivanov, P. Ch. (2015). Network Physiology: How Organ Systems Dynamically Interact. *PLOS ONE*, *10*(11), e0142143. https://doi.org/10.1371/journal.pone.0142143

Barttfeld, P., Uhrig, L., Sitt, J. D., Sigman, M., Jarraya, B., & Dehaene, S. (2015). Signature of consciousness in the dynamics of resting-state brain activity. *Proceedings of the National Academy of Sciences*, *112*(3), 887–892. https://doi.org/10.1073/pnas.1418031112

Bashan, A., Bartsch, R. P., Kantelhardt, Jan. W., Havlin, S., & Ivanov, P. Ch. (2012). Network physiology reveals relations between network topology and physiological function. *Nature Communications*, *3*(1), 702. https://doi.org/10.1038/ncomms1705

Basile, G. A., Bertino, S., Nozais, V., Bramanti, A., Ciurleo, R., Anastasi, G. P., Milardi, D., & Cacciola, A. (2022). White matter substrates of functional connectivity dynamics in the human brain. *NeuroImage*, *258*, 119391. https://doi.org/10.1016/j.neuroimage.2022.119391

Beckmann, C. F., DeLuca, M., Devlin, J. T., & Smith, S. M. (2005). Investigations into resting-state connectivity using independent component analysis. *Philosophical Transactions of the Royal Society B: Biological Sciences*, *360*(1457), 1001–1013. https://doi.org/10.1098/rstb.2005.1634

Birn, R. M., Molloy, E. K., Patriat, R., Parker, T., Meier, T. B., Kirk, G. R., Nair, V. A., Meyerand, M. E., & Prabhakaran, V. (2013). The effect of scan length on the reliability of resting-state fMRI connectivity estimates. *NeuroImage*, *83*, 550–558. https://doi.org/10.1016/j.neuroimage.2013.05.099

Biswal, B. B., Kylen, J. V., & Hyde, J. S. (1997). Simultaneous assessment of flow and BOLD signals in resting-state functional connectivity maps. *NMR in Biomedicine*, *10*(4–5), 165–170. https://doi.org/10.1002/(SICI)1099-1492(199706/08)10:4/5<165::AID-NBM454>3.0.CO;2-7

Biswal, B., Zerrin Yetkin, F., Haughton, V. M., & Hyde, J. S. (1995). Functional connectivity in the motor cortex of resting human brain using echo-planar mri. *Magnetic Resonance in Medicine*, *34*(4), 537–541. https://doi.org/10.1002/mrm.1910340409

Bloomberg, J. J., Peters, B. T., Cohen, H. S., & Mulavara, A. P. (2015). Enhancing astronaut performance using sensorimotor adaptability training. *Frontiers in Systems Neuroscience*, *9*. https://doi.org/10.3389/fnsys.2015.00129

Blumenfeld, H. (2012). Impaired consciousness in epilepsy. *The Lancet Neurology*, *11*(9), 814–826. https://doi.org/10.1016/S1474-4422(12)70188-6

Bogenschutz, M. P., Forcehimes, A. A., Pommy, J. A., Wilcox, C. E., Barbosa, P., & Strassman, R. J. (2015). Psilocybin-assisted treatment for alcohol dependence: A proof-of-concept study. *Journal of Psychopharmacology*, *29*(3), 289–299. https://doi.org/10.1177/0269881114565144

Bridi, M. C. D., Zong, F.-J., Min, X., Luo, N., Tran, T., Qiu, J., Severin, D., Zhang, X.-T., Wang, G., Zhu, Z.-J., He, K.-W., & Kirkwood, A. (2020). Daily Oscillation of the Excitation-Inhibition Balance in Visual Cortical Circuits. *Neuron*, *105*(4), 621-629.e4. https://doi.org/10.1016/j.neuron.2019.11.011

Bukhari, Q., Schroeter, A., & Rudin, M. (2018). Increasing isoflurane dose reduces homotopic correlation and functional segregation of brain networks in mice as revealed by resting-state fMRI. *Scientific Reports*, *8*(1), Article 1. https://doi.org/10.1038/s41598-018-28766-3

Bullmore, E., & Sporns, O. (2012). The economy of brain network organization. *Nature Reviews Neuroscience*, *13*(5), 336–349. https://doi.org/10.1038/nrn3214

Cabral, J., Vidaurre, D., Marques, P., Magalhães, R., Silva Moreira, P., Miguel Soares, J., Deco, G., Sousa, N., & Kringelbach, M. L. (2017). Cognitive performance in healthy older adults relates to spontaneous switching between states of functional connectivity during rest. *Scientific Reports*, *7*(1), 5135. https://doi.org/10.1038/s41598-017-05425-7

Calamante, F., Smith, R. E., Liang, X., Zalesky, A., & Connelly, A. (2017). Track-weighted dynamic functional connectivity (TW-dFC): A new method to study time-resolved functional connectivity. *Brain Structure and Function*, *222*(8), 3761–3774. https://doi.org/10.1007/s00429-017-1431-1

Carhart-Harris, R. L., Bolstridge, M., Day, C. M. J., Rucker, J., Watts, R., Erritzoe, D. E., Kaelen, M., Giribaldi, B., Bloomfield, M., Pilling, S., Rickard, J. A., Forbes, B., Feilding, A., Taylor, D., Curran, H. V., & Nutt, D. J. (2018). Psilocybin with psychological support for treatment-resistant depression: Six-month follow-up. *Psychopharmacology*, *235*(2), 399–408. https://doi.org/10.1007/s00213-017-4771-x

Carhart-Harris, R. L., Bolstridge, M., Rucker, J., Day, C. M. J., Erritzoe, D., Kaelen, M., Bloomfield, M., Rickard, J. A., Forbes, B., Feilding, A., Taylor, D., Pilling, S., Curran, V. H., & Nutt, D. J. (2016). Psilocybin with psychological support for treatment-resistant depression: An open-label feasibility study. *The Lancet Psychiatry*, *3*(7), 619–627. https://doi.org/10.1016/S2215-0366(16)30065-7

Carhart-Harris, R. L., Erritzoe, D., Williams, T., Stone, J. M., Reed, L. J., Colasanti, A., Tyacke, R. J., Leech, R., Malizia, A. L., Murphy, K., Hobden, P., Evans, J., Feilding,

A., Wise, R. G., & Nutt, D. J. (2012). Neural correlates of the psychedelic state as determined by fMRI studies with psilocybin. *Proceedings of the National Academy of Sciences*, *109*(6), 2138–2143. https://doi.org/10.1073/pnas.1119598109

Carhart-Harris, R. L., & Friston, K. J. (2019). REBUS and the Anarchic Brain: Toward a Unified Model of the Brain Action of Psychedelics. *Pharmacological Reviews*, *71*(3), 316–344. https://doi.org/10.1124/pr.118.017160

Carhart-Harris, R. L., Giribaldi, B., Watts, R., Baker-Jones, M., Murphy-Beiner, A., Murphy, R., Martell, J., Blemings, A., Erritzoe, D., & Nutt, D. J. (2021). Trial of Psilocybin versus Escitalopram for Depression. *New England Journal of Medicine*, *384*(15), 1402–1411. https://doi.org/10.1056/NEJMoa2032994

Carhart-Harris, R. L., Leech, R., Erritzoe, D., Williams, T. M., Stone, J. M., Evans, J., Sharp, D. J., Feilding, A., Wise, R. G., & Nutt, D. J. (2013). Functional Connectivity Measures After Psilocybin Inform a Novel Hypothesis of Early Psychosis. *Schizophrenia Bulletin*, *39*(6), 1343–1351. https://doi.org/10.1093/schbul/sbs117

Carhart-Harris, R. L., Leech, R., Hellyer, P. J., Shanahan, M., Feilding, A., Tagliazucchi, E., Chialvo, D. R., & Nutt, D. (2014). The entropic brain: A theory of conscious states informed by neuroimaging research with psychedelic drugs. *Frontiers in Human Neuroscience*, *8*. https://doi.org/10.3389/fnhum.2014.00020

Carhart-Harris, R. L., Roseman, L., Bolstridge, M., Demetriou, L., Pannekoek, J. N., Wall, M. B., Tanner, M., Kaelen, M., McGonigle, J., Murphy, K., Leech, R., Curran, H. V., & Nutt, D. J. (2017). Psilocybin for treatment-resistant depression: FMRI-measured brain mechanisms. *Scientific Reports*, *7*(1), 13187. https://doi.org/10.1038/s41598-017-13282-7

Casorso, J., Kong, X., Chi, W., Van De Ville, D., Yeo, B. T. T., & Liégeois, R. (2019). Dynamic mode decomposition of resting-state and task fMRI. *NeuroImage*, *194*, 42–54. https://doi.org/10.1016/j.neuroimage.2019.03.019

Cavanna, F., Vilas, M. G., Palmucci, M., & Tagliazucchi, E. (2018). Dynamic functional connectivity and brain metastability during altered states of consciousness. *NeuroImage*, *180*, 383–395. https://doi.org/10.1016/j.neuroimage.2017.09.065

Chang, C., & Glover, G. H. (2010). Time–frequency dynamics of resting-state brain connectivity measured with fMRI. *NeuroImage*, *50*(1), 81–98. https://doi.org/10.1016/j.neuroimage.2009.12.011

Chen, J. E., Lewis, L. D., Chang, C., Tian, Q., Fultz, N. E., Ohringer, N. A., Rosen, B. R., & Polimeni, J. R. (2020). Resting-state "physiological networks". *NeuroImage*, *213*, 116707. https://doi.org/10.1016/j.neuroimage.2020.116707

Chou, Y., Sundman, M., Whitson, H. E., Gaur, P., Chu, M.-L., Weingarten, C. P., Madden, D. J., Wang, L., Kirste, I., Joliot, M., Diaz, M. T., Li, Y.-J., Song, A. W., & Chen, N. (2017). Maintenance and Representation of Mind Wandering during Resting-State fMRI. *Scientific Reports*, *7*(1), 40722. https://doi.org/10.1038/srep40722

Christoff, K., Irving, Z. C., Fox, K. C. R., Spreng, R. N., & Andrews-Hanna, J. R. (2016). Mind-wandering as spontaneous thought: A dynamic framework. *Nature Reviews Neuroscience*, *17*(11), Article 11. https://doi.org/10.1038/nrn.2016.113

Cliff, N. (1993). Dominance statistics: Ordinal analyses to answer ordinal questions. *Psychological Bulletin*, *114*(3), 494.

Cocchi, L., Harding, I. H., Lord, A., Pantelis, C., Yucel, M., & Zalesky, A. (2014). Disruption of structure–function coupling in the schizophrenia connectome. *NeuroImage: Clinical*, *4*, 779–787. https://doi.org/10.1016/j.nicl.2014.05.004

Cole, M. W., Bassett, D. S., Power, J. D., Braver, T. S., & Petersen, S. E. (2014). Intrinsic and Task-Evoked Network Architectures of the Human Brain. *Neuron*, *83*(1), 238–251. https://doi.org/10.1016/j.neuron.2014.05.014

Cole, M. W., Ito, T., Bassett, D. S., & Schultz, D. H. (2016). Activity flow over resting-state networks shapes cognitive task activations. *Nature Neuroscience*, *19*(12), 1718–1726. https://doi.org/10.1038/nn.4406

Colenbier, N., Van de Steen, F., Uddin, L. Q., Poldrack, R. A., Calhoun, V. D., & Marinazzo, D. (2020). Disambiguating the role of blood flow and global signal with partial information decomposition. *NeuroImage*, *213*, 116699. https://doi.org/10.1016/j.neuroimage.2020.116699

Collin, G., Scholtens, L. H., Kahn, R. S., Hillegers, M. H. J., & van den Heuvel, M. P. (2017). Affected Anatomical Rich Club and Structural–Functional Coupling in Young Offspring of Schizophrenia and Bipolar Disorder Patients. *Biological Psychiatry*, *82*(10), 746–755. https://doi.org/10.1016/j.biopsych.2017.06.013

Cox, R. W. (1996). AFNI: Software for Analysis and Visualization of Functional Magnetic Resonance Neuroimages. *Computers and Biomedical Research*, *29*(3), 162–173. https://doi.org/10.1006/cbmr.1996.0014

Criscuolo, A., Schwartze, M., & Kotz, S. A. (2022). Cognition through the lens of a body–brain dynamic system. *Trends in Neurosciences*, *45*(9), 667–677. https://doi.org/10.1016/j.tins.2022.06.004

Critchley, H. D., & Harrison, N. A. (2013). Visceral Influences on Brain and Behavior. *Neuron*, *77*(4), 624–638. https://doi.org/10.1016/j.neuron.2013.02.008

Critchley, H. D., Wiens, S., Rotshtein, P., Öhman, A., & Dolan, R. J. (2004). Neural systems supporting interoceptive awareness. *Nature Neuroscience*, *7*(2), 189–195. https://doi.org/10.1038/nn1176

Damoiseaux, J. S., Rombouts, S. A. R. B., Barkhof, F., Scheltens, P., Stam, C. J., Smith, S. M., & Beckmann, C. F. (2006). Consistent resting-state networks across healthy subjects. *Proceedings of the National Academy of Sciences*, *103*(37), 13848–13853. https://doi.org/10.1073/pnas.0601417103

D'Argembeau, A., Stawarczyk, D., Majerus, S., Collette, F., Van der Linden, M., & Salmon, E. (2010). Modulation of medial prefrontal and inferior parietal cortices when thinking about past, present, and future selves. *Social Neuroscience*, *5*(2), 187–200. https://doi.org/10.1080/17470910903233562

Davatzikos, C., Ruparel, K., Fan, Y., Shen, D. G., Acharyya, M., Loughead, J. W., Gur, R. C., & Langleben, D. D. (2005). Classifying spatial patterns of brain activity with machine learning methods: Application to lie detection. *NeuroImage*, *28*(3), 663–668. https://doi.org/10.1016/j.neuroimage.2005.08.009

Davis, A. K., Barrett, F. S., May, D. G., Cosimano, M. P., Sepeda, N. D., Johnson, M. W., Finan, P. H., & Griffiths, R. R. (2021). Effects of Psilocybin-Assisted Therapy on Major Depressive Disorder: A Randomized Clinical Trial. *JAMA Psychiatry*, *78*(5), 481. https://doi.org/10.1001/jamapsychiatry.2020.3285

De la Torre, G. (2014). Cognitive Neuroscience in Space. *Life*, *4*(3), 281–294. https://doi.org/10.3390/life4030281

De Luca, M., Beckmann, C. F., De Stefano, N., Matthews, P. M., & Smith, S. M. (2006). FMRI resting state networks define distinct modes of long-distance interactions in the human brain. *NeuroImage*, *29*(4), 1359–1367. https://doi.org/10.1016/j.neuroimage.2005.08.035

Dehaene, S., Changeux, J.-P., Naccache, L., Sackur, J., & Sergent, C. (2006). Conscious, preconscious, and subliminal processing: A testable taxonomy. *Trends in Cognitive Sciences*, *10*(5), 204–211. https://doi.org/10.1016/j.tics.2006.03.007

Dehaene, S., Sergent, C., & Changeux, J.-P. (2003). A neuronal network model linking subjective reports and objective physiological data during conscious perception. *Proceedings of the National Academy of Sciences*, *100*(14), 8520–8525. https://doi.org/10.1073/pnas.1332574100

Delamillieure, P., Doucet, G., Mazoyer, B., Turbelin, M.-R., Delcroix, N., Mellet, E., Zago, L., Crivello, F., Petit, L., Tzourio-Mazoyer, N., & Joliot, M. (2010). The resting state questionnaire: An introspective questionnaire for evaluation of inner experience during the conscious resting state. *Brain Research Bulletin*, *81*(6), 565–573. https://doi.org/10.1016/j.brainresbull.2009.11.014

Demertzi, A., Tagliazucchi, E., Dehaene, S., Deco, G., Barttfeld, P., Raimondo, F., Martial, C., Fernández-Espejo, D., Rohaut, B., Voss, H. U., Schiff, N. D., Owen, A. M., Laureys, S., Naccache, L., & Sitt, J. D. (2019). Human consciousness is supported by dynamic complex patterns of brain signal coordination. *Science Advances*, *5*(2), eaat7603. https://doi.org/10.1126/sciadv.aat7603

Demertzi, A., Van Ombergen, A., Tomilovskaya, E., Jeurissen, B., Pechenkova, E., Di Perri, C., Litvinova, L., Amico, E., Rumshiskaya, A., Rukavishnikov, I., Sijbers, J., Sinitsyn, V., Kozlovskaya, I. B., Sunaert, S., Parizel, P. M., Van de Heyning, P. H., Laureys, S., & Wuyts, F. L. (2016). Cortical reorganization in an astronaut's brain after long-duration spaceflight. *Brain Structure and Function*, *221*(5), 2873–2876. https://doi.org/10.1007/s00429-015-1054-3

Desjardins, A. E., Kiehl, K. A., & Liddle, P. F. (2001). Removal of Confounding Effects of Global Signal in Functional MRI Analyses. *NeuroImage*, *13*(4), 751–758. https://doi.org/10.1006/nimg.2000.0719

Dhollander, T., Mito, R., Raffelt, D., & Connelly, A. (2019). Improved white matter response function estimation for 3-tissue constrained spherical deconvolution. *Proc. Intl. Soc. Mag. Reson. Med.*, *555*.

Ding, J.-R., An, D., Liao, W., Li, J., Wu, G.-R., Xu, Q., Long, Z., Gong, Q., Zhou, D., Sporns, O., & Chen, H. (2013). Altered Functional and Structural Connectivity Networks in Psychogenic Non-Epileptic Seizures. *PLoS ONE*, *8*(5), e63850. https://doi.org/10.1371/journal.pone.0063850

Dittrich, A. (1998). The standardized psychometric assessment of altered states of consciousness (ASCs) in humans. *Pharmacopsychiatry*, *31*(S 2), 80–84.

Efklides, A. (2014). The Blank-in-the-Mind Experience: Another Manifestation of the Tip-of-the-Tongue State or Something Else? In A. S. Brown & B. L. Schwartz (Eds.), *Tip-of-the-Tongue States and Related Phenomena* (pp. 232–263). Cambridge University Press. https://doi.org/10.1017/CBO9781139547383.011

El-Baba, M., Lewis, D. J., Fang, Z., Owen, A. M., Fogel, S. M., & Morton, J. B. (2019). Functional connectivity dynamics slow with descent from wakefulness to sleep. *PLOS ONE*, *14*(12), e0224669. https://doi.org/10.1371/journal.pone.0224669

Erritzoe, D., Roseman, L., Nour, M. M., MacLean, K., Kaelen, M., Nutt, D. J., & Carhart-Harris, R. L. (2018). Effects of psilocybin therapy on personality structure. *Acta Psychiatrica Scandinavica*, *138*(5), 368–378. https://doi.org/10.1111/acps.12904

Filippi, M., van den Heuvel, M. P., Fornito, A., He, Y., Hulshoff Pol, H. E., Agosta, F., Comi, G., & Rocca, M. A. (2013). Assessment of system dysfunction in the brain through MRI-based connectomics. *The Lancet Neurology*, *12*(12), 1189–1199. https://doi.org/10.1016/S1474-4422(13)70144-3

Fornito, A., Harrison, B. J., Zalesky, A., & Simons, J. S. (2012). Competitive and cooperative dynamics of large-scale brain functional networks supporting recollection. *Proceedings of the National Academy of Sciences*, *109*(31), 12788–12793. https://doi.org/10.1073/pnas.1204185109

Fox, M. D., & Raichle, M. E. (2007). Spontaneous fluctuations in brain activity observed with functional magnetic resonance imaging. *Nature Reviews Neuroscience*, *8*(9), 700–711. https://doi.org/10.1038/nrn2201

Fox, M. D., Snyder, A. Z., Vincent, J. L., Corbetta, M., Van Essen, D. C., & Raichle, M. E. (2005). The human brain is intrinsically organized into dynamic, anticorrelated functional networks. *Proceedings of the National Academy of Sciences*, *102*(27), 9673–9678. https://doi.org/10.1073/pnas.0504136102

Fox, M. D., Zhang, D., Snyder, A. Z., & Raichle, M. E. (2009). The Global Signal and Observed Anticorrelated Resting State Brain Networks. *Journal of Neurophysiology*, *101*(6), 3270–3283. https://doi.org/10.1152/jn.90777.2008

Fukunaga, M., Horovitz, S. G., van Gelderen, P., de Zwart, J. A., Jansma, J. M., Ikonomidou, V. N., Chu, R., Deckers, R. H. R., Leopold, D. A., & Duyn, J. H. (2006). Large-amplitude, spatially correlated fluctuations in BOLD fMRI signals during extended rest and early sleep stages. *Magnetic Resonance Imaging*, *24*(8), 979–992. https://doi.org/10.1016/j.mri.2006.04.018

Gagniuc, P. A. (2017). *Markov chains: From theory to implementation and experimentation*. John Wiley & Sons.

Garcia-Romeu, A., Davis, A. K., Erowid, F., Erowid, E., Griffiths, R. R., & Johnson, M. W. (2019). Cessation and reduction in alcohol consumption and misuse after psychedelic use. *Journal of Psychopharmacology*, *33*(9), 1088–1101. https://doi.org/10.1177/0269881119845793

Ghoneim, M. M., & Weiskopf, R. B. (2000). Awareness during anesthesia. *The Journal of the American Society of Anesthesiologists*, *92*(2), 597–597.

Gilmore, A. W., Nelson, S. M., Chen, H.-Y., & McDermott, K. B. (2018). Task-related and resting-state fMRI identify distinct networks that preferentially support remembering the past and imagining the future. *Neuropsychologia*, *110*, 180–190.

Glasser, M. F., Coalson, T. S., Bijsterbosch, J. D., Harrison, S. J., Harms, M. P., Anticevic, A., Van Essen, D. C., & Smith, S. M. (2018). Using temporal ICA to selectively remove global noise while preserving global signal in functional MRI data. *NeuroImage*, *181*, 692–717. https://doi.org/10.1016/j.neuroimage.2018.04.076

Glynn, S. M., & Detre, J. A. (2013). Imaging Epilepsy and Epileptic Seizures Using fMRI. In S. Ulmer & O. Jansen (Eds.), *FMRI: Basics and Clinical Applications* (pp. 177–189). Springer. https://doi.org/10.1007/978-3-642-34342-1_14

Gomez-Pinilla, F., & Hillman, C. (2013). The Influence of Exercise on Cognitive Abilities. In R. Terjung (Ed.), *Comprehensive Physiology* (1st ed., pp. 403–428). Wiley. https://doi.org/10.1002/cphy.c110063

Gonzalez-Castillo, J., Caballero-Gaudes, C., Topolski, N., Handwerker, D. A., Pereira, F., & Bandettini, P. A. (2019). Imaging the spontaneous flow of thought: Distinct periods of cognition contribute to dynamic functional connectivity during rest. *NeuroImage*, *202*, 116129. https://doi.org/10.1016/j.neuroimage.2019.116129

Gorgolewski, K., Burns, C. D., Madison, C., Clark, D., Halchenko, Y. O., Waskom, M. L., & Ghosh, S. S. (2011). Nipype: A Flexible, Lightweight and Extensible Neuroimaging Data Processing Framework in Python. *Frontiers in Neuroinformatics*, *5*. https://doi.org/10.3389/fninf.2011.00013

Griffa, A., Amico, E., Liégeois, R., Van De Ville, D., & Preti, M. G. (2022). Brain structure-function coupling provides signatures for task decoding and individual fingerprinting. *NeuroImage*, *250*, 118970. https://doi.org/10.1016/j.neuroimage.2022.118970

Griffiths, R. R., Johnson, M. W., Carducci, M. A., Umbricht, A., Richards, W. A., Richards, B. D., Cosimano, M. P., & Klinedinst, M. A. (2016). Psilocybin produces substantial and sustained decreases in depression and anxiety in patients with life-threatening cancer: A randomized double-blind trial. *Journal of Psychopharmacology*, *30*(12), 1181–1197. https://doi.org/10.1177/0269881116675513

Griffiths, R. R., Johnson, M. W., Richards, W. A., Richards, B. D., Jesse, R., MacLean, K. A., Barrett, F. S., Cosimano, M. P., & Klinedinst, M. A. (2018). Psilocybin-occasioned mystical-type experience in combination with meditation and other spiritual practices produces enduring positive changes in psychological functioning and in trait measures of prosocial attitudes and behaviors. *Journal of Psychopharmacology*, *32*(1), 49–69. https://doi.org/10.1177/0269881117731279

Griffiths, R. R., Johnson, M. W., Richards, W. A., Richards, B. D., McCann, U., & Jesse, R. (2011). Psilocybin occasioned mystical-type experiences: Immediate and persisting dose-related effects. *Psychopharmacology*, *218*(4), 649–665. https://doi.org/10.1007/s00213-011-2358-5

Griffiths, R. R., Richards, W. A., McCann, U., & Jesse, R. (2006). Psilocybin can occasion mystical-type experiences having substantial and sustained personal meaning and spiritual significance. *Psychopharmacology*, *187*(3), 268–283. https://doi.org/10.1007/s00213-006-0457-5

Grob, C. S., Danforth, A. L., Chopra, G. S., Hagerty, M., McKay, C. R., Halberstadt, A. L., & Greer, G. R. (2011). Pilot Study of Psilocybin Treatment for Anxiety in Patients With Advanced-Stage Cancer. *Archives of General Psychiatry*, *68*(1), 71. https://doi.org/10.1001/archgenpsychiatry.2010.116

Gu, S., Cieslak, M., Baird, B., Muldoon, S. F., Grafton, S. T., Pasqualetti, F., & Bassett, D. S. (2018). The Energy Landscape of Neurophysiological Activity Implicit in Brain Network Structure. *Scientific Reports*, *8*(1), 2507. https://doi.org/10.1038/s41598-018-20123-8

Gu, Z., Jamison, K. W., Sabuncu, M. R., & Kuceyeski, A. (2020). *Regional structural-functional connectome coupling is heritable and associated with age, sex and cognitive scores in adults* [Preprint]. Neuroscience. https://doi.org/10.1101/2020.12.09.417725

Hagmann, P., Sporns, O., Madan, N., Cammoun, L., Pienaar, R., Wedeen, V. J., Meuli, R., Thiran, J.-P., & Grant, P. E. (2010). White matter maturation reshapes structural connectivity in the late developing human brain. *Proceedings of the National Academy of Sciences*, *107*(44), 19067–19072. https://doi.org/10.1073/pnas.1009073107

Hansen, E. C. A., Battaglia, D., Spiegler, A., Deco, G., & Jirsa, V. K. (2015). Functional connectivity dynamics: Modeling the switching behavior of the resting state. *NeuroImage*, *105*, 525–535. https://doi.org/10.1016/j.neuroimage.2014.11.001

Hanson, S. J., & Halchenko, Y. O. (2008). Brain Reading Using Full Brain Support Vector Machines for Object Recognition: There Is No "Face" Identification Area. *Neural Computation*, *20*(2), 486–503. https://doi.org/10.1162/neco.2007.09-06-340

Hasler, F., Grimberg, U., Benz, M. A., Huber, T., & Vollenweider, F. X. (2004). Acute psychological and physiological effects of psilocybin in healthy humans: A double-blind, placebo-controlled dose?effect study. *Psychopharmacology*, *172*(2), 145–156. https://doi.org/10.1007/s00213-003-1640-6

Haynes, J.-D., & Rees, G. (2006). Decoding mental states from brain activity in humans. *Nature Reviews Neuroscience*, *7*(7), 523–534. https://doi.org/10.1038/nrn1931

He, H., & Liu, T. T. (2012). A geometric view of global signal confounds in resting-state functional MRI. *NeuroImage*, *59*(3), 2339–2348. https://doi.org/10.1016/j.neuroimage.2011.09.018

He, Y., & Evans, A. (2010). Graph theoretical modeling of brain connectivity. *Current Opinion in Neurology*, *23*(4), 341–350. https://doi.org/10.1097/WCO.0b013e32833aa567

Heine, L., Soddu, A., Gómez, F., Vanhaudenhuyse, A., Tshibanda, L., Thonnard, M., Charland-Verville, V., Kirsch, M., Laureys, S., & Demertzi, A. (2012). Resting State Networks and Consciousness. *Frontiers in Psychology*, *3*. https://doi.org/10.3389/fpsyg.2012.00295

Hupfeld, K. E., McGregor, H. R., Lee, J. K., Beltran, N. E., Kofman, I. S., De Dios, Y. E., Reuter-Lorenz, P. A., Riascos, R. F., Pasternak, O., Wood, S. J., Bloomberg, J. J., Mulavara, A. P., Seidler, R. D., & Alzheimer's Disease Neuroimaging Initiative. (2020). The Impact of 6 and 12 Months in Space on Human Brain Structure and Intracranial Fluid Shifts. *Cerebral Cortex Communications*, *1*(1), tgaa023. https://doi.org/10.1093/texcom/tgaa023

Ikeda, S., Kawano, K., Watanabe, S., Yamashita, O., & Kawahara, Y. (2022). Predicting behavior through dynamic modes in resting-state fMRI data. *NeuroImage*, *247*, 118801. https://doi.org/10.1016/j.neuroimage.2021.118801

Ito, T., Kulkarni, K. R., Schultz, D. H., Mill, R. D., Chen, R. H., Solomyak, L. I., & Cole, M. W. (2017). Cognitive task information is transferred between brain regions via resting-state network topology. *Nature Communications*, *8*(1), 1027. https://doi.org/10.1038/s41467-017-01000-w

Ivanov, P. Ch. (2021). The New Field of Network Physiology: Building the Human Physiolome. *Frontiers in Network Physiology*, *1*, 711778. https://doi.org/10.3389/fnetp.2021.711778

Jenkinson, M., Beckmann, C. F., Behrens, T. E. J., Woolrich, M. W., & Smith, S. M. (2012). FSL. *NeuroImage*, *62*(2), 782–790. https://doi.org/10.1016/j.neuroimage.2011.09.015

Jeurissen, B., Tournier, J.-D., Dhollander, T., Connelly, A., & Sijbers, J. (2014a). Multi-tissue constrained spherical deconvolution for improved analysis of multi-shell diffusion MRI data. *NeuroImage*, *103*, 411–426. https://doi.org/10.1016/j.neuroimage.2014.07.061

Jeurissen, B., Tournier, J.-D., Dhollander, T., Connelly, A., & Sijbers, J. (2014b). Multi-tissue constrained spherical deconvolution for improved analysis of multi-shell diffusion MRI data. *NeuroImage*, *103*, 411–426. https://doi.org/10.1016/j.neuroimage.2014.07.061

Jezzard, P. (2012). Correction of geometric distortion in fMRI data. *NeuroImage*, *62*(2), 648–651. https://doi.org/10.1016/j.neuroimage.2011.09.010

Jillings, S., Pechenkova, E., Tomilovskaya, E., Rukavishnikov, I., Jeurissen, B., Van Ombergen, A., Nosikova, I., Rumshiskaya, A., Litvinova, L., Annen, J., De Laet, C., Schoenmaekers, C., Sijbers, J., Petrovichev, V., Sunaert, S., Parizel, P. M., Sinitsyn, V., Eulenburg, P. zu, Laureys, S., … Wuyts, F. L. (2023). Prolonged microgravity induces reversible and persistent changes on human cerebral

connectivity. *Communications Biology*, *6*(1), 46. https://doi.org/10.1038/s42003-022-04382-w

Jillings, S., Van Ombergen, A., Tomilovskaya, E., Rumshiskaya, A., Litvinova, L., Nosikova, I., Pechenkova, E., Rukavishnikov, I., Kozlovskaya, I. B., Manko, O., Danilichev, S., Sunaert, S., Parizel, P. M., Sinitsyn, V., Petrovichev, V., Laureys, S., zu Eulenburg, P., Sijbers, J., Wuyts, F. L., & Jeurissen, B. (2020). Macro- and microstructural changes in cosmonauts' brains after long-duration spaceflight. *Science Advances*, *6*(36), eaaz9488. https://doi.org/10.1126/sciadv.aaz9488

Jobst, B. M., Atasoy, S., Ponce-Alvarez, A., Sanjuán, A., Roseman, L., Kaelen, M., Carhart-Harris, R., Kringelbach, M. L., & Deco, G. (2021). Increased sensitivity to strong perturbations in a whole-brain model of LSD. *NeuroImage*, *230*, 117809. https://doi.org/10.1016/j.neuroimage.2021.117809

Johnson, M. W., Garcia-Romeu, A., Cosimano, M. P., & Griffiths, R. R. (2014). Pilot study of the 5-HT $_{2A}$ R agonist psilocybin in the treatment of tobacco addiction. *Journal of Psychopharmacology*, *28*(11), 983–992. https://doi.org/10.1177/0269881114548296

Johnson, M. W., Garcia-Romeu, A., & Griffiths, R. R. (2017). Long-term follow-up of psilocybin-facilitated smoking cessation. *The American Journal of Drug and Alcohol Abuse*, *43*(1), 55–60. https://doi.org/10.3109/00952990.2016.1170135

Kane, M. J., Brown, L. H., McVay, J. C., Silvia, P. J., Myin-Germeys, I., & Kwapil, T. R. (2007). For Whom the Mind Wanders, and When: An Experience-Sampling Study of Working Memory and Executive Control in Daily Life. *Psychological Science*, *18*(7), 614–621. https://doi.org/10.1111/j.1467-9280.2007.01948.x

Karapanagiotidis, T., Bernhardt, B. C., Jefferies, E., & Smallwood, J. (2017). Tracking thoughts: Exploring the neural architecture of mental time travel during mind-wandering. *NeuroImage*, *147*, 272–281. https://doi.org/10.1016/j.neuroimage.2016.12.031

Karapanagiotidis, T., Vidaurre, D., Quinn, A. J., Vatansever, D., Poerio, G. L., Turnbull, A., Ho, N. S. P., Leech, R., Bernhardt, B. C., Jefferies, E., Margulies, D. S., Nichols, T. E., Woolrich, M. W., & Smallwood, J. (2020). The psychological correlates of distinct neural states occurring during wakeful rest. *Scientific Reports*, *10*(1), 21121. https://doi.org/10.1038/s41598-020-77336-z

Kawagoe, T., Onoda, K., & Yamaguchi, S. (2018). Different pre-scanning instructions induce distinct psychological and resting brain states during functional magnetic resonance imaging. *The European Journal of Neuroscience*, *47*(1), 77–82. https://doi.org/10.1111/ejn.13787

Kawagoe, T., Onoda, K., & Yamaguchi, S. (2019). The neural correlates of 'mind blanking': When the mind goes away. *Human Brain Mapping*, *40*(17), 4934–4940. https://doi.org/10.1002/hbm.24748

Kellner, E., Dhital, B., Kiselev, V. G., & Reisert, M. (2016). Gibbs-ringing artifact removal based on local subvoxel-shifts: Gibbs-Ringing Artifact Removal. *Magnetic Resonance in Medicine*, *76*(5), 1574–1581. https://doi.org/10.1002/mrm.26054

Koch, M. A., Norris, D. G., & Hund-Georgiadis, M. (2002). An Investigation of Functional and Anatomical Connectivity Using Magnetic Resonance Imaging. *NeuroImage*, *16*(1), 241–250. https://doi.org/10.1006/nimg.2001.1052

Koppelmans, V., Bloomberg, J. J., Mulavara, A. P., & Seidler, R. D. (2016). Brain structural plasticity with spaceflight. *Npj Microgravity*, *2*(1), 2. https://doi.org/10.1038/s41526-016-0001-9

Kornilova, L. N., Naumov, I. A., Glukhikh, D. O., Ekimovskiy, G. A., Pavlova, A. S., Khabarova, V. V., Smirnov, Yu. I., & Yarmanova, E. N. (2017). Vestibular function and space motion sickness. *Human Physiology*, *43*(5), 557–568. https://doi.org/10.1134/S0362119717050085

Kramer, L. A., Hasan, K. M., Stenger, M. B., Sargsyan, A., Laurie, S. S., Otto, C., Ploutz-Snyder, R. J., Marshall-Goebel, K., Riascos, R. F., & Macias, B. R. (2020). Intracranial Effects of Microgravity: A Prospective Longitudinal MRI Study. *Radiology*, *295*(3), 640–648. https://doi.org/10.1148/radiol.2020191413

Kucyi, A. (2018). Just a thought: How mind-wandering is represented in dynamic brain connectivity. *NeuroImage*, *180*, 505–514. https://doi.org/10.1016/j.neuroimage.2017.07.001

Kucyi, A., & Davis, K. D. (2014). Dynamic functional connectivity of the default mode network tracks daydreaming. *NeuroImage*, *100*, 471–480. https://doi.org/10.1016/j.neuroimage.2014.06.044

Kucyi, A., Tambini, A., Sadaghiani, S., Keilholz, S., & Cohen, J. R. (2018). Spontaneous cognitive processes and the behavioral validation of time-varying brain connectivity. *Network Neuroscience*, *2*(4), 397–417. https://doi.org/10.1162/netn_a_00037

Larson-Prior, L. J., Zempel, J. M., Nolan, T. S., Prior, F. W., Snyder, A. Z., & Raichle, M. E. (2009). Cortical network functional connectivity in the descent to sleep. *Proceedings of the National Academy of Sciences*, *106*(11), 4489–4494. https://doi.org/10.1073/pnas.0900924106

Lee, D., Quattrocki Knight, E., Song, H., Lee, S., Pae, C., Yoo, S., & Park, H.-J. (2021). Differential structure-function network coupling in the inattentive and combined types of attention deficit hyperactivity disorder. *PLoS ONE*, *16*(12), e0260295. https://doi.org/10.1371/journal.pone.0260295

Lee, H., Golkowski, D., Jordan, D., Berger, S., Ilg, R., Lee, J., Mashour, G. A., Lee, U., Avidan, M. S., Blain-Moraes, S., Golmirzaie, G., Hardie, R., Hogg, R., Janke, E., Kelz, M. B., Maier, K., Mashour, G. A., Maybrier, H., McKinstry-Wu, A., … Vlisides, P. E. (2019). Relationship of critical dynamics, functional connectivity, and states of consciousness in large-scale human brain networks. *NeuroImage*, *188*, 228–238. https://doi.org/10.1016/j.neuroimage.2018.12.011

Lee, J. K., Koppelmans, V., Riascos, R. F., Hasan, K. M., Pasternak, O., Mulavara, A. P., Bloomberg, J. J., & Seidler, R. D. (2019). Spaceflight-Associated Brain White Matter Microstructural Changes and Intracranial Fluid Redistribution. *JAMA Neurology*, *76*(4), 412. https://doi.org/10.1001/jamaneurol.2018.4882

Leonardi, N., Richiardi, J., Gschwind, M., Simioni, S., Annoni, J.-M., Schluep, M., Vuilleumier, P., & Van De Ville, D. (2013). Principal components of functional connectivity: A new approach to study dynamic brain connectivity during rest. *NeuroImage*, *83*, 937–950. https://doi.org/10.1016/j.neuroimage.2013.07.019

Leopold, D. A. (2003). Very Slow Activity Fluctuations in Monkey Visual Cortex: Implications for Functional Brain Imaging. *Cerebral Cortex*, *13*(4), 422–433. https://doi.org/10.1093/cercor/13.4.422

Li, J., Bolt, T., Bzdok, D., Nomi, J. S., Yeo, B. T. T., Spreng, R. N., & Uddin, L. Q. (2019). Topography and behavioral relevance of the global signal in the human brain. *Scientific Reports*, *9*(1), 14286. https://doi.org/10.1038/s41598-019-50750-8

Li, J., Kong, R., Liégeois, R., Orban, C., Tan, Y., Sun, N., Holmes, A. J., Sabuncu, M. R., Ge, T., & Yeo, B. T. T. (2019). Global signal regression strengthens association between resting-state functional connectivity and behavior. *NeuroImage*, *196*, 126–141. https://doi.org/10.1016/j.neuroimage.2019.04.016

Liégeois, R., Li, J., Kong, R., Orban, C., Van De Ville, D., Ge, T., Sabuncu, M. R., & Yeo, B. T. T. (2019). Resting brain dynamics at different timescales capture distinct aspects of human behavior. *Nature Communications*, *10*(1), 2317. https://doi.org/10.1038/s41467-019-10317-7

Liu, T. T., Nalci, A., & Falahpour, M. (2017). The global signal in fMRI: Nuisance or Information? *NeuroImage*, *150*, 213–229. https://doi.org/10.1016/j.neuroimage.2017.02.036

Liu, X., de Zwart, J. A., Schölvinck, M. L., Chang, C., Ye, F. Q., Leopold, D. A., & Duyn, J. H. (2018). Subcortical evidence for a contribution of arousal to fMRI studies of brain activity. *Nature Communications*, *9*(1), 395. https://doi.org/10.1038/s41467-017-02815-3

Liu, X., Yanagawa, T., Leopold, D. A., Chang, C., Ishida, H., Fujii, N., & Duyn, J. H. (2015). Arousal transitions in sleep, wakefulness, and anesthesia are characterized by

an orderly sequence of cortical events. *NeuroImage*, *116*, 222–231. https://doi.org/10.1016/j.neuroimage.2015.04.003

Lledo, P.-M., Alonso, M., & Grubb, M. S. (2006). Adult neurogenesis and functional plasticity in neuronal circuits. *Nature Reviews Neuroscience*, *7*(3), 179–193. https://doi.org/10.1038/nrn1867

Lord, L.-D., Expert, P., Atasoy, S., Roseman, L., Rapuano, K., Lambiotte, R., Nutt, D. J., Deco, G., Carhart-Harris, R. L., Kringelbach, M. L., & Cabral, J. (2019). Dynamical exploration of the repertoire of brain networks at rest is modulated by psilocybin. *NeuroImage*, *199*, 127–142. https://doi.org/10.1016/j.neuroimage.2019.05.060

Luppi, A. I., Vohryzek, J., Kringelbach, M. L., Mediano, P. A. M., Craig, M. M., Adapa, R., Carhart-Harris, R. L., Roseman, L., Pappas, I., Peattie, A. R. D., Manktelow, A. E., Sahakian, B. J., Finoia, P., Williams, G. B., Allanson, J., Pickard, J. D., Menon, D. K., Atasoy, S., & Stamatakis, E. A. (2023). Distributed harmonic patterns of structure-function dependence orchestrate human consciousness. *Communications Biology*, *6*(1), 117. https://doi.org/10.1038/s42003-023-04474-1

MacLean, K. A., Johnson, M. W., & Griffiths, R. R. (2011). Mystical experiences occasioned by the hallucinogen psilocybin lead to increases in the personality domain of openness. *Journal of Psychopharmacology*, *25*(11), 1453–1461. https://doi.org/10.1177/0269881111420188

Madsen, M. K., Fisher, P. M., Stenbæk, D. S., Kristiansen, S., Burmester, D., Lehel, S., Páleníček, T., Kuchař, M., Svarer, C., Ozenne, B., & Knudsen, G. M. (2020). A single psilocybin dose is associated with long-term increased mindfulness, preceded by a proportional change in neocortical 5-HT2A receptor binding. *European Neuropsychopharmacology*, *33*, 71–80. https://doi.org/10.1016/j.euroneuro.2020.02.001

Madsen, M. K., Stenbæk, D. S., Arvidsson, A., Armand, S., Marstrand-Joergensen, M. R., Johansen, S. S., Linnet, K., Ozenne, B., Knudsen, G. M., & Fisher, P. M. (2021). Psilocybin-induced changes in brain network integrity and segregation correlate with plasma psilocin level and psychedelic experience. *European Neuropsychopharmacology*, *50*, 121–132. https://doi.org/10.1016/j.euroneuro.2021.06.001

Majić, T., Schmidt, T. T., & Gallinat, J. (2015). Peak experiences and the afterglow phenomenon: When and how do therapeutic effects of hallucinogens depend on psychedelic experiences? *Journal of Psychopharmacology*, *29*(3), 241–253. https://doi.org/10.1177/0269881114568040

Marzbanrad, F., Yaghmaie, N., & Jelinek, H. F. (2020). A framework to quantify controlled directed interactions in network physiology applied to cognitive function

assessment. *Scientific Reports*, *10*(1), 18505. https://doi.org/10.1038/s41598-020-75466-y

Mason, M. F., Norton, M. I., Van Horn, J. D., Wegner, D. M., Grafton, S. T., & Macrae, C. N. (2007). Wandering Minds: The Default Network and Stimulus-Independent Thought. *Science*, *315*(5810), 393–395. https://doi.org/10.1126/science.1131295

Mason, N. L., Kuypers, K. P. C., Müller, F., Reckweg, J., Tse, D. H. Y., Toennes, S. W., Hutten, N. R. P. W., Jansen, J. F. A., Stiers, P., Feilding, A., & Ramaekers, J. G. (2020). Me, myself, bye: Regional alterations in glutamate and the experience of ego dissolution with psilocybin. *Neuropsychopharmacology*, *45*(12), Article 12. https://doi.org/10.1038/s41386-020-0718-8

Mazoyer, B., Zago, L., Mellet, E., Bricogne, S., Etard, O., Houdé, O., Crivello, F., Joliot, M., Petit, L., & Tzourio-Mazoyer, N. (2001). Cortical networks for working memory and executive functions sustain the conscious resting state in man. *Brain Research Bulletin*, *54*(3), 287–298. https://doi.org/10.1016/S0361-9230(00)00437-8

McCulloch, D. E.-W., Madsen, M. K., & Stenb, D. S. (2022). Lasting effects of a single psilocybin dose on resting-state functional connectivity in healthy individuals. *Journal of Psychopharmacology*, 11.

Mckeown, B., Strawson, W. H., Wang, H.-T., Karapanagiotidis, T., Vos de Wael, R., Benkarim, O., Turnbull, A., Margulies, D., Jefferies, E., McCall, C., Bernhardt, B., & Smallwood, J. (2020). The relationship between individual variation in macroscale functional gradients and distinct aspects of ongoing thought. *NeuroImage*, *220*, 117072. https://doi.org/10.1016/j.neuroimage.2020.117072

Medaglia, J. D., Huang, W., Karuza, E. A., Kelkar, A., Thompson-Schill, S. L., Ribeiro, A., & Bassett, D. S. (2018). Functional Alignment with Anatomical Networks is Associated with Cognitive Flexibility. *Nature Human Behaviour*, *2*(2), 156–164. https://doi.org/10.1038/s41562-017-0260-9

Metzner, R. (1998). Hallucinogenic Drugs and Plants in Psychotherapy and Shamanism. *Journal of Psychoactive Drugs*, *30*(4), 333–341. https://doi.org/10.1080/02791072.1998.10399709

Mihalik, A., Chapman, J., Adams, R. A., Winter, N. R., Ferreira, F. S., Shawe-Taylor, J., & Mourão-Miranda, J. (2022). Canonical Correlation Analysis and Partial Least Squares for Identifying Brain–Behavior Associations: A Tutorial and a Comparative Study. *Biological Psychiatry: Cognitive Neuroscience and Neuroimaging*, *7*(11), 1055–1067. https://doi.org/10.1016/j.bpsc.2022.07.012

Mišić, B., Betzel, R. F., de Reus, M. A., van den Heuvel, M. P., Berman, M. G., McIntosh, A. R., & Sporns, O. (2016). Network-Level Structure-Function Relationships in

Human Neocortex. *Cerebral Cortex (New York, N.Y.: 1991)*, *26*(7), 3285–3296. https://doi.org/10.1093/cercor/bhw089

Molholm, S., Sehatpour, P., Mehta, A. D., Shpaner, M., Gomez-Ramirez, M., Ortigue, S., Dyke, J. P., Schwartz, T. H., & Foxe, J. J. (2006). Audio-Visual Multisensory Integration in Superior Parietal Lobule Revealed by Human Intracranial Recordings. *Journal of Neurophysiology*, *96*(2), 721–729. https://doi.org/10.1152/jn.00285.2006

Monsell, S. (2003). Task switching. *Trends in Cognitive Sciences*, *7*(3), 134–140. https://doi.org/10.1016/S1364-6613(03)00028-7

Monti, M. M., Vanhaudenhuyse, A., Coleman, M. R., Boly, M., Pickard, J. D., Tshibanda, L., Owen, A. M., & Laureys, S. (2010). Willful Modulation of Brain Activity in Disorders of Consciousness. *New England Journal of Medicine*, *362*(7), 579–589. https://doi.org/10.1056/NEJMoa0905370

Moreno, et al. (2006). *Safety, Tolerability, and Efficacy of Psilocybin in 9 Patients With Obsessive-Compulsive Disorder*.

Mortaheb, S., Van Calster, L., Raimondo, F., Klados, M. A., Boulakis, P. A., Georgoula, K., Majerus, S., Van De Ville, D., & Demertzi, A. (2022). Mind blanking is a distinct mental state linked to a recurrent brain profile of globally positive connectivity during ongoing mentation. *Proceedings of the National Academy of Sciences*, *119*(41), e2200511119. https://doi.org/10.1073/pnas.2200511119

Murphy, K., Birn, R. M., Handwerker, D. A., Jones, T. B., & Bandettini, P. A. (2009). The impact of global signal regression on resting state correlations: Are anti-correlated networks introduced? *NeuroImage*, *44*(3), 893–905. https://doi.org/10.1016/j.neuroimage.2008.09.036

Murphy, K., & Fox, M. D. (2017). Towards a consensus regarding global signal regression for resting state functional connectivity MRI. *NeuroImage*, *154*, 169–173. https://doi.org/10.1016/j.neuroimage.2016.11.052

Newberg, A. B., & Alavi, A. (1998). Changes in the central nervous system during long-duration space flight: Implications for neuro-imaging. *Advances in Space Research*, *22*(2), 185–196. https://doi.org/10.1016/S0273-1177(98)80010-0

Nichols, D. E. (2016). Psychedelics. *Pharmacological Reviews*, *68*(2), 264–355. https://doi.org/10.1124/pr.115.011478

Nilsonne, G., Tamm, S., Schwarz, J., Almeida, R., Fischer, H., Kecklund, G., Lekander, M., Fransson, P., & Åkerstedt, T. (2017). Intrinsic brain connectivity after partial sleep deprivation in young and older adults: Results from the Stockholm Sleepy Brain study. *Scientific Reports*, *7*(1), Article 1. https://doi.org/10.1038/s41598-017-09744-7

Nisbett, R. E., & Wilson, T. D. (1977). *Telling more than we can know: Verbal reports on mental processes*. *84*(3), 231–259.

Nour, M. M., & Carhart-Harris, R. L. (2017). Psychedelics and the science of self-experience. *British Journal of Psychiatry*, *210*(3), 177–179. https://doi.org/10.1192/bjp.bp.116.194738

Nour, M. M., Evans, L., Nutt, D., & Carhart-Harris, R. L. (2016). Ego-Dissolution and Psychedelics: Validation of the Ego-Dissolution Inventory (EDI). *Frontiers in Human Neuroscience*, *10*. https://www.frontiersin.org/articles/10.3389/fnhum.2016.00269

Ortega, A., Frossard, P., Kovačević, J., Moura, J. M. F., & Vandergheynst, P. (2018). Graph Signal Processing: Overview, Challenges, and Applications. *Proceedings of the IEEE*, *106*(5), 808–828. https://doi.org/10.1109/JPROC.2018.2820126

Panda, R., Thibaut, A., Lopez-Gonzalez, A., Escrichs, A., Bahri, M. A., Hillebrand, A., Deco, G., Laureys, S., Gosseries, O., Annen, J., & Tewarie, P. (2022). Disruption in structural–functional network repertoire and time-resolved subcortical fronto-temporoparietal connectivity in disorders of consciousness. *ELife*, *11*, e77462. https://doi.org/10.7554/eLife.77462

Pascual-Leone, A., Amedi, A., Fregni, F., & Merabet, L. B. (2005). THE PLASTIC HUMAN BRAIN CORTEX. *Annual Review of Neuroscience*, *28*(1), 377–401. https://doi.org/10.1146/annurev.neuro.27.070203.144216

Pechenkova, E., Nosikova, I., Rumshiskaya, A., Litvinova, L., Rukavishnikov, I., Mershina, E., Sinitsyn, V., Van Ombergen, A., Jeurissen, B., Jillings, S., Laureys, S., Sijbers, J., Grishin, A., Chernikova, L., Naumov, I., Kornilova, L., Wuyts, F. L., Tomilovskaya, E., & Kozlovskaya, I. (2019). Alterations of Functional Brain Connectivity After Long-Duration Spaceflight as Revealed by fMRI. *Frontiers in Physiology*, *10*, 761. https://doi.org/10.3389/fphys.2019.00761

Penny, W. D., Friston, K. J., Ashburner, J. T., Kiebel, S. J., & Nichols, T. E. (2011). *Statistical Parametric Mapping: The Analysis of Functional Brain Images*. Elsevier.

Pernice, R., Antonacci, Y., Zanetti, M., Busacca, A., Marinazzo, D., Faes, L., & Nollo, G. (2021). Multivariate Correlation Measures Reveal Structure and Strength of Brain–Body Physiological Networks at Rest and During Mental Stress. *Frontiers in Neuroscience*, *14*, 602584. https://doi.org/10.3389/fnins.2020.602584

Petri, G., Expert, P., Turkheimer, F., Carhart-Harris, R., Nutt, D., Hellyer, P. J., & Vaccarino, F. (2014). Homological scaffolds of brain functional networks. *Journal of The Royal Society Interface*, *11*(101), 20140873. https://doi.org/10.1098/rsif.2014.0873

Pitts, M. A., Lutsyshyna, L. A., & Hillyard, S. A. (2018). The relationship between attention and consciousness: An expanded taxonomy and implications for 'no-report'

paradigms. *Philosophical Transactions of the Royal Society B: Biological Sciences*, *373*(1755), 20170348. https://doi.org/10.1098/rstb.2017.0348

Poldrack, R. (2006). Can cognitive processes be inferred from neuroimaging data? *Trends in Cognitive Sciences*, *10*(2), 59–63. https://doi.org/10.1016/j.tics.2005.12.004

Poldrack, R. A. (2011). Inferring Mental States from Neuroimaging Data: From Reverse Inference to Large-Scale Decoding. *Neuron*, *72*(5), 692–697. https://doi.org/10.1016/j.neuron.2011.11.001

Popp, J. L., Thiele, J. A., Faskowitz, J., Seguin, C., Sporns, O., & Hilger, K. (2023). *Structural-Functional Brain Network Coupling Predicts Human Cognitive Ability* [Preprint]. Neuroscience. https://doi.org/10.1101/2023.02.09.527639

Power, J. D., Mitra, A., Laumann, T. O., Snyder, A. Z., Schlaggar, B. L., & Petersen, S. E. (2014). Methods to detect, characterize, and remove motion artifact in resting state fMRI. *NeuroImage*, *84*, 320–341. https://doi.org/10.1016/j.neuroimage.2013.08.048

Power, J. D., Plitt, M., Laumann, T. O., & Martin, A. (2017). Sources and implications of whole-brain fMRI signals in humans. *NeuroImage*, *146*, 609–625. https://doi.org/10.1016/j.neuroimage.2016.09.038

Preller, K. H., Duerler, P., Burt, J. B., Ji, J. L., Adkinson, B., Stämpfli, P., Seifritz, E., Repovš, G., Krystal, J. H., Murray, J. D., Anticevic, A., & Vollenweider, F. X. (2020). Psilocybin Induces Time-Dependent Changes in Global Functional Connectivity. *Biological Psychiatry*, *88*(2), 197–207. https://doi.org/10.1016/j.biopsych.2019.12.027

Preller, K. H., & Vollenweider, F. X. (2018). Phenomenology, structure, and dynamic of psychedelic states. *Behavioral Neurobiology of Psychedelic Drugs*, 221–256.

Preti, M. G., & Van De Ville, D. (2019). Decoupling of brain function from structure reveals regional behavioral specialization in humans. *Nature Communications*, *10*(1), Article 1. https://doi.org/10.1038/s41467-019-12765-7

Raffelt, D., Dhollander, T., Tournier, J.-D., Tabbara, R., Smith, R., Pierre, E., & Connelly, A. (2017). *Bias Field Correction and Intensity Normalisation for Quantitative Analysis of Apparent Fibre Density*.

Raichle, M. E. (2011). The Restless Brain. *Brain Connectivity*, *1*(1), 3–12. https://doi.org/10.1089/brain.2011.0019

Ramyachitra, D. D., & Manikandan, P. (2014). Imbalanced Dataset Classification and Solutions: A Review. *International Journal of Computing and Business Research*, *5*(4).

Raut, R. V., Snyder, A. Z., Mitra, A., Yellin, D., Fujii, N., Malach, R., & Raichle, M. E. (2021). Global waves synchronize the brain's functional systems with fluctuating

arousal. *Science Advances*, *7*(30), eabf2709. https://doi.org/10.1126/sciadv.abf2709

Reed, L., & Mihaly, C. (2014). The experience sampling method. In *Flow and the Foundations of Positive Psychology*. Springer Netherlands. https://doi.org/10.1007/978-94-017-9088-8

Roberts, D. R., Albrecht, M. H., Collins, H. R., Asemani, D., Chatterjee, A. R., Spampinato, M. V., Zhu, X., Chimowitz, M. I., & Antonucci, M. U. (2017). Effects of Spaceflight on Astronaut Brain Structure as Indicated on MRI. *New England Journal of Medicine*, *377*(18), 1746–1753. https://doi.org/10.1056/NEJMoa1705129

Roberts, D. R., Brown, T. R., Nietert, P. J., Eckert, M. A., Inglesby, D. C., Bloomberg, J. J., George, M. S., & Asemani, D. (2019). Prolonged Microgravity Affects Human Brain Structure and Function. *American Journal of Neuroradiology*, ajnr;ajnr.A6249v1. https://doi.org/10.3174/ajnr.A6249

Roseman, L., Leech, R., Feilding, A., Nutt, D. J., & Carhart-Harris, R. L. (2014). The effects of psilocybin and MDMA on between-network resting state functional connectivity in healthy volunteers. *Frontiers in Human Neuroscience*, *8*. https://doi.org/10.3389/fnhum.2014.00204

Ross, S., Bossis, A., Guss, J., Agin-Liebes, G., Malone, T., Cohen, B., Mennenga, S. E., Belser, A., Kalliontzi, K., Babb, J., Su, Z., Corby, P., & Schmidt, B. L. (2016). Rapid and sustained symptom reduction following psilocybin treatment for anxiety and depression in patients with life-threatening cancer: A randomized controlled trial. *Journal of Psychopharmacology*, *30*(12), 1165–1180. https://doi.org/10.1177/0269881116675512

Roy-O'Reilly, M., Mulavara, A., & Williams, T. (2021). A review of alterations to the brain during spaceflight and the potential relevance to crew in long-duration space exploration. *Npj Microgravity*, *7*(1), 5. https://doi.org/10.1038/s41526-021-00133-z

Schaefer, A., Kong, R., Gordon, E. M., Laumann, T. O., Zuo, X.-N., Holmes, A. J., Eickhoff, S. B., & Yeo, B. T. T. (2018). Local-Global Parcellation of the Human Cerebral Cortex from Intrinsic Functional Connectivity MRI. *Cerebral Cortex*, *28*(9), 3095–3114. https://doi.org/10.1093/cercor/bhx179

Schölvinck, M. L., Maier, A., Ye, F. Q., Duyn, J. H., & Leopold, D. A. (2010). Neural basis of global resting-state fMRI activity. *Proceedings of the National Academy of Sciences*, *107*(22), 10238–10243. https://doi.org/10.1073/pnas.0913110107

Schooler, J., Reichle, E. D., & Halpern, D. V. (2004). Zoning-out during reading: Evidence for dissociations between experience and meta-consciousness. *Thinking and Seeing: Visual Metacognition in Adults and Children*, 204–226.

Schrouff, J., Kussé, C., Wehenkel, L., Maquet, P., & Phillips, C. (2012). Decoding Semi-Constrained Brain Activity from fMRI Using Support Vector Machines and Gaussian Processes. *PLOS ONE*, *7*(4), e35860. https://doi.org/10.1371/journal.pone.0035860

Searle, J. R. (2000). *Consciousness*. *23*, 557–578.

Sergent, C., & Dehaene, S. (2004). Neural processes underlying conscious perception: Experimental findings and a global neuronal workspace framework. *Journal of Physiology-Paris*, *98*(4–6), 374–384. https://doi.org/10.1016/j.jphysparis.2005.09.006

Shine, J. M. (2019). Neuromodulatory Influences on Integration and Segregation in the Brain. *Trends in Cognitive Sciences*, *23*(7), 572–583. https://doi.org/10.1016/j.tics.2019.04.002

Shirer, W. R., Ryali, S., Rykhlevskaia, E., Menon, V., & Greicius, M. D. (2012). Decoding Subject-Driven Cognitive States with Whole-Brain Connectivity Patterns. *Cerebral Cortex*, *22*(1), 158–165. https://doi.org/10.1093/cercor/bhr099

Shulman, G. L., Corbetta, M., Buckner, R. L., Fiez, J. A., Miezin, F. M., Raichle, M. E., & Petersen, S. E. (1997). Common Blood Flow Changes across Visual Tasks: I. Increases in Subcortical Structures and Cerebellum but Not in Nonvisual Cortex. *Journal of Cognitive Neuroscience*, *9*(5), 624–647. https://doi.org/10.1162/jocn.1997.9.5.624

Siebner, H. R., Bergmann, T. O., Bestmann, S., Massimini, M., Johansen-Berg, H., Mochizuki, H., Bohning, D. E., Boorman, E. D., Groppa, S., Miniussi, C., Pascual-Leone, A., Huber, R., Taylor, P. C. J., Ilmoniemi, R. J., De Gennaro, L., Strafella, A. P., Kähkönen, S., Klöppel, S., Frisoni, G. B., … Rossini, P. M. (2009). Consensus paper: Combining transcranial stimulation with neuroimaging. *Brain Stimulation*, *2*(2), 58–80. https://doi.org/10.1016/j.brs.2008.11.002

Signorelli, C. M., Boils, J. D., Tagliazucchi, E., Jarraya, B., & Deco, G. (2022). From brain-body function to conscious interactions. *Neuroscience & Biobehavioral Reviews*, *141*, 104833. https://doi.org/10.1016/j.neubiorev.2022.104833

Singleton, S. P., Luppi, A. I., Carhart-Harris, R. L., Cruzat, J., Roseman, L., Nutt, D. J., Deco, G., Kringelbach, M. L., Stamatakis, E. A., & Kuceyeski, A. (2022). Receptor-informed network control theory links LSD and psilocybin to a flattening of the brain's control energy landscape. *Nature Communications*, *13*(1), 5812. https://doi.org/10.1038/s41467-022-33578-1

Skudlarski, P., Jagannathan, K., Anderson, K., Stevens, M. C., Calhoun, V. D., Skudlarska, B. A., & Pearlson, G. (2010). Brain Connectivity Is Not Only Lower but Different in Schizophrenia: A Combined Anatomical and Functional Approach. *Biological Psychiatry*, *68*(1), 61–69. https://doi.org/10.1016/j.biopsych.2010.03.035

Slater, D. A., Melie-Garcia, L., Preisig, M., Kherif, F., Lutti, A., & Draganski, B. (2019). Evolution of white matter tract microstructure across the life span. *Human Brain Mapping*, *40*(7), 2252–2268. https://doi.org/10.1002/hbm.24522

Small, D. M. (2010). Taste representation in the human insula. *Brain Structure and Function*, *214*(5–6), 551–561. https://doi.org/10.1007/s00429-010-0266-9

Smallwood, J., Beach, E., Schooler, J. W., & Handy, T. C. (2008). *Going AWOL in the Brain: Mind Wandering Reduces Cortical Analysis of External Events*. *20*(3), 12.

Smallwood, J., Turnbull, A., Wang, H., Ho, N. S. P., Poerio, G. L., Karapanagiotidis, T., Konu, D., Mckeown, B., Zhang, M., Murphy, C., Vatansever, D., Bzdok, D., Konishi, M., Leech, R., Seli, P., Schooler, J. W., Bernhardt, B., Margulies, D. S., & Jefferies, E. (2021). The neural correlates of ongoing conscious thought. *IScience*, *24*(3), 102132. https://doi.org/10.1016/j.isci.2021.102132

Smith, R. E., Tournier, J.-D., Calamante, F., & Connelly, A. (2012). Anatomically-constrained tractography: Improved diffusion MRI streamlines tractography through effective use of anatomical information. *NeuroImage*, *62*(3), 1924–1938. https://doi.org/10.1016/j.neuroimage.2012.06.005

Smith, R. E., Tournier, J.-D., Calamante, F., & Connelly, A. (2013). SIFT: Spherical-deconvolution informed filtering of tractograms. *NeuroImage*, *67*, 298–312. https://doi.org/10.1016/j.neuroimage.2012.11.049

Smith, S. M. (2002). Fast robust automated brain extraction. *Human Brain Mapping*, *17*(3), 143–155. https://doi.org/10.1002/hbm.10062

Smith, S. M., Fox, P. T., Miller, K. L., Glahn, D. C., Fox, P. M., Mackay, C. E., Filippini, N., Watkins, K. E., Toro, R., Laird, A. R., & Beckmann, C. F. (2009). Correspondence of the brain's functional architecture during activation and rest. *Proceedings of the National Academy of Sciences*, *106*(31), 13040–13045. https://doi.org/10.1073/pnas.0905267106

Sporns, O., Tononi, G., & Kötter, R. (2005). The Human Connectome: A Structural Description of the Human Brain. *PLoS Computational Biology*, *1*(4), e42. https://doi.org/10.1371/journal.pcbi.0010042

Stahn, A. C., Gunga, H.-C., Kohlberg, E., Gallinat, J., Dinges, D. F., & Kühn, S. (2019). Brain changes in response to long Antarctic expeditions. *New England Journal of Medicine*, *381*(23), 2273–2275.

Stawarczyk, D., & D'Argembeau, A. (2016). Conjoint influence of mind-wandering and sleepiness on task performance. *Journal of Experimental Psychology. Human Perception and Performance*, *42*(10), 1587–1600. https://doi.org/10.1037/xhp0000254

Stawarczyk, D., François, C., Wertz, J., & D'Argembeau, A. (2020). Drowsiness or mind-wandering? Fluctuations in ocular parameters during attentional lapses. *Biological Psychology*, *156*, 107950. https://doi.org/10.1016/j.biopsycho.2020.107950

Stawarczyk, D., Majerus, S., Maquet, P., & D'Argembeau, A. (2011). Neural Correlates of Ongoing Conscious Experience: Both Task-Unrelatedness and Stimulus-Independence Are Related to Default Network Activity. *PLoS ONE*, *6*(2), e16997. https://doi.org/10.1371/journal.pone.0016997

Stevens, A. A., Skudlarski, P., Gatenby, J. C., & Gore, J. C. (2000). Event-related fMRI of auditory and visual oddball tasks. *Magnetic Resonance Imaging*, *18*, 495–502.

Studerus, E., Gamma, A., & Vollenweider, F. X. (2010). Psychometric Evaluation of the Altered States of Consciousness Rating Scale (OAV). *PLoS ONE*, *5*(8), e12412. https://doi.org/10.1371/journal.pone.0012412

Suárez, L. E., Markello, R. D., Betzel, R. F., & Misic, B. (2020). Linking Structure and Function in Macroscale Brain Networks. *Trends in Cognitive Sciences*, *24*(4), 302–315. https://doi.org/10.1016/j.tics.2020.01.008

Tagliazucchi, E., Carhart-Harris, R., Leech, R., Nutt, D., & Chialvo, D. R. (2014). Enhanced repertoire of brain dynamical states during the psychedelic experience: Enhanced Repertoire of Brain Dynamical States. *Human Brain Mapping*, *35*(11), 5442–5456. https://doi.org/10.1002/hbm.22562

Tagliazucchi, E., Roseman, L., Kaelen, M., Orban, C., Muthukumaraswamy, S. D., Murphy, K., Laufs, H., Leech, R., McGonigle, J., Crossley, N., Bullmore, E., Williams, T., Bolstridge, M., Feilding, A., Nutt, D. J., & Carhart-Harris, R. (2016). Increased Global Functional Connectivity Correlates with LSD-Induced Ego Dissolution. *Current Biology*, *26*(8), 1043–1050. https://doi.org/10.1016/j.cub.2016.02.010

Tavor, I., Jones, O. P., Mars, R. B., Smith, S. M., Behrens, T. E., & Jbabdi, S. (2016). Task-free MRI predicts individual differences in brain activity during task performance. *Science*, *352*(6282), 216–220. https://doi.org/10.1126/science.aad8127

Tononi, G. (2008). Consciousness as Integrated Information: A Provisional Manifesto. *The Biological Bulletin*, *215*(3), 216–242. https://doi.org/10.2307/25470707

Tournier, J. D., Calamante, F., & Connelly, A. (2010). *Improved probabilistic streamlines tractography by 2nd order integration over fibre orientation distributions*. *1670*.

Tournier, J. D., Calamante, F., & Connelly, A. (2013). Determination of the appropriate *b* value and number of gradient directions for high-angular-resolution diffusion-weighted imaging: APPROPRIATE *b* VALUE AND NUMBER OF GRADIENT

DIRECTIONS FOR HARDI. *NMR in Biomedicine*, *26*(12), 1775–1786. https://doi.org/10.1002/nbm.3017

Tournier, J.-D., Calamante, F., & Connelly, A. (2010). Improved probabilistic streamlines tractography by 2nd order integration over fibre orientation distributions. *Proceedings of the International Society for Magnetic Resonance in Medicine*, *1670*(ISMRM).

Tournier, J.-D., Smith, R., Raffelt, D., Tabbara, R., Dhollander, T., Pietsch, M., Christiaens, D., Jeurissen, B., Yeh, C.-H., & Connelly, A. (2019). MRtrix3: A fast, flexible and open software framework for medical image processing and visualisation. *NeuroImage*, *202*, 116137. https://doi.org/10.1016/j.neuroimage.2019.116137

Tu, Y., Cao, J., Guler, S., Chai-Zhang, T., Camprodon, J. A., Vangel, M., Gollub, R. L., Dougherty, D. D., & Kong, J. (2021). Perturbing fMRI brain dynamics using transcranial direct current stimulation. *NeuroImage*, *237*, 118100.

Turnbull, A., Wang, H. T., Murphy, C., Ho, N. S. P., Wang, X., Sormaz, M., Karapanagiotidis, T., Leech, R. M., Bernhardt, B., Margulies, D. S., Vatansever, D., Jefferies, E., & Smallwood, J. (2019). Left dorsolateral prefrontal cortex supports context-dependent prioritisation of off-task thought. *Nature Communications*, *10*(1), 3816. https://doi.org/10.1038/s41467-019-11764-y

Tustison, N. J., Avants, B. B., Cook, P. A., Yuanjie Zheng, Egan, A., Yushkevich, P. A., & Gee, J. C. (2010). N4ITK: Improved N3 Bias Correction. *IEEE Transactions on Medical Imaging*, *29*(6), 1310–1320. https://doi.org/10.1109/TMI.2010.2046908

Tustison, N. J., Avants, B. B., Cook, P. A., Zheng, Y., Egan, A., Yushkevich, P. A., & Gee, J. C. (2010). N4ITK: Improved N3 Bias Correction. *IEEE Transactions on Medical Imaging*, *29*(6), 1310–1320. https://doi.org/10.1109/TMI.2010.2046908

Tylš, F., Páleníček, T., & Horáček, J. (2014). Psilocybin – Summary of knowledge and new perspectives. *European Neuropsychopharmacology*, *24*(3), 342–356. https://doi.org/10.1016/j.euroneuro.2013.12.006

Uddin, L. Q. (2021). Cognitive and behavioural flexibility: Neural mechanisms and clinical considerations. *Nature Reviews Neuroscience*, *22*(3), Article 3. https://doi.org/10.1038/s41583-021-00428-w

Unsworth, N., & Robison, M. K. (2016). Pupillary correlates of lapses of sustained attention. *Cognitive, Affective & Behavioral Neuroscience*, *16*(4), 601–615. https://doi.org/10.3758/s13415-016-0417-4

Van Calster, L., D'Argembeau, A., Salmon, E., Peters, F., & Majerus, S. (2017). Fluctuations of Attentional Networks and Default Mode Network during the Resting State Reflect Variations in Cognitive States: Evidence from a Novel

Resting-state Experience Sampling Method. *Journal of Cognitive Neuroscience*, *29*(1), 95–113. https://doi.org/10.1162/jocn_a_01025

Van den Driessche, C., Bastian, M., Peyre, H., Stordeur, C., Acquaviva, É., Bahadori, S., Delorme, R., & Sackur, J. (2017). Attentional Lapses in Attention-Deficit/Hyperactivity Disorder: Blank Rather Than Wandering Thoughts. *Psychological Science*, *28*(10), 1375–1386. https://doi.org/10.1177/0956797617708234

Van den Heuvel, M. P., & Hulshoff Pol, H. E. (2010). Exploring the brain network: A review on resting-state fMRI functional connectivity. *European Neuropsychopharmacology*, *20*(8), 519–534. https://doi.org/10.1016/j.euroneuro.2010.03.008

Van Ombergen, A., Jillings, S., Jeurissen, B., Tomilovskaya, E., Rühl, R. M., Rumshiskaya, A., Nosikova, I., Litvinova, L., Annen, J., & Pechenkova, E. V. (2018). Brain tissue–volume changes in cosmonauts. *New England Journal of Medicine*, *379*(17), 1678–1680.

Van Ombergen, A., Jillings, S., Jeurissen, B., Tomilovskaya, E., Rumshiskaya, A., Litvinova, L., Nosikova, I., Pechenkova, E., Rukavishnikov, I., Manko, O., Danylichev, S., Rühl, R. M., Kozlovskaya, I. B., Sunaert, S., Parizel, P. M., Sinitsyn, V., Laureys, S., Sijbers, J., zu Eulenburg, P., & Wuyts, F. L. (2019). Brain ventricular volume changes induced by long-duration spaceflight. *Proceedings of the National Academy of Sciences*, *116*(21), 10531–10536. https://doi.org/10.1073/pnas.1820354116

Vanhaudenhuyse, A., Demertzi, A., Schabus, M., Noirhomme, Q., Bredart, S., Boly, M., Phillips, C., Soddu, A., Luxen, A., Moonen, G., & Laureys, S. (2011). Two distinct neuronal networks mediate the awareness of environment and of self. *Journal of Cognitive Neuroscience*, *23*(3), 570–578. https://doi.org/10.1162/jocn.2010.21488

Varley, T. F., Carhart-Harris, R., Roseman, L., Menon, D. K., & Stamatakis, E. A. (2020). Serotonergic psychedelics LSD & psilocybin increase the fractal dimension of cortical brain activity in spatial and temporal domains. *NeuroImage*, *220*, 117049. https://doi.org/10.1016/j.neuroimage.2020.117049

Veraart, J., Novikov, D. S., Christiaens, D., Ades-aron, B., Sijbers, J., & Fieremans, E. (2016). Denoising of diffusion MRI using random matrix theory. *NeuroImage*, *142*, 394–406. https://doi.org/10.1016/j.neuroimage.2016.08.016

Vollenweider, F. X., & Kometer, M. (2010). The neurobiology of psychedelic drugs: Implications for the treatment of mood disorders. *Nature Reviews Neuroscience*, *11*(9), 642–651. https://doi.org/10.1038/nrn2884

Vyazovskiy, V. V., Olcese, U., Hanlon, E. C., Nir, Y., Cirelli, C., & Tononi, G. (2011). Local sleep in awake rats. *Nature*, *472*(7344), 443–447. https://doi.org/10.1038/nature10009

Wang, J., Khosrowabadi, R., Ng, K. K., Hong, Z., Chong, J. S. X., Wang, Y., Chen, C.-Y., Hilal, S., Venketasubramanian, N., Wong, T. Y., Chen, C. L.-H., Ikram, M. K., & Zhou, J. (2018). Alterations in Brain Network Topology and Structural-Functional Connectome Coupling Relate to Cognitive Impairment. *Frontiers in Aging Neuroscience*, *10*, 404. https://doi.org/10.3389/fnagi.2018.00404

Wang, Z., Dai, Z., Gong, G., Zhou, C., & He, Y. (2015). Understanding Structural-Functional Relationships in the Human Brain: A Large-Scale Network Perspective. *The Neuroscientist*, *21*(3), 290–305. https://doi.org/10.1177/1073858414537560

Ward, A. F., & Wegner, D. M. (2013). Mind-blanking: When the mind goes away. *Frontiers in Psychology*, *4*. https://doi.org/10.3389/fpsyg.2013.00650

Watanabe, T., Hirose, S., Wada, H., Imai, Y., Machida, T., Shirouzu, I., Konishi, S., Miyashita, Y., & Masuda, N. (2014). Energy landscapes of resting-state brain networks. *Frontiers in Neuroinformatics*, *8*. https://doi.org/10.3389/fninf.2014.00012

Watts, F. N., MacLeod, A. K., & Morris, L. (1988). Associations between phenomenal and objective aspects of concentration problems in depressed patients. *British Journal of Psychology*, *79*(2), 241–250. https://doi.org/10.1111/j.2044-8295.1988.tb02285.x

Weinstein, Y., De Lima, H. J., & van der Zee, T. (2018). Are you mind-wandering, or is your mind on task? The effect of probe framing on mind-wandering reports. *Psychonomic Bulletin & Review*, *25*(2), 754–760. https://doi.org/10.3758/s13423-017-1322-8

Winter, U., LeVan, P., Borghardt, T. L., Akin, B., Wittmann, M., Leyens, Y., & Schmidt, S. (2020). Content-Free Awareness: EEG-fcMRI Correlates of Consciousness as Such in an Expert Meditator. *Frontiers in Psychology*, *10*, 3064. https://doi.org/10.3389/fpsyg.2019.03064

Wong, C. W., Olafsson, V., Tal, O., & Liu, T. T. (2013). The amplitude of the resting-state fMRI global signal is related to EEG vigilance measures. *NeuroImage*, *83*, 983–990. https://doi.org/10.1016/j.neuroimage.2013.07.057

Xu, H., Su, J., Qin, J., Li, M., Zeng, L.-L., Hu, D., & Shen, H. (2018). Impact of global signal regression on characterizing dynamic functional connectivity and brain states. *NeuroImage*, *173*, 127–145. https://doi.org/10.1016/j.neuroimage.2018.02.036

Ye, C., Huang, J., Liang, L., Yan, Z., Qi, Z., Kang, X., Liu, Z., Dong, H., Lv, H., & Ma, T. (2022). Coupling of brain activity and structural network in multiple sclerosis: A graph

frequency analysis study. *Journal of Neuroscience Research*, *100*(5), 1226–1238.

Zhang, J., Huang, Z., Tumati, S., & Northoff, G. (2020). Rest-task modulation of fMRI-derived global signal topography is mediated by transient coactivation patterns. *PLOS Biology*, *18*(7), e3000733. https://doi.org/10.1371/journal.pbio.3000733

Zhang, J., & Northoff, G. (2022). Beyond noise to function: Reframing the global brain activity and its dynamic topography. *Communications Biology*, *5*(1), 1350. https://doi.org/10.1038/s42003-022-04297-6

Zhang, Y., Wang, C., Wang, Y., Yan, F., Wang, Q., & Huang, L. (2019). Investigating dynamic functional network patterns after propofol-induced loss of consciousness. *Clinical Neurophysiology*, *130*(3), 331–340. https://doi.org/10.1016/j.clinph.2018.11.028

Zhang, Z., Liao, W., Chen, H., Mantini, D., Ding, J.-R., Xu, Q., Wang, Z., Yuan, C., Chen, G., Jiao, Q., & Lu, G. (2011). Altered functional–structural coupling of large-scale brain networks in idiopathic generalized epilepsy. *Brain*, *134*(10), 2912–2928. https://doi.org/10.1093/brain/awr223

Zhou, S., Zou, G., Xu, J., Su, Z., Zhu, H., Zou, Q., & Gao, J. (2019). Dynamic functional connectivity states characterize NREM sleep and wakefulness. *Human Brain Mapping*, *40*(18), 5256–5268. https://doi.org/10.1002/hbm.24770

Zhu, D. C., Tarumi, T., Khan, M. A., & Zhang, R. (2015). Vascular Coupling in Resting-State FMRI: Evidence from Multiple Modalities. *Journal of Cerebral Blood Flow & Metabolism*, *35*(12), 1910–1920. https://doi.org/10.1038/jcbfm.2015.166